CURRENT RESEARCH IN SCIENCE AND MATHEMATICS

EDITORS

ASSOC. PROF. DR. NESLIHAN İYİT

MARCH 2022

gece kitaplığı

İmtiyaz Sahibi / Publisher • Yaşar Hız
Genel Yayın Yönetmeni / Editor in Chief • Eda Altunel
Kapak & İç Tasarım / Cover & Interior Design • Gece Kitaplığı
Editörler / Edıtors • Assoc. Prof. Dr. Neslihan İYİT
Birinci Basım / First Edition • © Mart 2022
ISBN • 978-625-430-052-3

© copyright
Bu kitabın yayın hakkı Gece Kitaplığı'na aittir.

Kaynak gösterilmeden alıntı yapılamaz, izin
almadan hiçbir yolla çoğaltılamaz.

The r ight to publish this book belongs to Gece Kitaplığı.
Citation can not be shown without the source, reproduced in any way
without permission.

Gece Kitaplığı / Gece Publishing
Türkiye Adres / Turkey Address: Kızılay Mah. Fevzi Çakmak 1. Sokak
Ümit Apt. No: 22/A Çankaya / Ankara / TR
Telefon / Phone: +90 312 384 80 40
web: www.gecekitapligi.com
e-mail: gecekitapligi@gmail.com

Baskı & Cilt / Printing & Volume
Sertifika / Certificate No: 47083

Current Research in Science and Mathematics

March 2022

EDITORS

Assoc. Prof. Dr. Neslihan İYİT

CONTENTS

Chapter 1

A GENERAL OVERVIEW FOR DETERMINATION OF SAMPLE SIZE IN PARAMETRIC T-TESTS BY A MONTE-CARLO SIMULATION STUDY

Neslihan İYİT , Hediye Nagehan BÜYÜKBAYRAM,
Mehmet Emin TEKİN 1

Chapter 2

INVESTIGATION OF EFFECT OF ROASTED SESAME SEED EXTRACT ON OXIDATIVE EVENTS IN EXPERIMENTAL ANIMAL WOUND MODEL

Sibel GOKSEN, Kaan KALTALIOGLU,
Sule COSKUN-CEVHER 17

Chapter 3

RNAi MANAGEMENT STRATEGIES OF FUNGAL DISEASES AND MYCOTOXIN CONTAMINATION IN PLANT

Fatma AYDINOGLU 31

Chapter 4

DETERMINATION OF ELECTRON TRAJECTORIES FOR SEM-EDS ANALYSIS OF BI-(2212) BULK SUPERCONDUCTORS: A MONTE CARLO SIMULATION FOR SURFACE IMPURITY DIFFUSION

Şenol KAYA 57

Chapter 5

MICROPLASTICS AND RECENT IDENTIFICATION TECHNIQUES

Sabahattin DENIZ 77

A GENERAL OVERVIEW FOR DETERMINATION OF SAMPLE SIZE IN PARAMETRIC T-TESTS BY A MONTE-CARLO SIMULATION STUDY

Neslihan İYİT [1], Hediye Nagehan BÜYÜKBAYRAM[2], Mehmet Emin TEKİN [3]

1 Assoc.Prof.Dr., Statistics Department, Faculty of Science, Selcuk University, Konya, Türkiye *Corresponding Author: Email: niyit@selcuk.edu.tr
ORCID ID: 0000-0002-5727-6441
2 P.Hd. Student, Department of Biostatistics, Selçuk University, Faculty of Veterinary Medicine, Konya, Türkiye
ORCID ID: 0000-0002-6540-6007
3 Prof.Dr., Department of Biostatistics, Selçuk University, Faculty of Veterinary Medicine, Konya, Türkiye
ORCID ID: 0000-0002-3449-9984

1.Introduction

Statistical analysis is the science of collecting, discovering and presenting quantitative and qualitative data to make hypothesis tests of the interested populations and/or determining relationships between dependent and independent variables and also dealt with making forecastings based on the data (Cohen, 1977; Fick, 1995; Asraf and Brewer, 2004; Demirel and Gürler, 2010). Statistics has a wide range of uses as follows; Pharmaceutical companies use statistics to determine the most effective production of viral vaccines for COVID-19 pandemics. Communication companies use statistics to learn more about subscriber requirements, to optimize network resources, to improve service, and to reduce customer churn. Statistics can also be used to produce better quality fabrics for manufacturers, to accelerate the airline industry, to help musicians make better music. In summary; from the toothpaste tube in your bathroom to the planes in the sky, from the clothes you use to the communication operator you prefer, statistics have a wide range of uses.

In a statistical analysis, a sample is a set of subjects randomly taken from the interested population, representing the characteristics of whole population, by the most appropriate sampling method. Before starting a statistical analysis, sampling is done in cases where it is not possible to reach the entire population, in order to save time, cost and human resources, and most importantly, to cause minimum damage to living things and nature. In the sampling stages, the population should be well defined; the population frame, the sampling method and the sample size should be determined exactly. (Julious, 2004; Maxwell et al., 2008; Chow et al., 2018).

Many factors affect the accuracy of the results of a statistical analysis, such as researcher's perspective, the design of the research, data collection methods, data analysis techniques (Goldstein, 1989; Keppel, 1991; John and Dennis, 2001). In this context, there are four basic concepts that will affect the accuracy of a statistical analysis. These are "statistical power $(1-\beta)$", "effect size (d)", "sample size (n)" and "significance level (α)". In a statistical analysis, these four important concepts are strongly related in the aspect of each being a function of the other three. In other words, if three of these concepts are taken as fixed, then the fourth concept is fully determined (Cohen, 1988; Kang, 2021). G*Power is a free program to calculate the sample size, statistical power, and the effect size for a wide variety of statistical parametric tests including t-test, F-test, correlation, regression analysis and etc (Paxton, Curran and Bollen, 2001; Faul et al., 2007; Faul et al., 2009). In this study G*Power program and R-Studio program, Stats Package, Power calculations for one and two sample t-tests (pwr) library, and Multivariate normal density and random deviates

(mvtnorm) library are used.

In the literature, there are many studies such as Cohen (1962), Cohen (1977), Cohen (1988), Verma and Goodale (1995), Erdfelder et al. (1996), Wood and Lambert (1999), Lewis (2000), Julious (2004), Asraf and Brewer (2004), Ellis (2010), Demirel and Gürler (2010), Kelly and Preacher (2012), Luke (2017), Kelter (2020), Kang (2021) and etc. avaliable on sample size determination in parametric t-tests. In addition to the literature, in this study, paired/independent samples t-tests, which are the hypothesis tests for comparing two dependent/independent group means are studied to determine the optimal sample size. The reason for this is our opinion that the impact of the "effect size" concept on the sample size is primarily necessary in statistical hypothesis tests where two group means are compared. Therefore, in this study, sample sizes are estimated by taking into account the different standard deviations, statistical powers and effect sizes to be used in the comparison of two dependent/independent samples mean differences in parametric tests. In this study, the estimated sample sizes are given with the aim of providing convenience to the researchers who will work with this statistical hypothesis tests in this field.

2.Materials and Method

2.1. Sample Size

When choosing a sample from the population, care should be taken to ensure that the sample is sufficient in number. The sample size (n) should always be "large enough". This is the heart of the statistics to estimate the parameters of the interested population and hypothesis tests.

If the sample size is too small;

When the sample size (n) is less than enough, there is a possibility of failing to reject a statistically significant effect/relationship in fact when there is a statistically significant actual effect/relationship as a result of the hypothesis test called Type II error (β).

If the sample size is too large;

When the sample size (n) is greater than enough, there is a possibility of rejecting a statistically significant effect/relationship in fact when there is a statistically insignificant actual effect/relationship as a result of the hypothesis test called Type I error (α).

Therefore, determining the optimum sample size and performing statistical power analysis in a statistical research is very important to prevent the possibility of making Type I error and Type II error.

While determining the optimal sample size (n), it is very important to

- determine the most appropriate statistical analysis method to test the main hypothesis of the statistical research,
- determine effect size as a measure of the strength of the relationship between two/more variables or dependent/independent variables in statistics calculated from a sample of the population,
- determine standard deviation of the interested variable(s) from the previous studies in the literature, significance level, and Type II error.

Four different possible states that can occur on a given sample to make statistical inferences about a population as a result of hypothesis test are given in Table 1 (Schmidt, 1996).

Table 1. *The relationships between Type I error, Type II error, and statistical power in a statistical hypothesis test*

		Decision as a Result of Hypothesis Test	
		H_0 can be rejected	**H_0 can not rejected**
The Actual Situation	**When H_0 is true**	Type I Error (α)	Right Decision (1- α)
	When H_0 is false	Power (1- β)	Type II Error (β)

2.2. Statistical Power

Statistical power is the probability of making the right decision when the null hypothesis is false (Cohen, 1962). In other words; statistical power reflects the degree to which differences in data taken from samples can be detected in a statistical hypothesis test (Keppel, 1991; Kramer and Rosenthal, 1999; Kelly and Preacher, 2012). Performing a statistical power analysis is an important part of doing proper scientific research, since it doesn't really make sense to conduct a study with insufficient statistical power (Lewis, 2000, Bausell and Li, 2002).

Knowing the relationships between the factors that affect the statistical power of a study is so important for obtaining as high statistical power as possible for the hypothesis tests (Verma and Goodale, 1995, Smith and Bayen, 2005, Dalgaard, 2008). Statistical power defines the relationship between significance level (α), sample size (n) and effect size (d) in statistical inference.

The concept of statistical power is a function of three parameters given as follows (Verma and Goodale, 1995);

$$Statistical\ Power = (1-\beta) = f(\alpha, n, d) \tag{1}$$

where α is the probability of rejecting the null hypothesis (H_0) when H_0 is true (Dallgard, 2008, Sheppard, 1999). For an ideal scientific study, the researcher should decide on the appropriate level of the Type I and

Type II errors, estimate the effect size, and determine the required sample size (Cohen, 1977, 1988).

2.3. Effect Size

In hypothesis tests, p-value is the probability value of making Type I error from the sample taken from the interested population (Lipsey, 1990; John and Dennis, 2001). The effect size is complementary to the p-value, which is an inferential statistics. While the p-value explains whether a finding is statistically significant or not, the effect size provides information about the measure of mean difference in the hypothesis test (McGraw and Wong, 1992; Kramer and Rosenthal, 1999; Parks et al., 1999). Of course, the easier it is to test the difference between population means that are quite different from each other, the harder it will be to detect differences between population means that are very close to each other. For example, if a diet program is guaranteed to lose 10 kilos in a month, this is the effect size of the diet program to be applied (Ellis, 2010).

Regarding the determination of the effect size, Cohen divided the effect sizes into three classes as small, medium and large as given in Table 2.

Table 2. *Effect sizes for parametric t-tests reported by Cohen (1977)*

Statistical Test		Effect Sizes		
		Small	**Medium**	**Large**
Parametric t-tests	*Cohen's d statistics*	0,2	0,5	0,8

The effect size levels determined by Cohen have been used by researchers since 1977 as a standard definition. If the statistical power $(1-\beta)$ and level of significance (α) are certain in a study, it is possible to determine the sample size (n) by using Cohen's effect size Table 1 given above (Deng, 2000). Also effect sizes formulas for parametric t-tests are given in Table 3 (Faul et al., 2007);

Table 3. *Effect sizes formulas for parametric t-tests*

Parametric t-tests	***Hypothesis***	***Effect Sizes***
One sample t-test	$H_0 : \mu = \mu_0$ $H_1 : \mu \neq \mu_0$ $H_1 : \mu > \mu_0$ $H_1 : \mu < \mu_0$	$d = \frac{\mu - \mu_0}{\sigma}$

Paired groups t-test	$H_0 : \mu_{x-y} = 0$ $H_1 : \mu_{x-y} \neq 0$ $H_1 : \mu_{x-y} > 0$ $H_1 : \mu_{x-y} < 0$	$d_{x-y} = \frac{\lvert \mu_{x-y} \rvert}{\sigma_{x-y}}$ $\sigma_{x-y} = \sqrt{\sigma_x^2 + \sigma_y^2 - 2\rho\sigma_x\sigma_y}$
Independent groups t-test	$H_0 : \mu_1 = \mu_2$ $H_1 : \mu_1 \neq \mu_2$ $H_1 : \mu_1 > \mu_2$ $H_1 : \mu_1 < \mu_2$	$d = \frac{\mu_1 - \mu_2}{\sigma}$

3. Results and Discussion

In this section, Monte Carlo simulation method is used to determine the appropriate sample size for parametric t-test applications. In the simulation study, 20.000 Monte Carlo trials are conducted in R-Studio and appropriate sample sizes are estimated for different standard deviations, statistical powers and effect sizes in order to test the paired samples t-test and independent samples t-test.

Sample sizes (n) for paired samples t-test are estimated at different standard deviations (σ), statistical powers $(1-\beta)$ and effect sizes (d) determined by Cohen (1977, 1988) given in Table 4.

Table 4. *Sample sizes for different statistical powers and effect sizes in one/two sided alternative hypotheses at different standard deviations for paired samples t-test*

			Effect Size					
			d=0.2		**d=0.5**		**d=0.8**	
		Power	**One-Sided**	**Two-Sided**	**One-Sided**	**Two-Sided**	**One-Sided**	**Two-Sided**
Standard Deviation	**S. d =1**	**1-β= 0.80**	n=158	n=200	n=27	n=33	n=11	n=14
		1-β= 0.85	n=178	n=227	n=30	n=38	n=13	n=16
		1-β= 0.90	n=216	n=263	n=35	n=44	n=15	n=19
		1-β= 0.95	n=271	n=326	n=45	n=54	n=18	n=23
	S.d =1.5	**1-β= 0.80**	n=349	n=445	n=57	n=73	n=23	n=30
		1-β= 0.85	n=406	n=505	n=66	n=83	n=27	n=34
		1-β= 0.90	n=486	n=592	n=79	n=97	n=32	n=39
		1-β= 0.95	n=608	n=733	n=99	n=118	n=39	n=48
	S.d =2	**1-β= 0.80**	n=619	n=782	n=100	n=128	n=40	n=51
		1-β= 0.85	n=719	n=894	n=116	n=145	n=47	n=59
		1-β= 0.90	n=855	n=1057	n=138	n=171	n=54	n=69
		1-β= 0.95	n=1092	n=1296	n=175	n=210	n=70	n=84
	S.d =2.5	**1-β= 0.80**	n=965	n=1225	n=156	n=199	n=62	n=79
		1-β= 0.85	n=1121	n=1413	n=181	n=225	n=72	n=90
		1-β= 0.90	n=1341	n=1641	n=215	n=263	n=85	n=104
		1-β= 0.95	n=1691	n=2026	n=271	n=325	n=108	n=129
	S.d =3	**1-β= 0.80**	n=1386	n=1771	n=224	n=282	n=87	n=113
		1-β= 0.85	n=1618	n=2027	n=260	n=325	n=103	n=129
		1-β= 0.90	n=1259	n=2359	n=311	n=378	n=121	n=148
		1-β= 0.95	n=2430	n=2916	n=387	n=461	n=155	n=185
	S.d =3.5	**1-β= 0.80**	n=1897	n=2385	n=304	n=385	n=119	n=152
		1-β= 0.85	n=2205	n=2766	n=356	n=439	n=138	n=175
		1-β= 0.90	n=2613	n=3220	n=420	n=518	n=165	n=203
		1-β= 0.95	n=3308	n=3987	n=530	n=638	n=208	n=251

According to Table 4;

When the standard deviation is taken as $\sigma = 1.0$, the statistical power $(1-\beta)$ is taken as 0.80; for the effect size d=0.2 in one/two sided alternative hypotheses, the sample sizes are estimated as 158 and 200, respectively. For the effect size d=0.5 in one/two sided alternative hypotheses, the sample sizes are estimated as 27 and 33, respectively. For the effect size d=0.8 in one/two sided alternative hypotheses, the sample sizes are estimated as 11 and 14, respectively.

When the standard deviation is taken as $\sigma = 1.0$, the statistical power $(1-\beta)$ is taken as 0.95; for the effect size d=0.2 in one/two sided alternative hypotheses, the sample sizes are estimated as 271 and 326, respectively. For the effect size d=0.5 in one/two sided alternative hypotheses, the sample sizes are estimated as 45 and 54, respectively. For the effect size d=0.8 in one/two sided alternative hypotheses, the sample sizes are estimated as 18 and 23, respectively.

When the standard deviation is taken as $\sigma = 1.5$, the statistical power $(1-\beta)$ is taken as 0.80; for the effect size d=0.2 in one/two sided alternative hypotheses, the sample sizes are estimated as 349 and 445, respectively. For the effect size d=0.5 in one/two sided alternative hypotheses, the sample sizes are estimated as 57 and 73, respectively. For the effect size d=0.8 in one/two sided alternative hypotheses, the sample sizes are estimated as 23 and 30, respectively.

When the standard deviation is taken as $\sigma = 1.5$, the statistical power $(1-\beta)$ is taken as 0.95; for the effect size d=0.2 in one/two sided alternative hypotheses, the sample sizes are estimated as 608 and 733, respectively. For the effect size d=0.5 in one/two sided alternative hypotheses, the sample sizes are estimated as 99 and 118, respectively. For the effect size d=0.8 in one/two sided alternative hypotheses, the sample sizes are estimated as 39 and 48, respectively.

When the standard deviation is taken as $\sigma = 2.0$, the statistical power $(1-\beta)$ is taken as 0.80; for the effect size d=0.2 in one/two sided alternative hypotheses, the sample sizes are estimated as 619 and 782, respectively. For the effect size d=0.5 in one/two sided alternative hypotheses, the sample sizes are estimated as 100 and 128, respectively. For the effect size d=0.8 in one/two sided alternative hypotheses, the sample sizes are estimated as 40 and 51, respectively.

When the standard deviation is taken as $\sigma = 2.0$, the statistical power $(1-\beta)$ is taken as 0.95; for the effect size d=0.2 in one/two sided alternative hypotheses, the sample sizes are estimated as 1092 and 1296, respectively. For the effect size d=0.5 in one/two sided alternative hypotheses, the sample sizes are estimated as 175 and 210, respectively. For the effect size d=0.8 in one/two sided alternative hypotheses, the sample sizes are estimated as 70 and 84, respectively.

When the standard deviation is taken as $\sigma = 2.5$, the statistical power $(1-\beta)$ is taken as 0.80; for the effect size d=0.2 in one/two sided alternative hypotheses, the sample sizes are estimated as 965 and 1225, respectively. For the effect size d=0.5 in one/two sided alternative hypotheses, the sample sizes are estimated as 156 and 199, respectively. For the effect size d=0.8 in one/two sided alternative hypotheses, the sample sizes are estimated as

62 and 79, respectively.

When the standard deviation is taken as $\sigma = 2.5$, the statistical power $(1-\beta)$ is taken as 0.95; for the effect size d=0.2 in one/two sided alternative hypotheses, the sample sizes are estimated as 1691 and 2026, respectively. For the effect size d=0.5 in one/two sided alternative hypotheses, the sample sizes are estimated as 271 and 325, respectively. For the effect size d=0.8 in one/two sided alternative hypotheses, the sample sizes are estimated as 108 and 129, respectively.

When the standard deviation is taken as $\sigma = 3.0$, the statistical power $(1-\beta)$ is taken as 0.80; for the effect size d=0.2 in one/two sided alternative hypotheses, the sample sizes are estimated as 1386 and 1771, respectively. For the effect size d=0.5 in one/two sided alternative hypotheses, the sample sizes are estimated as 224 and 282, respectively. For the effect size d=0.8 in one/two sided alternative hypotheses, the sample sizes are estimated as 87 and 113, respectively.

When the standard deviation is taken as $\sigma = 3.0$, the statistical power $(1-\beta)$ is taken as 0.95; for the effect size d=0.2 in one/two sided alternative hypotheses, the sample sizes are estimated as 2430 and 2916, respectively. For the effect size d=0.5 in one/two sided alternative hypotheses, the sample sizes are estimated as 387 and 461, respectively. For the effect size d=0.8 in one/two sided alternative hypotheses, the sample sizes are estimated as 155 and 185, respectively.

When the standard deviation is taken as $\sigma = 3.5$, the statistical power $(1-\beta)$ is taken as 0.80; for the effect size d=0.2 in one/two sided alternative hypotheses, the sample sizes are estimated as 1897 and 2385, respectively. For the effect size d=0.5 in one/two sided alternative hypotheses, the sample sizes are estimated as 304 and 385, respectively. For the effect size d=0.8 in one/two sided alternative hypotheses, the sample sizes are estimated as 119 and 152, respectively.

When the standard deviation is taken as $\sigma = 3.5$, the statistical power $(1-\beta)$ is taken as 0.95; for the effect size d=0.2 in one/two sided alternative hypotheses, the sample sizes are estimated as 3308 and 3987, respectively. For the effect size d=0.5 in one/two sided alternative hypotheses, the sample sizes are estimated as 530 and 638, respectively. For the effect size d=0.8 in one/two sided alternative hypotheses, the sample sizes are estimated as 208 and 251, respectively.

Sample sizes (n) for indepentdent samples t-test are estimated at different standard deviations (σ), statistical powers $(1-\beta)$ and effect sizes (d) determined by Cohen (1977, 1988) given in Table 5.

Table 5. *Sample sizes for different statistical powers and effect sizes in one/two sided alternative hypotheses at different standard deviations for independent samples t-test*

			Effect Size					
			d=0.2		**d=0.5**		**d=0.8**	
		Power	**One-Sided**	**Two-Sided**	**One-Sided**	**Two-Sided**	**One-Sided**	**Two-Sided**
Standard Deviation	**S. d =1**	**1-β= 0.80**	n=308	n=392	n=51	n=63	n=20	n=26
		1-β= 0.85	n=361	n=450	n=59	n=72	n=23	n=29
		1-β= 0.90	n=429	n=525	n=69	n=85	n=28	n=34
		1-β= 0.95	n=541	n=651	n=87	n=105	n=35	n=42
	S.d =1.5	**1-β= 0.80**	n=697	n=885	n=112	n=143	n=44	n=56
		1-β= 0.85	n=813	n=1017	n=130	n=162	n=51	n=64
		1-β= 0.90	n=963	n=1186	n=154	n=190	n=61	n=75
		1-β= 0.95	n=1218	n=1468	n=197	n=235	n=77	n=92
	S.d =2	**1-β= 0.80**	n=1240	n=1570	n=198	n=253	n=78	n=99
		1-β= 0.85	n=1444	n=1798	n=230	n=288	n=91	n=113
		1-β= 0.90	n=1715	n=2107	n=275	n=335	n=108	n=134
		1-β= 0.95	n=2162	n=2600	n=346	n=414	n=136	n=163
	S.d =2.5	**1-β= 0.80**	n=1937	n=2446	n=309	n=392	n=122	n=154
		1-β= 0.85	n=2242	n=2802	n=363	n=451	n=141	n=176
		1-β= 0.90	n=2679	n=3295	n=429	n=528	n=168	n=207
		1-β= 0.95	n=3376	n=4071	n=541	n=653	n=212	n=255
	S.d = 3	**1-β= 0.80**	n=2782	n=3508	n=448	n=571	n=174	n=221
		1-β= 0.85	n=3251	n=4024	n=521	n=646	n=203	n=253
		1-β= 0.90	n=3837	n=4753	n=617	n=759	n=242	n=297
		1-β= 0.95	n=4857	n=5852	n=781	n=934	n=306	n=367
	S.d =3.5	**1-β= 0.80**	n=3815	n=4812	n=604	n=766	n=237	n=301
		1-β= 0.85	n=4408	n=5501	n=704	n=883	n=276	n=343
		1-β= 0.90	n=5267	n=6445	n=839	n=1028	n=329	n=403
		1-β= 0.95	n=6607	n=7963	n=1059	n=1271	n=415	n=502

According to Table 5;

When the standard deviation is taken as $\sigma = 1.0$, the statistical power $(1-\beta)$ is taken as 0.80; for the effect size d=0.2 in one/two sided alternative hypotheses, the sample sizes are estimated as 308 and 392, respectively. For the effect size d=0.5 in one/two sided alternative hypotheses, the sample sizes are estimated as 51 and 63, respectively. For the effect size d=0.8 in one/two sided alternative hypotheses, the sample sizes are estimated as 20 and 26, respectively.

When the standard deviation is taken as $\sigma = 1.0$, the statistical power $(1-\beta)$ is taken as 0.95; for the effect size d=0.2 in one/two sided alternative

hypotheses, the sample sizes are estimated as 541 and 651, respectively. For the effect size d=0.5 in one/two sided alternative hypotheses, the sample sizes are estimated as 87 and 105, respectively. For the effect size d=0.8 in one/two sided alternative hypotheses, the sample sizes are estimated as 35 and 42, respectively.

When the standard deviation is taken as $\sigma = 1.5$, the statistical power $(1-\beta)$ is taken as 0.80; for the effect size d=0.2 in one/two sided alternative hypotheses, the sample sizes are estimated as 697 and 885, respectively. For the effect size d=0.5 in one/two sided alternative hypotheses, the sample sizes are estimated as 112 and 143, respectively. For the effect size d=0.8 in one/two sided alternative hypotheses, the sample sizes are estimated as 44 and 56, respectively.

When the standard deviation is taken as $\sigma = 1.5$, the statistical power $(1-\beta)$ is taken as 0.95; for the effect size d=0.2 in one/two sided alternative hypotheses, the sample sizes are estimated as 1218 and 1468, respectively. For the effect size d=0.5 in one/two sided alternative hypotheses, the sample sizes are estimated as 197 and 235, respectively. For the effect size d=0.8 in one/two sided alternative hypotheses, the sample sizes are estimated as 77 and 92, respectively.

When the standard deviation is taken as $\sigma = 2.0$, the statistical power $(1-\beta)$ is taken as 0.80; for the effect size d=0.2 in one/two sided alternative hypotheses, the sample sizes are estimated as 619 and 782, respectively. For the effect size d=0.5 in one/two sided alternative hypotheses, the sample sizes are estimated as 100 and 128, respectively. For the effect size d=0.8 in one/two sided alternative hypotheses, the sample sizes are estimated as 40 and 51, respectively.

When the standard deviation is taken as $\sigma = 2.0$, the statistical power $(1-\beta)$ is taken as 0.95; for the effect size d=0.2 in one/two sided alternative hypotheses, the sample sizes are estimated as 1240 and 1570, respectively. For the effect size d=0.5 in one/two sided alternative hypotheses, the sample sizes are estimated as 198 and 253, respectively. For the effect size d=0.8 in one/two sided alternative hypotheses, the sample sizes are estimated as 78 and 99, respectively.

When the standard deviation is taken as $\sigma = 2.5$, the statistical power $(1-\beta)$ is taken as 0.80; for the effect size d=0.2 in one/two sided alternative hypotheses, the sample sizes are estimated as 1937 and 2446, respectively. For the effect size d=0.5 in one/two sided alternative hypotheses, the sample

sizes are estimated as 309 and 392, respectively. For the effect size d=0.8 in one/two sided alternative hypotheses, the sample sizes are estimated as 122 and 154, respectively.

When the standard deviation is taken as $\sigma = 2.5$, the statistical power $(1-\beta)$ is taken as 0.95; for the effect size d=0.2 in one/two sided alternative hypotheses, the sample sizes are estimated as 3376 and 4071, respectively. For the effect size d=0.5 in one/two sided alternative hypotheses, the sample sizes are estimated as 541 and 653, respectively. For the effect size d=0.8 in one/two sided alternative hypotheses, the sample sizes are estimated as 212 and 255, respectively.

When the standard deviation is taken as $\sigma = 3.0$, the statistical power $(1-\beta)$ is taken as 0.80; for the effect size d=0.2 in one/two sided alternative hypotheses, the sample sizes are estimated as 2782 and 3508, respectively. For the effect size d=0.5 in one/two sided alternative hypotheses, the sample sizes are estimated as 448 and 571, respectively. For the effect size d=0.8 in one/two sided alternative hypotheses, the sample sizes are estimated as 174 and 221, respectively.

When the standard deviation is taken as $\sigma = 3.0$, the statistical power $(1-\beta)$ is taken as 0.95; for the effect size d=0.2 in one/two sided alternative hypotheses, the sample sizes are estimated as 4857 and 5852, respectively. For the effect size d=0.5 in one/two sided alternative hypotheses, the sample sizes are estimated as 781 and 934, respectively. For the effect size d=0.8 in one/two sided alternative hypotheses, the sample sizes are estimated as 306 and 367, respectively.

When the standard deviation is taken as $\sigma = 3.5$, the statistical power $(1-\beta)$ is taken as 0.80; for the effect size d=0.2 in one/two sided alternative hypotheses, the sample sizes are estimated as 3815 and 4812, respectively. For the effect size d=0.5 in one/two sided alternative hypotheses, the sample sizes are estimated as 604 and 766, respectively. For the effect size d=0.8 in one/two sided alternative hypotheses, the sample sizes are estimated as 237 and 301, respectively.

When the standard deviation is taken as $\sigma = 3.5$, the statistical power $(1-\beta)$ is taken as 0.95; for the effect size d=0.2 in one/two sided alternative hypotheses, the sample sizes are estimated as 6607 and 7963, respectively. For the effect size d=0.5 in one/two sided alternative hypotheses, the sample sizes are estimated as 1059 and 1271, respectively. For the effect size d=0.8 in one/two sided alternative hypotheses, the sample sizes are estimated as 415 and 502, respectively.

4.CONCLUSION

In this study, paired/independent samples t-tests, which are the hypothesis tests for comparing two dependen/independent group means are studied to determine the optimal sample size. The reason for this is our opinion that the effect of the "effect size" concept on the sample size is primarily necessary in statistical hypothesis tests where two group means are compared. Therefore, in this study, sample sizes are estimated by taking into account the different standard deviations, statistical powers and effect sizes to be used in the comparison of two dependent/independent samples mean differences in parametric tests. The estimated sample sizes are presented in Table 4 and Table 5 with the aim of providing convenience to the researchers who will work with this statistical hypothesis tests in this field.

So one of the most important requirements for making the right decision as a result of a statistical hypothesis is to be able to estimate the "optimum" sample size. Before starting the research, the researcher should determine the effect size, statistical power and significance level and then estimate the appropriate sample size for the study. Because appropriate sample size estimation will minimize the possibility of the researcher making a Type I or Type II errors.

While the sample size increases as the statistical power increases, it decreases as the effect size expands and increases as the standard deviation of the study gets larger.

In other words, the sample size is directly proportional to the statistical power and standard deviation, and inversely proportional to the effect size. Therefore, the larger the effect size for paired or independent samples t-test, the easier it will be to test the hypothesis, and a smaller sample size will be sufficient for the study. However, in this case, the probability of making Type I error or Type II error will increase considerably.

In our next study, the decisions of the statistical hypotheses according to the statistical powers and effect sizes of the studies will be investigated in one/two-sided hypotheses, with a similar simulation study for the one-sample t-test, which we could not include in this section.

REFERENCES

Asraf, R. M. and Brewer, J. K. (2004). Conducting Tests of Hypotheses: The Need for an Adequate Sample Size, The Australian Educational Researcher, 31 (1), 79-94.

Bausell, B. R. and Li, Y. (2002). Power analysis for experimantal research: A practical guide for the biological, medical and social sciences.

Chow, S-C., Shao, J., Wang. H. and Lokhnygina, Y. (2018). Sample Size Calculations In Clinical Research, Taylor and Francis, NY., 30-33.

Cohen J. (1962). The statistical power of abnormal-social psychological research: A review, Journal of Abnormal Psychology, 65,145-153.

Cohen, J. (1977). Statistical Power Analysis for the Behavioral Sciences, Academic Press, New York.

Cohen, J. (1988). Statistical power analysis for the behavioral sciences (2nd ed.), Hillsdale, NJ: Erlbaum.

Dalgaard, Peter (2008). Power and the computation of sample size. Introductory Statistics with R. Statistics and Computing. New York: Springer, 155–56.

Demirel, N. and Gürler, S. (2010). Klinik çalışmalarda örneklem genişliğinin belirlenmesine pratik yaklaşımlar, Kafkas Üniversitesi Vet. Fak. Dergisi, 15(2), 205-211.

Ellis, P. D. (2010). The Essential Guide to Effect Size, Statistical Power, Meta-Analysis and Interpretation Research Results. United Kingdom: Cambridge University Press.

Erdfelder, E., Faul, F. and Buchner, A. (1996). GPower: A General Power Analysis Program, Behavior Research Methods, Instruments and Computers, 28 (1), 1-11.

Faul, F., Erdfelder, E., Lang, A. G., and Buchner, A. (2007). G*Power 3: A Flexible Statistical Power Analysis Program for the Social, Behavioral, and Biomedical Sciences, Behavior Research Methods, 39 (2), 175-191.

Faul F., Erdfelder E., Buchner A. and Lang AG. (2009). Statistical power analyses using G*Power 3.1: tests for correlation and regression analyses. Behav Res Methods; 41:1149-1160.

Fick, R L. (1995). Accepting the null hypothesis. Memory and Cognition, 23, 132-138.

Goldstein, R. (1989). Power and sample size via MS/PC-DOS computers. American Statistician, 43, 253-262.

John, M. and Dennis M. (2001). The abuse of power: the pervasive fallacy of power calculations for data analysis, The American Statistician, 55(1):19–24.

Julious, S.A. (2004) Tutorial in biostatistics - Sample sizes for clinical trials with Normal data. Statistics in Medicine, 23 (12),1921-1986.

Kang, H. (2021). Sample size determination and power analysis using the G*Power software, Journal of Educational Evaluation for Health Professions.

Kelly, K. and Preacher, J. K. (2012). On Effect Size, Psychological Methods, 17 (2), 137-152.

Kelter, R. (2020). Analysis of type I and II error rates of Bayesian and frequentist parametric and nonparametric two-sample hypothesis tests under preliminary assessment of normality, Computational Statistics, 36, 1263–1288.

Keppel, G. (1991). Design and Analysis: A Researcher's Handbook, Prentice Hall, Englewood Cliffs, 3rd Edition.

Kramer, S. H. and Rosenthal, R. (1999). Effect sizes and significance levels in small-sample research. Statistical strategies for small sample research, 59-79.

Lewis, R. J. (2000). Power Analysis and Sample Size Determination: Concepts and Software Tools,

Lipsey, M. W. (1990). Design sensitivity: Statistical power for experimental research. Newbury Park, CA: Sage.

Luke, S. G. (2017). Evaluating significance in linear mixed-effects models in R, (September 2016), 1494–1502.

Maxwell, S. E., Kelley, K. and Rausch, J. R. (2008). Sample Size Planning for Statistical Power and Accuracy in Parameter Estimation. Annual Review of Psychology, 59(1), 537–563.

McGraw, K. O. and Wong, S. P. 1992. A common language effect size statistic. Psychological Bulletin, 111: 361–365.

Parks, J. B., Shewokis, P. A. and Costa, C. A. (1999) "Using Statistical Power Analysis in Sport Management Research". Journal of Sport Management, 13 (2),139-147

Paxton, P., Curran, P. J. and Bollen, K. A. (2001). Monte Carlo Experiments: Design and Implementation, University of North Carolina at Chapel Hill.

Schmidt, F. F. (1996). Statistical significance testing and cumulative knowledge in psychology: Implications for the training of researchers. Psychological Methods, 1, 115–129.

Sheppard, C. (1999). How large should my sample be? Some quick guides to sample size and the power of tests. Marine Pollution Bulletin, 38, 439-447

Smith, R. E. and Bayen, U. J. (2005). The effects of working memory resource availability on prospective memory: A formal modeling approach. Experimental Psychology, 52, 243-256.

Verma, R. and Goodale, J. C. (1995). Statistical Power in Operations Management Research. Journal of Operations Management, 13 (2), 139-152.

Wood J. and Lambert M. (1999). Sample-size calculations for trials in health services research Journal of Health Services and Research and Policy; 4:226-9.

INVESTIGATION OF EFFECT OF ROASTED SESAME SEED EXTRACT ON OXIDATIVE EVENTS IN EXPERIMENTAL ANIMAL WOUND MODEL

Sibel GOKSEN[1], Kaan KALTALIOGLU[2], Sule COSKUN-CEVHER[3]

1 Department of Biology, Faculty of Science, Gazi University, 06500, Ankara, Turkey Department of Medical and Surgical Research, Institute of Health Sciences, Hacettepe University, 06100, Ankara, Turkey ORCID ID: 0000-0003-1595-2816

2 Vocational School of Espiye, Giresun University, 28600, Giresun, Turkey ORCID ID: 0000-0002-4995-2657

3 Department of Biology, Faculty of Science, Gazi University, 06500, Ankara, Turkey Prof. Dr. Sule Coskun-Cevher, sule@gazi.edu.tr, coskuncevher@hotmail.com ORCID ID: 0000-0001-6204-2845

INTRODUCTION

Human beings have been interested in wound healing for centuries. Some of the Ebers papyri found in Ancient Egypt are related to wound healing (Özler, Şimşek, Topal, Öter, & Korkmaz, 2010). Wound is the disruption of the normal anatomical structure and function of soft tissues. Wound healing is the process of cellular and biochemical events that begin with trauma and result in new tissue formation. Dermal wound healing, it is a dynamic event contains various components such as cell proliferation, cell migration and collagen synthesis (Karasu & Bakır 2008). Wound healing, which is an easily affected process, can be affected by factors such as infection, oxidative events, diabetes, systemic steroid and radiation applications.

As in many natural processes in the organism, oxidative events occur throughout the complex wound healing process. Increased reactive oxygen and nitrogen species (ROS and RNS) levels may suggest oxidative/ nitrosative damage to nucleic acids, proteins, and lipids. On the other hand, these species are required to maintain healing process at low levels (Ben Othman et al., 2016; Goksen, Balabanli, & Coskun-Cevher, 2017; Alver, Kaltalioglu, & Coskun-Cevher, 2021)such as neurodegenerative diseases. Dietary antioxidants that can protect neuronal cells from oxidative damage play an important role in preventing such diseases. Previously, we reported that water-soluble fractions purified from defatted sesame seed flour exhibit good antioxidant activity in vitro. In the present study, we investigated the protective effects of white and gold sesame seed water-soluble fractions (WS-wsf and GS-wsf, respectively. Therefore, it is significant to examine the changes in oxidative parameters and maintain the balance.

Sesamum indicum L. (sesame) belongs to the *Sesamum* genus of the *Pedaliaceae* family. It is an annual, herbaceous plant that can be grown in tropical and subtropical climate zones and microclimate regions where the combination of temperature is favorable, grows upright, varies between 80-180 cm in height depending on the variety, climate conditions and soil characteristics (Bozkurt, 2006). Sesame is one of the world's oldest oilseeds, having been grown for over 4000 years (Morris, 2002; Bozkurt, 2006) and is thought to have nutritional and medicinal properties (Shenoy et al., 2011). Sesame seeds provide a considerable protein content (20-30%) (Bozkurt, 2006). Sesame seed, especially roasted form, is a significant oilseed containing powerful antioxidant compounds. Naturally, sesame and products are used to improve healing process in wounds (Kiran & Asad, 2008; Shenoy et al., 2011). The most significant attribute of sesame oil is its strength to oxidative degradation. High stability of sesame oil; It is due to the antioxidant effects of tocopherols, some hydrocarbons and some sterols found in other edible oils, as well as compounds with strong

antioxidant effects specific to this oil, such as sesamol and sesaminol in its composition (Mohamed & Awatif, 1998; Bozkurt, 2006). Unlike the fatty acids found in other vegetable oils, sesame oil contains 41.5-47.9% linoleic acid and 35.9-42.3% oleic acid (Baydar, 2005; Bozkurt, 2006).

Sesame and its oil and seed are related with wound healing process. Kiran et al. (2008) examined the effect of *S. indicum* seeds and oil on rats induced by excisional, incisional, burn and dead space wound models. They observed a decrease in the healing time of wound (via contraction and epithelialization) and a significant eleavation of hydroxyproline content in rats treated with sesame seed and oil. In conclusion, they stated that *S. indicum* seed and oil have wound healing activity when applied topically or given orally. In the study published by Canpolat et al. (2021), it was reported that ozonated sesame oil improved the healing in their macroscopic and microscopic examinations. In another study in rats, it was shown that sesame oil significantly increased the percentage of wound contraction, improved tissue regeneration, and also showed antioxidant and antimicrobial activity (Moalla Rekik et al., 2016). Shenoy et al. (2011) investigated the effect of sesamol, the active ingredient of *S. indicum*, on both normal and dexamethasone-induced healing in incisional, excisional and dead space wounds in albino rats. While they observed a significant strengthen in tensile strength and hydroxyproline levels in sesamol-treated rats, they did not observe a significant change in wound contraction duration and lysyl oxidase. In conclusion, they stated that sesamol could be an encouraging agent for wound healing. In another study with sesamol, it was reported that sesamol-loaded nano formulation accelerated the collagen deposition, reepithelialization and fibroblast migration, and increased the expression of vascular endothelial growth factor (VEGF) and platelet-derived growth factor-B (PDGF-B) of the wound tissue in diabetic foot ulcer (Gourishetti et al., 2020).

In addition to the health problems, the wound affects the psychology and social life of the patients negatively. In this respect, phytotherapeutic approaches to wound healing are gaining in importance. In this study, it was aimed to examine the effects of roasted sesame seed extract, which is thought to have high antioxidant properties, on oxidative events throughout dermal healing process.

MATERIALS AND METHODS

The Local Animal Experimentation Ethics Committee of Gazi University authorized the animal protocol, which was assigned the proven number G.U.ET-12.044.

Roasting and Extraction

In the study using Kesput 99 of sesame variety was elicited ETAE (Ege Tarımsal Araştırma Enstitüsü). Sesame (*Sesamum indicum* L.) seeds were roasted (180 °C, 15 min.) with bakery. According to Yoshida et al., roasting sesame seeds at 180 °C results in a high-quality product (Yoshida & Takagi, 1997). Sesamol is formed from sesamol during the roasting, frying and hydrogenation processes of the seed (Yoshida & Takagi, 1999; Bozkurt, 2006). It is said that roasted sesame seed oil has more sesamol and less sesamolin than unroasted sesame seed oil (Fukuda,Nagata, Osawa, & Namiki, 1986). Sesamol is a good antioxidant for edible oils due to its non-toxicity, soluble in both aqueous and oily systems, free radical scavenging effect, resistance to high cooking temperatures, and increased antioxidant capacity with heat application (Joshi et al., 2005; Bozkurt 2006; Khan et al., 2015). The antioxidant effect of roasted sesame seed oil is much greater than that of unroasted sesame seed oil (Bozkurt, 2006). Fresh roasted sesame seeds (20 g) were extracted with 200 ml of %80 ethanol (at 60-70 °C) using soxhlet extractor for 8 h. Ethanolic extracts were evaporated with rotary evaporator (60 °C). The roasted sesame extracts were filtered through Whatman paper and steriled syringe tip filter (Sartorius 0.45 µm 26 mm) for sterilization. According to day using sterile tube seperate the roasted sesame extracts were kept at +4 °C until using. Roasted sesame extracts (1 ml/each wound) were applied topically once day to the treatment groups.

Animals and Experimental Incisional Wound Model

Three groups of male Wistar albino rats (n=30, 200–250 g) were established (Table 1). Rats were kept at 20-22 °C in a 12-hour light/12-hour dark cycle with regular rat diet and water *(ad libitum*). All surgical procedures carried out under anaesthesia (xylazine and ketamine). Rats were shaved, and skin prepared with baticonol. A linear full-thickness 40 mm incision wounds were made on both sides of spine and sutured with 4/0 silk suture (Figure 1). Following the operations, the animals were killed under anaesthesia on the 3rd and 7th days of healing, except for the control group. The tissue samples were taken from the wounds and immediately frozen in liquid nitrogen.

Table 1. Group specifications

Groups	Specifications
Control Group	Non-wounded, n=6, sacrificed on day 0
Negative Control Groups	Incisional wound, untreated, n=6, sacrificed on day 3
	Incisional wound, untreated, n=6, sacrificed on day 7
Sesame Groups	Incisional wound, roasted sesame extracts (1 ml/each wound) treated, n=6, sacrificed on day 3
	Incisional wound, roasted sesame extracts (1 ml/each wound) treated, n=6, sacrificed on day 7

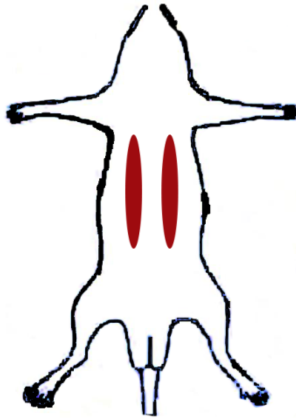

Figure 1. *Incisional full-thickness wound model*

Determination of TBARs levels

TBAR levels in wound tissues were determined spectrophotometrically (Casini et al., 1988). To summarize, samples were homogenized in 10% trichloroacetic acid. Following 2000 g centrifugation, 750 µl of the supernatant was added to an equivalent amount of 0.67% thiobarbituric acid and heated to 100 °C. At 535 nm, absorbance was determined. As a control, a solution of tetraethoxypropane was used.

Determination of GSH levels

Aykaç et al. (1985) method was used to measure GSH levels. To summarize, wounds were homogenized using the TBARs method. After centrifugation, 0.5 ml of supernatant was added to 2 ml of 0.3 M $Na_2HPO_4.2H_2O$ solutions. The absorbance at 412 nm was recorded after adding 0.2 ml of 5,5-dithiobis-2-nitrobenzoic acid.

Determination of NOx levels

NOx levels in wound tissues were determined using the Griess reaction (Miranda, Espey, & Wink, 2001). The tissues were homogenized in phosphate buffer (pH 7) and centrifuged at 3500 rpm; 0.3 M NaOH was added to the supernatants. This mixture was then centrifuged for 5 minutes at 14000 g. Vanadium trichloride (VCI_3) was added following centrifugation. As a control, sodium nitrite was used.

Determination of AA levels

The levels of AA were determined using a spectrophotometric method (Berger, Shepard, Morrow, & Taylor, 1989). On ice, wounds were homogenized in 0.35 M perchloric acid containing EDTA. Supernatants were obtained after centrifuging samples at 15000 g. In a tube, the standard or sample was mixed with the color reagent. Following incubation, 300 µl of 65% H_2SO_4 was added. At 520 nm, the absorbance of the samples was determined.

Statistical Analysis

The Mann-Whitney U test was used to compare the groups statistically. Statistically, $P<0.05$ was assessed. We estimated the data's mean and standard deviation.

RESULTS

TBARs levels

The control group had a significantly greater amount of TBARs than the other groups ($p<0.05$). On the 3rd day, the sesame group's TBARs level was statistically lower than the negative control group's ($p<0.05$). On the 7th day, no significant change was seen between the sesame group and the negative control group ($p>0.05$) (Table 2 and Figure 2).

Table 2. *The effects of roasted sesame seed extract application on oxidative parameters in wound tissue. a p<0.05 as compared with the control group b p<0.05 as compared with the negative control group on same day*

		TBARs (nmol/g tissue)	GSH (µmol/g tissue)	NOx (µmol/g tissue)	AA (mg/g tissue)
Control Group (n=6)	Day 0 (n=6)	65.85 ± 13.86	0.45 ± 0.11	16.66 ± 3.27	103.52 ± 10.30
Negative Control Groups (n=12)	Day 3 (n=6)	16.29 ± 2.17[a]	0.11 ± 0.01[a]	47.35 ± 11.15[a]	127.63 ± 10.37[a]
	Day 7 (n=6)	14.18 ± 4.57[a]	0.17 ± 0.02[a]	42.11 ± 7.73[a]	134.64 ± 10.66[a]
Sesame Groups (n=12)	Day 3 (n=6)	11.71 ± 1.44[a,b]	0.23 ± 0.07[a,b]	29.02 ± 3.67[a,b]	85.21 ± 11.21[a,b]
	Day 7 (n=6)	9.65 ± 2.75[a]	0.23 ± 0.09[a]	39.20 ± 8.71[a]	95.34 ± 23.86[b]

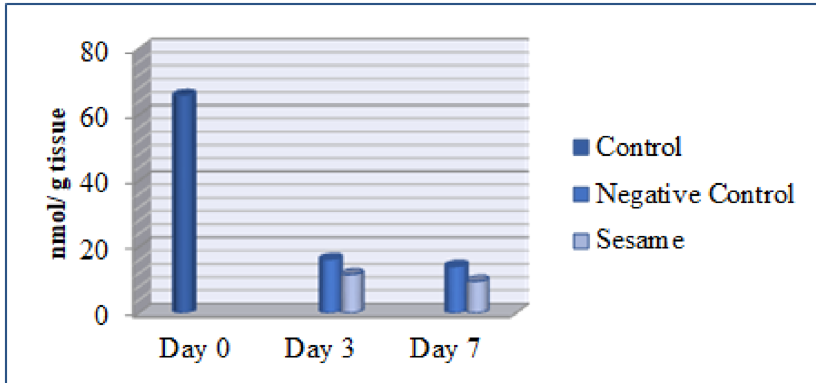

Figure 2. *Wound tissue TBARs levels*

GSH levels

When GSH levels were compared, it was found that it was higher in the control group than in the other groups (p<0.05). As shown in Figure 3, a significant increase was detected in the GSH level of sesame group on the 3rd compared to negative control groups (p<0.05). No significant change was noticed on the 7th day in the same group (p>0.05) (Table 2).

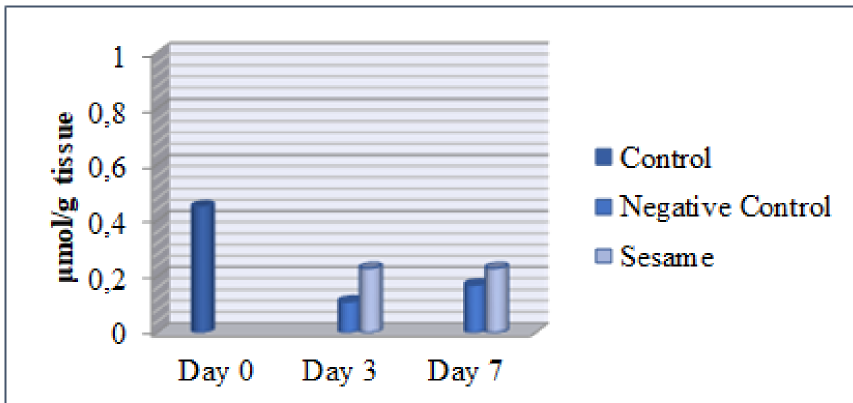

Figure 3. *Wound tissue GSH levels*

NOx levels

The control group's NOx level was found to be statistically lower than that of the other groups (p0.05). On the 3rd day, the sesame group's NOx level was statistically lower than the negative control group's (Table 2 and Figure 4).

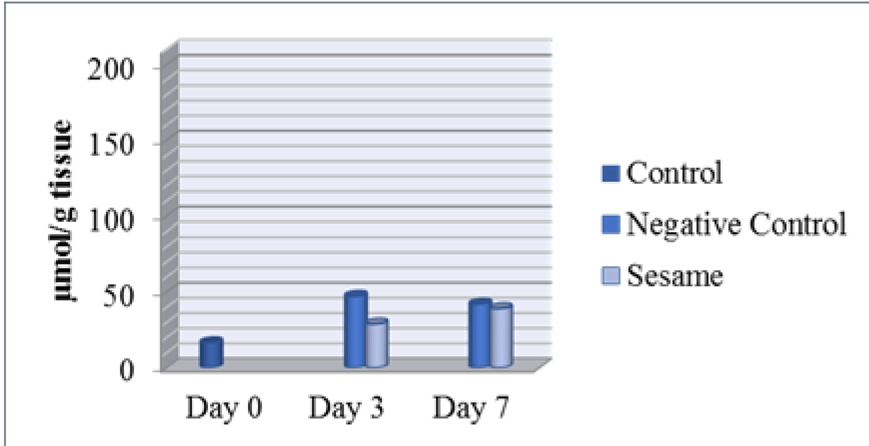

Figure 4. *Wound tissue NOx levels*

AA levels

The control group's AA levels were lower than those of the negative control group but greater than those of the sesame group. The sesame group's AA level was shown to be statistically lower than that of the negative control group on the 3rd and 7th days ($p<0.05$) (Table 2 and Figure 5).

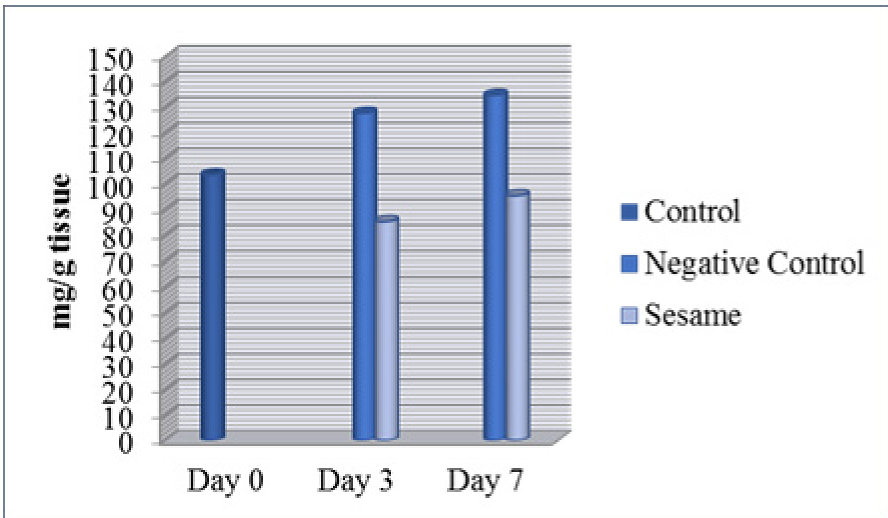

Figure 5. *Wound tissue AA levels*

DISCUSSION

During the wound healing process, important oxidative events occur that improve or damage the process. The purpose of this study was to determine the oxidative events that occurred in wound tissue as a result of topically administered roasted sesame seed extract. Recent studies have shown that seeds, oil or active constituent of *Sesamum indicum* are promoted almost all phases of wound healing (Kiran & Asad, 2008; Shenoy et al., 2011; Gourishetti et al., 2020).

In the sesame group, TBARs level was statistically decreased on 3rd day when compared to the negative control group ($p<0.05$). The level of lipid peroxidation that occurs as a result of oxidative stress caused by ROS is determined by the concentration of malondialdehyde (MDA), one of the most important end products. The fact the TBARs level used in the determination of MDA was significantly decreased in sesame group on the 3rd day compared to negative control group, it is thought that topical roasted sesame seed extract application may have stimulated antioxidant defence mechanism and ROS detoxification in the early stages of healing. Sesame seeds contain various tocopherols such as α, γ and δ (Bozkurt, 2006). Tocopherols have a defensive effect against lipid peroxidation in tissue. Sankar et al. (2006) reported that sesame oil decreased lipid peroxidation in hypertensive patients. It has been shown by Saleem et al. that sesame oil treatment decreased TBARs levels and increased endogenous antioxidants in rats (Mohamed Saleem et al. 2012). Taking into consideration, it is evaluated that the application of roasted sesame seed extract may have contributed to the healing by showing a protective effect due to its high antioxidant capacity (Bozkurt, 2006).

Our results demonstrated that sesame application elevated GSH levels of wound tissue as compared to negative control group on 3rd day ($p<0.05$). GSH is a tripeptide consisting of glutamic acid, glycine and cysteine. It takes part in making the free radicals and various toxic substances harmless in the organism. Ramesh et al. (2005) indicated that GSH level increased in diabetic rats fed with sesame oil. Similar results have been found in other studies (Sankar, Rao, Sambandam, & Pugalendi, 2006; Mohamed Saleem, Madhusudhana Chetty, & Kavimani, 2012; Hanci et al., 2018). In our study, the increase in GSH level in the sesame group shows that roasted sesame seed extract application can increase the antioxidant level of the wound tissue.

In the sesame group, NOx level was statistically decreased on 3rd day when compared to the negative control groups ($p<0.05$). Nitric oxide plays a role in cytotoxic and antimicrobial activity, which also plays a role in macrophages. At the same time, high levels of nitric oxide may have detrimental effect on healthy tissue. Nitric oxide has been implicated in a number of mechanisms involving cell destruction. Nitric oxide synthase

(NOS) enzyme is known to produce NO through 3 isoforms. iNOS, which is induced by immunologic stimuli and found in almost all nucleated cells, is one of them. Inflammatory cytokines take part in coordination of early response to inflammation, and superoxide production and iNOS are well known inducers (Cheng et al., 1999)the role of the radicals in the cytokine-induced myocardial dysfunction in vivo remains unclear. The present study was designed to address this point in our novel canine model of cytokine-induced myocardial dysfunction in vivo. Methods: Studies were performed in mongrel dogs, in which microspheres (MS, 15 μm in diameter. Hsu et al. (2013) showed that pulmonary nitric oxide production, iNOS expression, and neutrophil infiltration were decreased by sesame oil application in ovalbumin-treated rats. Roasted sesame seed extract application may improve healing by reducing nitric oxide level and protecting wound tissue against its harmful effects.

AA or vit C is an important chain breaking antioxidant, and it plays a vital role in scavenging of ROS. Additionally, it is involved in every phases of healing (Moores, 2013; Yimcharoen et al., 2019)also known as ascorbic acid (AA. In the sesame group, AA levels were statistically decreased on 3rd and 7th days when compared to the negative control group ($p<0.05$). This decline was not parallel with some previous studies (Sankar, Rao, Sambandam, & Pugalendi, 2006; Ikeda et al., 2007). This result may be explained by alternative antioxidant mechanism (such as vit E, GSH) or the increased utilization of AA. Another view is that ascorbic acid may have been used to eliminate the increased lipid preoxidation and maintain tissue homeostasis in the groups treated with sesame, that is, on both the 3rd and 7th days of wound healing. At the same time, a balanced behavior between GSH and AA antioxidants, in terms of maintaining the balance, when one increases, the other decreases, is also seen in the wound healing processes. In this study, decreased AA levels may have manifested themselves in this way with the increase of GSH antioxidant in wound healing processes.

CONCLUSION

In addition to medical treatment, phytotherapeutic applications are keeping up to date with an increasing interest. Sesame seed oil has a higher oxidation resistance than other vegetable oils. These findings imply that topically applied roasted sesame seed extract may aid in preventing oxidative damage during the inflammatory phase of the healing process. The roasted sesame seed extract application is thought to contribute to the increase of antioxidant capacity by non-enzymatic antioxidants in the early stage in accordance with increasing oxidative events in wounds. This information has suggested that roasted sesame seed extract application plays a stabilizing role in oxidative events in the early stage of healing. In this respect, the results of the study have the potential to constitute a preliminary step for future studies to regulate and balance the prolonged inflammatory phase in diabetic wounds.

REFERENCES

Alver, E., Kaltalioglu, K., Coskun-Cevher, S. (2021) Reactive oxygen species and wound healing. In: Akgül H, Doğan HH, Yükse l M, Karaman O (eds) *Research & Reviews in Science and Mathematics - May, 2021*, 1st edn. Gece Publishing, pp 65–78.

Aykaç, G., Uysal, M., Yalçın, A.S., Koçak-Toker, N., Sivas, A., & Oz, H. (1985) The effect of chronic ethanol ingestion on hepatic lipid peroxide, glutathione, glutathione peroxidase and glutathione transferase in rats. *Toxicology* 36:71–76.

Baydar, H. (2005) Susamda (Sesamum indicum L.) Verim, Yağ, Oleik ve Linoleik Tipi Hatların Tarımsal ve Teknolojik Özellikleri. *Akdeniz Üniversitesi Ziraat Fakültesi Derg* 18:267–272.

Ben Othman, S., Katsuno, N., Kitayama, A., Fujimura, M., Kitaguchi, K., Yabe, T. (2016) Water-soluble fractions from defatted sesame seeds protect human neuroblast cells against peroxyl radicals and hydrogen peroxide-induced oxidative stress. *Free Radic Res* 50:949–958.

Berger, J., Shepard, D., Morrow, F., Taylor, A. (1989) Relationship between dietary intake and tissue levels of reduced and total vitamin C in the nonscorbutic guinea pig. *J Nutr* 119:734–740.

Bozkurt, G. (2006) Susam yağının antioksidan özellikteki başlıca bileşenlerinin nitelik ve nicelikleri üzerine araştırmalar. (Master's thesis) Ege University (182777).

Canpolat, İ., Eröksüz, Y., Rızaoğlu, T. (2021) Effects on the Wound Healing Process Using Ozonated Oils (Sesame, Nigella Sativa , Hypericum Perforatum) in Rats. *Turkish J Vet Res*. 5 (1) , 25-33.

Casini, A.F., Maellaro, E., Pompella, A., Ferrali, M., Comporti, M. (1988) Lipid Peroxidation, Protein Thiols, Calcium Homeostasis and Imbalance of Antioxidant Systems in Bromobenzene Induced Liver Damage. In: *Chemical Carcinogenesis*. Springer, USA, pp 153–163.

Cheng, X.S., Shimokawa, H., Momii, H., Oyama, J., Fukuyama, N., Egashira, K., Nakazawa, H., Takeshita, A. (1999) Role of superoxide anion in the pathogenesis of cytokine-induced myocardial dysfunction in dogs in vivo. *Cardiovasc Res* 42:651–659.

Fukuda, Y., Nagata, M., Osawa, T., Namiki, M. (1986) Chemical aspects of the antioxidative activity of roasted sesame seed oil, and the effect of using the oil for frying. *Agric Biol Chem* 50:857–862.

Goksen, S., Balabanli, B., Coskun-Cevher, S. (2017) Application of platelet derived growth factor-BB and diabetic wound healing: the relationship with oxidative events. *Free Radic Res* 51:498–505.

Gourishetti, K., Keni, R., Nayak, P. G., Jitta, S. R., Bhaskaran, N. A., Kumar, L., Kumar, N., Krishnadas, N., & Shenoy, R. R. (2020) Sesamol-loaded plga

nanosuspension for accelerating wound healing in diabetic foot ulcer in rats. *Int J Nanomedicine* 15:9265–9282.

Hancı, N. , Odabasoglu, F. , Atalay Dumlu, F. , Aydın Berktaş, O., Kutlu, Z., Halici, M. & Halici, Z. (2018) Sesame Oil Has Gastroprotective And Anti-Oxidative Properties: An Experimental Study In Rats With Indomethacin-Induced Gastric Ulcers. *Eurasian J Food Sci Technol* 2:53–68.

Hsu, D.Z., Liu, C.T., Chu, P.Y., Li, Y.H., Periasamy, S., Liu, M.Y. (2013) Sesame oil attenuates ovalbumin-induced pulmonary edema and bronchial neutrophilic inflammation in mice. *Biomed Res Int* 2013:1–7.

Ikeda S., Abe, C., Uchida, T., Ichikawa, T., Horio, F., Yamashita, K. (2007) Dietary sesame seed and its lignan increase both ascorbic acid concentration in some tissues and urinary excretion by stimulating biosynthesis in rats. *J Nutr Sci Vitaminol (Tokyo)* 53:383–392.

Joshi, R., Kumar, M.S., Satyamoorthy, K., Unnikrisnan, M.K., Mukherjee, T. (2005) Free radical reactions and antioxidant activities of sesamol: Pulse radiolytic and biochemical studies. *J Agric Food Chem* 53:2696–2703.

Karasu, A., & Bakır, B. (2008) Yara ve yara iyileşmesi. *Vet Cerrahi Derg* 14:36–43.

Khan, S., Kumar, A., Adhikari, J.S., Rizvi, M.A., Chaudhury, N.K. (2015) Protective effect of sesamol against 60Co γ-ray-induced hematopoietic and gastrointestinal injury in C57BL/6 male mice. *Free Radic Res* 49:1344–1361.

Kiran, K., Asad, M. (2008) Wound healing activity of Sesamum indicum L seed and oil in rats. *Indian J Exp Biol* 46:777–82.

Miranda, K.M., Espey, M.G., Wink, D.A. (2001) A rapid, simple spectrophotometric method for simultaneous detection of nitrate and nitrite. *Nitric Oxide - Biol Chem* 5:62–71.

Moalla Rekik, D., Ben Khedir, S., Ksouda Moalla, K., Kammoun, N. G., Rebai, T., & Sahnoun, Z. (2016) Evaluation of Wound Healing Properties of Grape Seed, Sesame, and Fenugreek Oils. *Evidence-based Complement Altern Med* 2016:1–12.

Mohamed, H. M. A., & Awatif I.I. (1998) The use of sesame oil unsaponifiable matter as a natural antioxidant. *Food Chem* 62:269–276.

Mohamed Saleem, T.S., Madhusudhana Chetty, C., Kavimani, S. (2012) Sesame oil enhances endogenous antioxidants in ischemic myocardium of rat. *Rev Bras Farmacogn* 22:669–675.

Moores, J. (2013) Vitamin C: a wound healing perspective. *Br J Community Nurs* Suppl:S6--S11.

Morris, J.B. (2002) Food, industrial, nutraceutical, and pharmaceutical uses of sesame genetic resources. In: Janick J, Whipkey A (eds) *Trends in new crops and new uses*. ASHS Press, Alexandria, VA, pp 153–156.

Özler, M., Şimşek, K., Topal, T., Öter, Ş., Korkmaz, A. (2010) Pinealektomili ratlarda yara iyileşmesi. *Gulhane Med J* 52:181–184.

Ramesh, B., Saravanan, R., Pugalendi, K.V. (2005) Influence of sesame oil on blood glucose, lipid peroxidation, and antioxidant status in streptozotocin diabetic rats. *J Med Food* 8:377–381.

Sankar, D., Rao, M.R., Sambandam, G., Pugalendi, K.V. (2006) Effect of sesame oil on diuretics or Beta-blockers in the modulation of blood pressure, anthropometry, lipid profile, and redox status. *Yale J Biol Med* 79:19–26.

Shenoy, R.R., Sudheendra, A.T., Nayak, P.G., Paul, P., Gopalan Kutty, N., Mallikarjuna Rao, C. (2011) Normal and delayed wound healing is improved by sesamol, an active constituent of Sesamum indicum (L.) in albino rats. *J Ethnopharmacol* 133:608–612.

Yimcharoen, M., Kittikunnathum, S., Suknikorn, C., Nak-On, W., Yeethong, P., Anthony, T.G., Bunpo, P. (2019) Effects of ascorbic acid supplementation on oxidative stress markers in healthy women following a single bout of exercise. *J Int Soc Sports Nutr* 16(1):2.

Yoshida, H., & Takagi, S. (1997) Effects of seed roasting temperature and time on the quality characteristics of sesame (Sesamum indicum) oil. *J Sci Food Agric* 75:19–26.

Yoshida, H., & Takagi, S. (1999) Antioxidative effects of sesamol and tocopherols at various concentrations in oils during microwave heating. *J Sci Food Agric* 79:220–226.

RNAI MANAGEMENT STRATEGIES OF FUNGAL DISEASES AND MYCOTOXIN CONTAMINATION IN PLANT

Fatma AYDINOGLU[1]

1 (Assoc. Prof. Dr.), Gebze Technical University, Molecular Biology and Genetics Department, Gebze/Kocaeli, Turkey, E-mail: faydinoglu@gtu.edu.tr, Orcid ID: 0000-0002-9974-045X

1.Introduction

Plant fungal disease and mycotoxins cause a reduction in yield and quality of crops in the field and post-harvest processes. Although symbiotic interaction between plants and fungi help colonize the land in past, today, pathogenic fungi are prominent biotic stress factors that limit plant productivity and becoming increasingly a more important aspect for human and animal health and the global economy. In the future, it is estimated that this interaction will be worst because of the threats to arable land accompanied by climate changes and population increase. In this context, unraveling the genetic regulation of the pathogenesis mechanism of fungi and the interaction between pathogens and their hosts will illuminate new insight to cope with plant fungal diseases and mycotoxins.

Many control strategies to prevent, delay or inhibit fungal development have been adopted to manage fungal diseases and mycotoxin production, including chemical control, genetic resistance, cultural practices, and irrigation management. Developing resistance varieties seems the most cost-effective strategy up to now. However, it keeps in some difficulties due to the slow and complex manner of disease resistance and mycotoxin accumulation as being inherited by many quantitative trait loci (QTLs) and influenced by environmental factors such as drought, temperature, and relative humidity. Chemical control with fungicides emerges as an alternative management strategy. The most used fungicides are demethylation inhibitors (DMI). These fungicides, such as the triazoles, act on fungi by targeting cytochrome P450 lanosterol C-14α-demethylase (CYP51), an enzyme operating in ergosterol biosynthesis, causing inhibition of fungal growth and virulence due to adversely affected cell membrane synthesis and permeability. However, this type of fungicides cannot achieve complete control due to mutations and paralogous *CYP51* gene in the genome of fungal pathogens. Another reason why fungicides do not provide full protection is the increasing resistance to fungicides of fungi. For example, a tebuconazole-resistant *F. graminearum* strain has been reported, representing the evolution of the fungal populations exposed to these fungicides (Spolti et al., 2014). Besides, there are also some growing concerns about fungicides due to their harmful impact on the environment, insects and animals, and humans because of food and feed contamination. Therefore, innovative, and sustainable management strategies must be employed to control disease and mycotoxin contamination.

To control disease and mycotoxins, it is essential to understand the lifestyles, cycles, and interactions of pathogenic fungi, their hosts, and the environment because they differ greatly among fungi genera. Fungi can be necrotrophic, biotrophic, obligately biotrophic, and hemibiotrophic. The most devastating plant pathogenic fungi can be listed as the following: *Puc-*

cinia spp., Fusarium oxysporum, Fusarium graminearum, Magnaporthe oryzae, Botrytis cinerea, Blumeria graminis, Mycosphaerella graminicola, Colletotrichum spp., Ustilago maydis, Melampsora lini, Rhizoctonia solani, and *Phakopsora pachyrhizi* (Dean et al., 2012). Some fungi growing on plants produce and accumulate mycotoxins. Mycotoxins are secondary metabolites produced by filamentous fungi. The 'mycotoxin' term is introduced due to its toxic or poison effects (Turner et al., 2009). Mycotoxins are not essential for fungal growth, but they gain extra advantages to the fungus such as inhibiting the growth of their competitors and regulating the ecology around itself (Calvo et al., 2002). The most mycotoxin-producing fungal genera are Aspergillus, Penicillium, Fusarium, Alternaria, and Claviceps, which mainly produced aflatoxin, ochratoxin, fumonisin, deoxynivalenol, and zearalenone. Mycotoxins cause cancer and birth defects in both humans and livestock. Therefore, arising concern about the mycotoxin contamination of foods and feeds directs the scientific effort to find innovative management and prevention solutions.

Although fungi have versatile lifestyles, the pathogenicity mechanism is conserved among plant fungal pathogens during infection processes. Pathogens share the conserved proteins during infection processes. Therefore, these proteins can be the potential targets for the biotechnological control strategies of pathogens. Recently, RNA interference (RNAi) has been employed to reduce the threat of pathogenic fungi by manipulating plant or fungal gene expression supplying a reduction in fungal growth, mating, conidiation, toxin biosynthesis, virulence, and mycotoxin production.

1.1. Major Plant Fungal Diseases and Pathogenesis

Fungal plant pathogens cause an enormous decrease in the quality and yield of plants and are a threat to the health of both animals and humans due to their mycotoxins. Therefore, understanding the biology of pathogenic fungus and unraveling pathogenesis will shed light on attempts to achieve management of diseases and mycotoxin production.

Plant fungal pathogens display a broad range of lifestyles while some are necrotrophic, others can be biotrophic, obligate biotrophic, or hemibiotrophic. *Botrytis cinerea* is a typical necrotrophic pathogen that induces host programmed cell death during infection processes (van Baarlen et al., 2007). It has a diverse host range, resulting in severe damage at both pre-and post-harvest stages. This fungus evades quite a lot of time before rotting and occurs from the seedling stage to ripening. The most effective control method is fungicide application, and also biocontrol agents can be applied in some crops. Its genome sequence is available, and it has a sufficient number of molecular tools. Therefore, RNAi represents a promising management strategy to control this pathogenic fungus.

Magnaporthe oryzae has arisen as a model fungus to establish a mechanism for host–fungal pathogen interactions because of its tendency to genetic manipulation (Dean et al., 2005). Therefore, RNAi is a promising control strategy of this fungus. It is a filamentous ascomycete fungus and the most destructive fungal pathogen of rice and wheat causing blast disease on foliar tissues. However, the symptoms occur on the head of wheat causing mistakenly with the wheat scab of *Fusarium graminearum*. It proliferates via conidia produced from lesions and dispersed and penetrates to a new host on which where they germinate in a few hours. Within 12 h, it forms 'appressorium' which is a highly melanized dome-shaped structure is required for infection. Tricyclazole fungicides were demonstrated as inhibitors of melanization of the appressorium that prevent penetration to the host. Following, turgor pressure of the appressorium increases within 24 h, which forces the formation of a penetration peg into the underlying tissues. The symptoms become visible at 7 days.

Puccinia spp. cause wheat rust diseases in three types; stripe (yellow) rust caused by *P. striiformisf. sp. tritici* (Pst), stem (black) rust caused by *Puccinia graminisf. sp. tritici* (Pgt), and leaf (brown) rust caused by *P. triticina* (Pt) (Duplessis et al., 2011). These diseases have historical importance and their pathogenic variability, all efficient dispersion, prolific sporulation, and extensive wheat cultivation have additive effects on the destructive feature of these fungi. There is a significant improvement in resolving of pathogenicity of Pgt at the molecular level. Pst, Pgt, and Pt display macrocyclic and heteroecious life cycles. They are obligate biotrophs within basidiomycete fungi (Leonard & Szabo, 2005; Bolton et al., 2008; Jin et al., 2010). They grow through plant cells via their 'haustoria' which are specific structures required for infection of obligate biotrophic pathogens. Haustoria facilitate nutrient uptake through the specialized feeding structures and efficiently represses the defense responses of the host (Micali et al., 2011; Voegele & Mendgen, 2011). The identified quantitative trait loci (QTL) coupled with genomics data and race analysis will enable the utilization of RNAi for sustainable management strategies for resistance to rust.

Fusarium graminearum (teleomorph *Gibberella zeae*) is an ascomycete fungus causing Fusarium head blight (FHB) disease on all cereal species. It co-founds with other Fusarium species (Magan et al., 2010; Machado et al., 2018). This disease occurs on floral tissues and deteriorate mainly the quality of the grain, rather than reducing the yield, and causes mycotoxin contamination in grain. The fungus infects wheat rachis tissue and produces deoxynivalenol (DON) mycotoxin which suppresses the plant defense. DON synthesis is tightly coordinated mainly by TRI6, TRI10, and TRI15 transcription factors. In addition, 160 virulence/pathogenicity factors, a

great number of which functions during the post-penetration process, are identified as responsible for floral infection of cereal (Urban & Hammond-Kosack, 2012). Due to the limitation of fungicide application timing on flowers, developing the resistance varieties to Fusarium are more efficient but requir identification of major QTLs. On the other hand, sufficient genomics resources are available for *F. graminearum*. Therefore, the RNAi technology will open a new way to control this fungus.

Fusarium oxysporum Schlecht. results in wilting of vascular tissue in a wide range of plants such as melon, tomato, cotton, banana, etc. It is a soil-borne and ubiquitous pathogen. The disease symptoms are seen as vascular browning, progressive wilting, defoliation, stunting, leaf epinasty, and plant death (Agrios, 2005). It is also an emerging human pathogen causing infections in immunocompromised patients (Nucci & Anaissie, 2007). Although it has a broad range of hosts, the disease only develops on a few plant species. It does not have a known sexual cycle. Many crops have been found to have plant *resistance* (*R*) genes to fight the diverse strains of *F. oxysporum* (Simons et al., 1998). To unravel the genetic basis of pathogenicity of fungus, the master regulators of pathogenic development, genome-wide insertional mutants, a novel mucin-type transmembrane sensor and a nitrogen response pathway functioning in invasive growth have been extensively studied (Michielse et al., 2009; Lopez-Berges et al., 2010; Perez-Nadales & Di Pietro, 2011). These studies illuminate the molecular mechanisms of fungal pathogenicity of *F. oxysporum* leading to new insights for the development of RNAi strategy to control the disease.

Blumeria graminisis is an ascomycete fungus within Erysiphales and causes powdery mildew on barley and wheat resulting in a reduction of grain yield (Takamatsu, 2004). The Erysiphales exhibit a versatile host range from broad in many fruits and vegetables to narrow in the case of *B. graminis* which infects only wheat and barley. All powdery mildews are strictly dependent on a live host plant due to being obligate biotrophic. *B. graminis* causes epidemy because of its rapid asexual cycles in which the conidia germinate within a few minutes and airborne conidia disperse on a host. Unlike other mildews, *B. graminis* initially forms a short primary germ tube functioning in surface sensing. Following a few hours, a secondary germ tube emerges from the conidium. Subsequently, it is differentiated to a septated, elongated, and hooked appressorium from which a peg penetrates through the host cuticle and epidermal cell wall. The peg develops into a complex haustorium which is surrounded by a specialized host membrane and a perihaustorial matrix (Hückelhoven & Panstruga, 2011). Like other obligate biotrophic, the haustorium facilitates feeding and regulates the immunity and metabolism of the host (Panstruga & Dodds, 2009). Within 3 days of infection, conidiophores produce a

large number of conidia which are ‘powder’ of these mildews. When the growth season of the host is completed, the compatible strains mate and produce ‘chasmothecia’ which is a resting structure at adverse conditions (Braun et al., 2002). Disease management is maintained by fungicides and developing disease-resistant plant varieties. Furthermore, two classes of effectors are currently recognized which are considered as targets to control pathogen by RNAi application. The first class is the ‘EKA’ effectors which are paralogous to the *Avrk1* and *Avra10* genes related to retrotransposons (Ridout et al., 2006; Sacristán et al., 2009). The second class is small, secreted proteins that are highly specific to lineage (Spanu et al., 2010).

Mycosphaerella graminicola (anamorph *Septoria tritici*) causes Septoria tritici blotch (STB) disease on wheat, especially in a temperate climate (Orton et al., 2011). This fungus is an ascomycete in the order Dothideales. Its hypha extends through the surface of the leaf and penetrates through stomata without an appressorium formation. It colonizes intercellularly for more than seven days without any symptoms and then switches to the necrotrophic stage in which the fungus produces asexual spores (Keon et al., 2007). Functional genomics analysis has illuminated several genes directing hyphal growth, stomatal penetration, cell wall-degrading, plant defense suppressor effector proteins during the infection process (Goodwin et al., 2011; Marshall et al., 2011).

Colletotrichum spp. belongs to Coelomycetes within the imperfect fungi. It represents the most common and important pathogenic fungi genera of the plant resulting in anthracnose spots and blights on above-ground parts of the plant (Sutto, 1992). The disease especially occurs as post-harvest rots due to latent infections, which are initiated before harvest and activated during storage. *Colletotrichum spp.* reproduced asexual conidia in ‘acervuli’. This genus serves as a model pathosystem to the establishment of systemic acquired/induced resistance (SAR) and the early studies on phytoalexins (Kuc, 1972; Durrant & Dong, 2004). It is unique with an intracellular hemibiotrophic lifestyle. The initial infection starts with a short biotrophic stage, identified with large intracellular primary hyphae (Takano et al., 2000). Subsequently, fungus switches to the necrotrophic stage which is more destructive. During this stage, narrower secondary hyphae grow through the tissue of the host.

Ustilago maydis is among the most devastating plant pathogenic fungi causing corn smut disease. The fungus is biotrophic and has a haploid genome. It divides by budding, mates, and becomes filamentous ‘dikaryon’. It serves as a model for research such as homologous recombination, motor-based microtubule organization, mitosis, and long-distance transport (Holliday, 2004). Within 5–6 days of infection, the symptoms can develop on all aerial parts of the plant. *Ustilago maydis* completes its

infection cycle in about 2 weeks. It does not have a known endogenous RNAi mechanism. But host-induced gene silencing can be preferred to the management of this disease.

Melampsora lini, causing flax rust, is an obligate biotroph. The fungus facilitated the establishment of a gene-for-gene relationship in which *avirulence* (*Avr*) genes of fungus were identified interacting with host *resistance* (*R*) genes (Lawrence et al., 2010). The flax rust system was also served the illumination of cytoplasmic nucleotide-binding leucine-rich repeat (NB-LRR) proteins, a new class of immune receptor, specific members of the host for resistance to several pathogenic organisms (Ellis et al., 2007). These studies further facilitated the improvement of an Agrobacterium transformation system for this pathogen.

Plants fight all the pathogens by the highly conserved molecular mechanisms which can be grouped into two. Firstly, pathogen-associated molecular patterns (PAMPs) are delivered to plants and perceived by plant microbial pattern recognition receptors (PRRs), triggering PAMP-triggered immunity (PTI) (Wang et al., 2017). Secondly, following PTI, plant defense against pathogens with R genes which are encode nuclear-binding leucine-rich repeat (NB-LRR)-type receptor-like proteins. Those proteins recognize pathogen effectors and induce effector-triggered immunity (ETI). During plant-pathogen interaction, dozens of pathogen effector proteins are secreted to repress PTI. To consult RNAi application to dispose of pathogens, to understand effector recognition and molecular regulation of plant immune systems and related pathways are crucial. Although secretion systems of bacterial pathogens for effector delivery, called the type-III and type-IV were revealed, the delivery of fungal effectors into the plant cells has recently been started to uncover. All this knowledge will make it possible for RNAi to be a beneficial application to control disease and mycotoxin.

1.2. Major Mycotoxins

Mycotoxins are secondary metabolites that are produced by many filamentous fungi belonging to Aspergillus, Fusarium, Penicillium, Alternaria, and Claviceps genera (Assefa & Geremew, 2018; Majeed et al., 2018). Mycotoxins are produced and accumulated in agricultural crops and cause contamination of feed and food resulting in harmful effects on both humans and animals consuming them (Jolly et al., 2011). Some mycotoxins cause phytotoxicity or have antimicrobial activity too. These low molecular weight metabolites (less than 1000 Da) are ubiquitous and practically inevitable. They are produced during pre-and-post harvest stages of plants, transportation, processing, and storage causing economic losses. Researchers have identified over 400 mycotoxins. Among them,

aflatoxin, ochratoxin A, fumonisins, zearalenone, trichothecenes including deoxynivalenol (DON), and T-2 toxin, and patulin are considered the most dangerous major mycotoxins (Wagacha & Muthomi, 2008). One type of mycotoxin can be produced by several fungal species. On the other hand, one fungal species may produce many different types of mycotoxins. Mycotoxin production is related to species of pathogenic fungus and its host plant, plant developmental stages, tissue and organs, environmental conditions, climate, pre-and-post harvest practices, storage, drying, and processing (Chilaka et al., 2016; Ogara et al., 2017).

Aflatoxins are polyketide-derived poisonous and carcinogenic mycotoxins produced by *Aspergillus flavus* and *A. parasiticus* (Khan et al., 2021; Jef et al., 2015). About 20 aflatoxin types are known, basically grouped into aflatoxin B1 (AFB1), B2, G1, G2, M1, and M2 according to their structure, fluorescent and chromatographic characteristics (Ephrem, 2015). They evade 25% of the food crops in the world mainly cereals, maize, rice, nuts, cassava, and spices. Drought and any other stress factors increase aflatoxin production in the plant, and they are very stable to food processes such as roasting, cooking, etc.

Ochratoxin A (OTA) is a phenylalanyl derivative produced by Aspergillus and Penicillium fungi. (el Khoury & Atoui, 2010). OTA is a mitochondrial poison resulting in cellular damage via oxidative burst, oxidative phosphorylation, and lipid peroxidation. It is heat stable and high temperatures (above 250°C) decrease its concentration.

Fumonisins are structurally similar metabolites to sphinganine produced by dominantly *Fusarium verticillioides* and *Fusarium proliferatum* and also by other fungal species such as *F. dlamini, F. nygamai* and *F. napiforme* (Aydinoglu, 2021). About 12 fumonisin types are identified. Among these, FB1, FB2, and FB3 are the most toxic. They occur mostly in maize prior to harvest or during the beginning of storage and do not increase anymore. They are heat stable.

Zearalenone (ZEA) is mainly produced by Fusarium species, especially *F. graminearum* and *F. semitectum*. It is structurally a macrocyclic β-resorcyclic acid lactone (Bhatnagar & Ehrlich, 2002). ZEA is mostly encountered in maize, barley, wheat, rye, and sorghum. Because it is structurally similar to estrogens, it causes estrogenic impact in animals and humans by binding to estrogen receptors (ERα and ERβ) (Kowalska et al., 2018). ZEA is stable during cooking but partially decays under high temperatures.

Trichothecenes (TCTC) are the most structurally diverse mycotoxins produced especially by Fusarium species and Cephalosporium, Dendrodochium, Cylindrocarpon, Trichoderma, Myrothecium, Trichothecium, and Stachybotrys genera. Deoxynivalenol (DON) is

the most common and well-studied among TCTC, but least toxic one. Meanwhile, TCTC producing *F. graminearum* and *F. culmorum* cause Fusarium Head Blight (FHB) which is among the most destructive disease of cereals. FHB causes big economic losses globally on wheat, rice, maize, rye, barley, and oats (Bottalico et al., 2002; Sobrova et al., 2010). TCTC can rapidly penetrate the cell membrane and pass through lipid bilayers to interact with RNA, DNA, and cellular organelles and inhibit the synthesis of protein (Rocha et al., 2005).

Patulin is a polyketide produced by Aspergillus, Penicillium, and Byssochlamys infecting fruits and vegetables. Initially, it was studied as a potential antibiotic, but later it was demonstrated as a carcinogenic agent (Baert et al., 2007; Barad et al., 2014; Zhong et al., 2018).

To the management of mycotoxin contamination, the best strategy is to prevent plant fungal infection by avoiding drought stress and insect damage, breeding resistant varieties, making crop rotation and harvesting after optimum maturity and supplying good storage conditions without humidity (Gabriel & Puleng, 2013). Physical control including hand sorting, washing, crushing and peeling off, gamma irradiation, cooking, and steaming are also used to control mycotoxins. The usage of chemical fungicides is another management strategy of mycotoxin contamination at pre-and-post harvest stages. Due to the hazards of chemicals to the environment, humans, and animals, biological control has been proposed as an alternative to chemical management strategies. In this context, microbial agents can be used to prevent mycotoxin production. Recent advances in genomics and marker development facilitate improving resistance plant varieties to the pathogenic fungi by identifying major QTLs related to pathogenicity. Furthermore, biotechnological approaches such as RNAi also open a way to reduce mycotoxin production by targeting the genes functioning in mycotoxin biosynthesis (Medina et al., 2017; Majumdar et al., 2017).

1.3. RNAi Mechanisms in Plants and Fungi

RNA interference (RNAi), or RNA-silencing, is a post-transcriptional gene silencing mechanism in which a double-stranded RNA (dsRNA) is cleaved into small RNA (sRNA) molecules that activate ribonucleases which direct to degradation of target mRNA via sequence-specific complementation (Agrawal et al., 2003). Plant and some fungal species have evolved endogenous RNAi mechanisms for protecting themselves against several parasitic bacterial or viral genomes (Li et al., 2010). RNAi phenomenon was proposed for the first time by Fire et al. (1998). They observed interference of the function of an endogenous gene following injection of dsRNA related to a 742-nucleotide segment of *unc22* into *Caenorhabditis elegans*. RNAi in *C. elegans* can be supplied easily by soaking the worms

in a dsRNAs-containing solution or by feeding the worms with dsRNAs expressing *Escherichia coli*. Recently, it became a useful tool not only for functional gene studies but also for many implementations in agricultural practice.

RNAi was observed in almost all eukaryotic organisms, including insects, flies, protozoa, nematodes, mouse and human cell lines. RNAi in all these organisms share mechanistic similarities but phenotypical differences with naming like 'PTGS' for plants, 'quelling' for fungi, and 'RNAi' for animals. The biogenesis and function of non-coding small RNAs (nc-sRNAs) called micro-RNAs (miRNAs) resemble extensively RNAi (Aydinoglu & Lucas, 2019; Aydinoglu et al., 2020). Eukaryotic cells have been identified to display another naturally occurring RNAi process called 'heterochromatinization'.

RNAi or PTGS in plants was firstly observed in 1990 during research on *chalcone synthase* (*chsA*)-overexpressed transgenic petunia flowers (Napoli et al., 1990). Subsequently, PTGS was reported by van der Krol et al. (1990) and Ingelbrecht et al. (1994) by cosuppression of introduced sense-oriented transgenes with homologous endogenous genes. It was also proved to initiate not only by sense-oriented sequences but also by antisense-oriented sequences (Di Serio et al., 2001).

Fungal RNAi or quelling was first observed in the saprotrophic species *Neurospora crassa* in a study to increase the production of an orange pigment by overexpressing *carotenogenic albino-3 (al-3)* and *albino-1 (al-1)* genes (Romano & Macino, 1992; Cogoni et al., 1996). The core RNAi machinery operating with RNA-dependent RNA-polymerases (RdRps), Dicers, and Argonautes are largely conserved among fungi species. However, some differences exist. For example, it was reported that additional genes and Dicer-independent pathways were identified in RNAi in *N. crassa* and several other fungi such as *Mucor circinelloides* (Billmyre et al., 2013). Furthermore, some components of, or the whole, RNAi machinery can be deficient in some fungal species including the budding yeast *Saccharomyces cerevisiae* and the corn smut fungus *Ustilago maydis* (Trieu et al., 2015).

RNAi-induced gene silencing is incorporated in several key components such as RNA-dependent RNA polymerase, Dicer, dsRNA endonucleases, and helicases. RNAi starts with cleavage of dsRNA molecules into 21 to 25 nucleotides long small interfering RNAs (siRNAs) by an RNase III-like endoribonuclease. Each strand of this siRNA has a 5′-phosphate and 3′-hydroxyl termini and 2- to 3-nucleotide 3′ overhangs. Subsequently, one strand of siRNA (the guide) is loaded to an RNase complex called RISC (RNA-induced silencing complex), whereas the other strand (the passenger) is degraded. RISC-loaded the antisense component of siRNA

is activated in the presence of ATP. siRNAs direct RISC to homologous target mRNA and lead to its degradation. RNase III family member of ds-RNA-specific nucleases was identified in Drosophila and was called Dicer (DCR) (Bernstein et al., 2001). Dicer has four distinct domains: dual RNase III motifs, a dsRNA binding domain, an amino-terminal helicase domain, and a PAZ domain (a 110-amino-acid domain present in proteins like Piwi, Argo, and Zwille/Pinhead), which is common in the proteins of RDE1/QDE2/Argonaute family. Because of this sequence-specific nuclease activity, it was called the RNA-induced silencing complex (RISC). The protein multicomponent of RNAi nucleases was characterized. One of them was identified as a member of the Argonaute family and was named Argonaute2 (AGO2). It is about 130 kDa and contains PAZ, PIWI domains, and polyglutamine residues, which are characteristic of the Argonaute family members. AGO2 is displayed homology to *C. elegans* RDE1 protein which is required for dsRNA-mediated gene silencing. RNA-dependent RNA polymerases (RdRPs) act as both trigger and booster the silencing effect. The RdRP enzymes can perceive these aberrant RNAs as templates and synthesize antisense RNAs. Meanwhile, siRNA is unwound by the activity of a helicase present in RISC. The antisense siRNAs in the activated RISC recognize the complementary cognate mRNAs. Finally, RISC cuts this cognate mRNA approximately in the middle of the duplex. An RNase protein called Argonaute forms the catalytic center of the RISC, leading to endonucleolytic cleavage of the mRNA.

1.4. Systemic or Cell-to-cell Transport of siRNAs and dsRNAs

The systemic or cell-to-cell transport of gene silencing has been initially observed in *C. elegans*. Winston et al. (2002) was engineered a transgenic strain of *C. elegans* (HC57) to illuminate the systemic spread of RNAi components from one tissue to another. Finally, they characterized a systemic *RNA interference-deficient* (*sid*) mutant. The SID1 is predicted as a 776-amino-acid membrane protein including a signal peptide and 11 putative transmembrane domains. Structural modeling of SID1 proposed its function as a channel protein or a receptor for the systemic RNAi signal via export or import or endocytosis.

The transport of the silencing signal from locally initiated place to other parts of the organisms through systemic or cell-to-cell spreading was also demonstrated in plants. The silencing signal in plants is proposed to be translocated by the phloem to long distances. This transportation of the RNAi signal is followed by flux from source to sink. Short and long-distance movement of silencing signal via cell-to-cell movement can follow a symplastic route through 'plasmodesmata', specialized channels between cells. RdRps are discovered as functioning in local and systemic gene silencing in *Arabidopsis thaliana*. It was demonstrated that the

necrotrophic ascomycete *Botrytis cinerea* is known to transfer small RNA 'effectors' into the cells of Arabidopsis and tomato plants (Cai et al., 2018a). For example, Weiberg et al. (2013) showed that fungal DICER-like (DCL)-dependent sRNAs secreted to the infected *A. thaliana*. These sRNAs are uptaken into plant cells and initiated the silencing of plant immune genes by interacting with plant AGO1 protein. Similarly, sRNA Bc-siR3.2 and Bc-siR37 were characterized as targeting mitogen-activated protein kinases, including MPK2 and MPK1 in Arabidopsis, and MAPKKK4 in tomato and several immune-related transcription factors including WRKY7, PMR6, and FEI2, respectively (Weiberg et al., 2013; Wang et al., 2017). Likewise, the oomycete *Hyaloperonospora arabidopsidis* produces 133 AGO1-bound sRNAs, which are crucial for virulence (Dunker et al., 2020). Furthermore, many sRNAs of wheat leaf rust fungus *Puccinia triticina* and wheat stripe rust fungus *Puccinia striiformis f. sp. tritici* were identified targeting wheat genes related to pathogen resistance, metabolism, biotic and abiotic stress, development, hormone signaling (Dubey et al., 2019; Mueth et al., 2015). microRNA-like RNA1 (Pst-milR1) from the yellow rust-causing biotrophic basidiomycete *Puccinia striiformis f.sp. tritici* (Pst) was revealed as a negative regulator of the Pathogenesis-related 2 (PR2) gene in wheat (Wang et al, 2017). Panwar et al. (2013) transformed wheat by BSMV-mediated HIGS targeting fungal genes *MAPK, CYC, and CNB* and observed translocation of siRNA molecules from host to fungus. These findings suggested that the local and systemic RNA silencing signal may transfer between fungus and plant cells, but RNAi pathways may consist of different components in different species. However, how both siRNAs and dsRNAs spread from local to the other parts of the organism still need to answer with further experiments.

1.5. RNA Communication Between Plant and Fungi Kingdoms and RNAi Implementations

RNAi signals (siRNA or dsRNA) can move between different organisms of the same or different species, and even across kingdoms in case of pathogenic or mutualistic interaction. The information is carried between organisms to determine the fate of the war between pathogen and host. RNAi signals are transported in exosomes (secreted vesicles) which was inferred because of their proliferation subsequent to pathogen attack and their abundance in extrahaustorial matrix where is the specialized pathogen-host interfaces (Rutter & Innes, 2017). Other siRNAs trafficking mechanisms have been hypothesized such as passive diffusion, membrane-associated transporters, and receptors. However, these mechanisms are not well-understood.

Based on this natural RNA fight between pathogen and host, a novel transgene-based plant-mediated approach called host-induced gene

silencing (HIGS) was improved to use siRNA that can target and silence the gene of fungal pathogens in the infection process (Cai et al., 2018b; Machado et al., 2018). Many studies were conducted to alleviate the disease and mycotoxin production in plants some of which have been transformed to field (Table 1). HIGS was initially found in 2010 in a maize pathogenic fungus *F. verticillioides* transgenic strain as a result of observation of the silencing of a β-glucuronidase (*GUS*) reporter gene during infection of transgenic tobacco plants expressing a hairpin GUS RNA (Tinoco et al., 2010). Afterward, transgenic wheat and barley were engineered to express dsRNA targeting the virulence factor Avra10 transcripts in the plant fungal pathogen *Blumeria graminis*, which resulted in a reduction in powdery mildew infection (Nowara et al., 2010). RNAi can be the opposite direction where pathogen-induced gene silencing targets host plant genes. For example, a necrotrophic plant pathogen *Botrytis cinerea* transfers small RNA 'effectors' into the cells of Arabidopsis and tomato (Weiberg et al., 2013). The fungus uses the plant RNAi machinery to produce sRNAs that can enter the plant cell.

An alternative approach to HIGS, spray-induced gene silencing (SIGS) was offered. SIGS supply exogenous application of long dsRNA and siRNAs, which utilizes the RNAi mechanism. Because SIGS offers a non-transgenic RNAi approach, it is more manageable compared to HIGS which is required stable transformation of plants. SIGS have been attempted to control *B. cinerea* and *F. graminearum* and obtained effective results (Koch et al., 2016; Wang et al., 2016). These studies demonstrate the potential applicability of SIGS methods and shed light on efforts for transformation from laboratory to field in the future (Table 1).

HIGS and SIGS present powerful applications to manage disease and mycotoxin production. They prevent off-target organisms which supply specific control of a single pathogen and offer environmentally friendly applications. Likewise, SIGS eliminates the production of transgenic plants which are concerned in public. Besides, because transgenic plants expressing dsRNA would not produce heterologous proteins, HIGS cause fewer concerns about allergies. Along with these advantages, there are some technical issues that must be overcome to use SIGS in field as an efficient management strategy. The first issue is application timing because SIGS application has a short life in the field lasting in a few days. To improve the SIGS effect on plants, dsRNA was offered to load into protective or gradually releasing nanoparticles. For example, it was demonstrated that dsRNA loaded into the double-layered hydroxide clay nanosheets has remained for up to 30 days on leaves after spray application (Mitter et al., 2017). The second issue is that SIGS is more expensive compared to chemical fungicides due to the high cost of RNA synthesis. This issue

can be overcome with the cost-efficient mass production of RNA for topical RNAi applications in agriculture. Another important issue is to develop a single application method to control multiple pathogens in a broad spectrum. It can be achieved to design a dsRNA targeting the same gene in different fungal species with the highest homology. For effective application of HIGS or SIGS in field, environmental conditions, soil type, irrigation regimes, and overall growing conditions through the season must be taken seriously.

Recently, the existence of siRNA or dsRNA in food is another public concern because of the probability of their effect on the gene expression of humans and animals. It was reported that the ingested plant siRNAs could not be found in the gut of mammals (Witwer et al., 2014). However, for sufficient gene silencing, the ingested siRNAs or dsRNA must be remaining intact and in a sufficient amount to promote RNAi machinery, require to be delivered to a target cell, and display sequence complementation to target mRNA transcript into the cell. Actually, plants naturally produce siRNAs, miRNAs, and dsRNAs through their developmental stages to coordinate their own gene expression. Therefore, exogenous siRNAs and dsRNAs produced by various plants have been ingested for years.

2. Conclusion

RNAi strategy has emerged as a promising alternative to fungicides and conventional management strategies of disease and mycotoxins. It allows effective control of the pathogen in a species-specific manner. It also presents an alternative control solution where the pathogenic species regularly became resistant. The recent advance in genomics and other omics technologies shed light on genetic mechanisms of pathogenesis which allow the improvement of RNAi technologies. In this context, HIGS and SIGS are effective on destructive fungal pathogens that became resistant to fungicides. Additionally, the deeper unraveling of the molecular mechanism of interaction between plants and fungal pathogens and mycotoxin production further will lead to the development of the most effective and environmentally friendly, sustainable agricultural implementations for their management of them.

Acknowledgment

This study was supported by The Scientific and Technological Research Council of Turkey (TUBITAK) with grant number 221O321.

Table 1. *RNAi Studies to Control Fungal Pathogen Growth and Mycotoxin Production in Plant.*

Pathogen/ Host	Disease/ Mycotoxin	Target gene/ function	Results	Method	References
Aspergillus flavus/ Peanut, maize	Aflatoxin	Fungal afl, aflR, aflC/aflotoxin biosythesis transcription factor/ Polyketide synthase;Fungal AILP/α-amylase inhibitor-like protein	Reduced aflatoxin, decreases fungal growth	HIGS-dsRNAs	Arias et al., 2015; Sobolev et al., 2019; Power et al., 2020; Masanga et al., 2015; Rajasekaran vd., 2019; Gilbert et al., 2018
Magnaporthe oryzae/rice	Fungal blast	Funggal DES1/ host-defense suppressor pathogenicity	Alteration on fungal growth, conidiation, ROS-scavenging ability, and pathogenic	SIGS-dsRNAs	Sarkar & Roy-Barman, 2021
Puccinia triticina/wheat	Wheat leaf rust	Fungal MAPK1/ phosphorylation of transcription factors, CYC1/ folding catalysts and chaperones, CNB/ relaying calcium signals	suppressed disease phenotype, reduction of the expression target fungal gene	VIGS-HIGS-dsRNA	Panvar et al., 2013
Fusarium graminearum/ Arabidopsis, barley	Fusarium head blight (FHB)	fungal CYP51/ biosynthesis of fungal ergosterol	Fungal growth inhibition and altered morphology, reduced infection	HIGS /SIGS-dsRNA	Koch et al., 2013
Fusarium graminearumm /Barley	Fusarium head blight (FHB) and Fusarium seedling blight (FSB)	CYP3- biosynthesis of fungal ergosterol	Inhibition of fungal growth	SIGS-dsRNA	Koch et al., 2016/2019; Höfle et al., 2020
Fusarium graminearum/Barley, *Brachypodium distachyon*	Fusarium head blight and crown rot/DON, nivalenol (NIV)	fungal dcl1/2	Reduced virulence	Double knock-out in fungus	Werner et al., 2021
Fusarium graminearum/ Wheat, barley	Fusarium head blight/ deoxynivale-nol (DON)	Fungal TRI6/, a transcription factor in DON synthesis	Deduced virulence and mycotoxin	dsRNA	Baldwin et al., 2018; Hao et al., 2021
Fusarium oxysporum f. sp. lycopersici (Fol) /Tomato	Fusarium wilt	Fungal peroxisomal biogenesis factor and β-1,3-glucanosyltransfer-ase	Enhanced resistance and delayed disease symptoms	HIGS-dsRNAs	Tetorya & Rajam, 2021
Blumeria graminis/ Barley, wheat	powdery mildew	Avra10 of fungus/ virulence factor	Reduced infection		Nowara et al, 2010
Botrytis cinerea /Arabidopsis, tomato	Grey mold	fungal DCL1 and DCL2	Inhibition fungal pathogenicity and growth	HIGS-sRNAs	Wang et al., 2016
Botrytis cinerea		Fungal KMO/ kynurenine 3-monooxygenase	Slower growth, no conidia but enhanced pathogenicity	dsRNA	Zhang et al., 2018
Slafroctonia leguminicola / legumes	Blackpatch/ slaframine and swainsonine	Fungal pks1/polyketide synthase gene	Reduced mycotoxin	dsRNA	Alhawatema et al., 2017
Arabidopsis thaliana	Fumonisin B_1	ORM1;2/orosomucoid-like proteins	Plant increase sensitivity to mycotoxin	dsRNA	Kimberlin et al., 2016
Setosphaeria turcica/maize	Northern Corn Leaf Blight	Fungal PBS2/Mitogen-activated protein kinase kinase (MAPKK)	Reduced conidia	dsRNA	Gong et al., 2017

References

Agrawal, N., Dasaradhi, P. V., Mohmmed, A., Malhotra, P., Bhatnagar, R. K., & Mukherjee, S. K. (2003). RNA interference: biology, mechanism, and applications. *Microbiology and molecular biology reviews: MMBR*, *67*(4), 657–685.

Agrios, G.N. (2005). Plant Pathology. Academic Press, St. Louis,

Alhawatema, M. S., Gebril, S., Cook, D., & Creamer, R. (2017). RNAi-mediated down-regulation of a melanin polyketide synthase (pks1) gene in the fungus *Slafractonia leguminicola*. *World journal of microbiology & biotechnology*, *33*(10), 179.

Arias, R. S., Dang, P. M., & Sobolev, V. S. (2015). RNAi-mediated Control of Aflatoxins in Peanut: Method to Analyze Mycotoxin Production and Transgene Expression in the Peanut/Aspergillus Pathosystem. *Journal of visualized experiments: JoVE*, (106), e53398.

Assefa, T., & Geremew, T. (2018). Major mycotoxins occurrence, prevention and control approaches. *Biotechnology and Molecular Biology Reviews 12(1):1-11*

Aydinoglu, F., & Lucas, S. J. (2019). Identification and expression profiles of putative leaf growth related microRNAs in maize (Zea mays L.) hybrid ADA313. *Gene*, *690*, 57–67.

Aydinoglu F. (2020). Elucidating the regulatory roles of microRNAs in maize (*Zea mays* L.) leaf growth response to chilling stress. *Planta*, *251*(2), 38.

Aydinoglu, F. (2021). Fumonisin mycotoxins: metabolism, toxicity, detection and prevention, in Mathematics and Natural Sciences, Livre de Lyon.

Baert, K., Devlieghere, F., Flyps, H., Oosterlinck, M., Ahmed, M. M., Rajković, A., Verlinden, B., Nicolaï, B., Debevere, J., & De Meulenaer, B. (2007). Influence of storage conditions of apples on growth and patulin production by *Penicillium expansum*. *International journal of food microbiology*, 119(3), 170–181.

Baldwin, T., Islamovic, E., Klos, K., Schwartz, P., Gillespie, J., Hunter, S., & Bregitzer, P. (2018). Silencing efficiency of dsRNA fragments targeting *Fusarium graminearum* TRI6 and patterns of small interfering RNA associated with reduced virulence and mycotoxin production. *PloS one*, *13*(8), e0202798. Barad, S., Horowitz, S. B., Kobiler, I., Sherman, A., & Prusky, D. (2014). Accumulation of the mycotoxin patulin in the presence of gluconic acid contributes to pathogenicity of *Penicillium expansum*. *Molecular plant-microbe interactions: MPMI*, *27*(1), 66–77.

Bernstein, E., Caudy, A.A., Hammond, S.M., & Hannon, G.J. (2001). Role for a bidentate ribonuclease in the initiation step of RNA interference. *Nature*. 409(6818):363-6.

Bhatnagar, D., Yu, J., & Ehrlich, K.C. (2002). Toxins of filamentous fungi. *Chem. Immunol.*, 81, 167–206.

Billmyre, R.B., Calo, S., Feretzaki, M., Wang, X.Y., & Heitman, J. (2013). RNAi function, diversity, and loss in the fungal kingdom. *Chromosome Res.,* 21:561–572.

Bolton, M.D., Kolmer, J.A. & Garvin, D.F. (2008). Wheat leaf rust caused by *Puccinia triticina*. *Mol. Plant Pathol.,* 9, 563–575.

Bottalico, A., & Perrone, G. (2002). Toxigenic Fusarium species and mycotoxins associated with head blight in small-grain cereals in Europe. *Eur. J. Plant Pathol.*, 108, 611–624.

Braun, U., Cook, R.T.A., Inman, A.J., & Shin, H.-D. (2002). The taxonomy of the powdery mildew fungi. The Powdery Mildews: A Comprehensive Treatise, APS Press.

Cai, Q., Qiao, L., Wang, M., He, B., Lin, F. M., Palmquist, J., Huang, S. D., & Jin, H. (2018a). Plants send small RNAs in extracellular vesicles to fungal pathogen to silence virulence genes. *Science*, *360*(6393), 1126–1129.

Cai Q., He B., Kogel K. H., & Jin H. (2018b). Cross-kingdom RNA trafficking and environmental RNAi—nature's blueprint for modern crop protection strategies. *Current opinion in microbiology*, 46, 58–64.

Calvo, A. M., Wilson, R. A., Bok, J. W., & Keller, N. P. (2002). Relationship between secondary metabolism and fungal development. *Microbiology and molecular biology reviews: MMBR*, 66(3), 447–459.

Chilaka, C.A., De Boevre, M., Atanda, O., & De Saeger, S. (2016). Occurrence of Fusarium mycotoxins in cereal crops and processed products (ogi) from Nigeria. Toxins 8:342.

Cogoni, C., Irelan, J.T., Schumacher, M., Schmidhauser, T.J., Selker, E.U., & Macino, G. (1996). Transgene silencing of the al-1 gene in vegetative cells of Neurospora is mediated by a cytoplasmic effector and does not depend on DNA-DNA interactions or DNA methylation. *EMBO J., 15*(12):3153-63.

Dean, R., Van Kan, J. A., Pretorius, Z. A., Hammond-Kosack, K. E., Di Pietro, A., Spanu, P. D., Rudd, J. J., Dickman, M., Kahmann, R., Ellis, J., & Foster, G. D. (2012). The Top 10 fungal pathogens in molecular plant pathology. *Molecular plant pathology*, *13*(4), 414–430.

Dean, R.A., Talbot, N.J., Ebbole, D.J., Farman, M.L., Mitchell, T.K., Orbach, M.J., Thon, M., Kulkarni, R., Xu, J.-R., Pan, H., Read, N.D., Lee, Y.-H., Carbone, I., Brown, D., Oh, Y.Y., Donofrio, N., Jeong, J.S., Soanes, D.M., Djonovic, S., Kolomiets, E., Rehmeyer, C., Li, W., Harding, M., Kim, S., Lebrun, M.-H., Bohnert, H., Coughlan, S., Butler, J., Calvo, S., Li-Jun Ma, L.-J., Nicol, R., Purcell, S., Nusbaum, C., Galagan, J.E. & Birren, B.W. (2005). The genome sequence of the rice blast fungus Magnaporthe grisea. Nature, 434, 980–986.

Di Serio, F., Schob, H., Iglesias, A., Tarina, C., Bouldoires, E., & Meins, F.Jr. (2001). Sense- and antisense-mediated gene silencing in tobacco is inhibited by the same viral suppressors and is associated with accumulation of small RNAs. *Proc Natl Acad Sci, 98*(11):6506-10.

Dubey, H., Kiran, K., Jaswal, R., Jain, P., Kayastha, A. M., Bhardwaj, S. C., Mondal, T. K., & Sharma, T. R. (2019). Discovery and profiling of small RNAs from *Puccinia triticina* by deep sequencing and identification of their potential targets in wheat. *Functional & integrative genomics*, *19*(3), 391–407.

Dunker, F., Trutzenberg, A., Rothenpieler, J.S., Kuhn, S., Pröls, R., Schreiber, T., ... (2020). Oomycete small RNAs bind to the plant RNA-induced silencing complex for virulence. *Elife*, 9, e56096.

Duplessis, S., Cuomo, C.A., Lin, Y.-C., Aerts, A., Tisserant, E., Veneault-Fourrey, C., … (2011). Obligate biotrophy features unraveled by the genomic analysis of rust fungi. *Proc. Natl. Acad. Sci.*, 108, 9166–9171.

Durrant, W.E. & Dong, X. (2004) Systemic acquired resistance. *Annu. Rev. Phytopathol*. 42, 185–209.

el Khoury, A., & Atoui, A. (2010). Ochratoxin a: general overview and actual molecular status. *Toxins*, *2*(4), 461–493.

Ellis, J.G., Dodds, P.N. & Lawrence, G.J. (2007). Flax rust resistance gene specificity is based on direct resistance–avirulence protein interaction. *Annu. Rev. Phytopathol*. 45, 12.1–12.18.

Ephrem, G. (2015). Aflatoxin Contamination in Groundnut (*Arachis hypogaea* L.) caused by Aspergillus Species in Ethiopia. *Journal of Applied & Environmental Microbiology*, *3*(1):11-19.

Fire, A., Xu, S., Montgomery, M.K., Kostas, S.A., Driver, S.E., & Mello, C.C. (1998). Potent and specific genetic interference by double-stranded RNA in *Caenorhabditis elegans*. *Nature. 391*(6669):806-11.

Gabriel, O.A., & Puleng, L. (2013). Strategies for the Prevention and Reduction of Mycotoxins in Developing Countries. Mycotoxin and Food Safety in Developing Countries. http://dx.doi.org/10.5772/52542.

Gilbert, M. K., Majumdar, R., Rajasekaran, K., Chen, Z. Y., Wei, Q., Sickler, C. M., Lebar, M. D., Cary, J. W., Frame, B. R., & Wang, K. (2018). RNA interference-based silencing of the alpha-amylase (amy1) gene in *Aspergillus flavus* decreases fungal growth and aflatoxin production in maize kernels. *Planta*, *247*(6), 1465–1473.

Gong, X. D., Feng, S. Z., Zhao, J., Tang, C., Tian, L., Fan, Y. S., Cao, Z. Y., Hao, Z. M., Jia, H., Zang, J. P., Zhang, Y. F., Han, J. M., Gu, S. Q., & Dong, J. G. (2017). *StPBS2*, a MAPK kinase gene, is involved in determining hyphal morphology, cell wall development, hypertonic stress reaction as well as the production of secondary metabolites in Northern Corn Leaf Blight pathogen Setosphaeria turcica. *Microbiological research*, *201*, 30–38.

Goodwin, S.B., Ben M'Barek, S., Dhillon, B., Wittenberg, A.H.J., Crane, C.F., Hane, J.K., ... (2011). Finished genome of the fungal wheat pathogen *Mycosphaerella graminicola* reveals dispensome structure, chromosome plasticity, and stealth pathogenesis. *PLoS Genet.,* 7, e1002070.

Hao, G., McCormick, S., & Vaughan, M. M. (2021). Effects of Double-Stranded RNAs Targeting *Fusarium graminearum TRI6* on Fusarium Head Blight and Mycotoxins. *Phytopathology*, *111*(11), 2080–2087.

Höfle, L., Biedenkopf, D., Werner, B. T., Shrestha, A., Jelonek, L., & Koch, A. (2020). Study on the efficiency of dsRNAs with increasing length in RNA-based silencing of the Fusarium *CYP51* genes. *RNA biology*, *17*(4), 463–473.

Holliday, R. (2004) Early studies on recombination and DNA repair in Ustilago maydis. *DNA Repair*, 3, 671–682.

Hückelhoven, R. & Panstruga, R. (2011). Cell biology of the plant–powdery mildew interaction. *Curr. Opin. Plant Biol.* 14, 738–746.

Ingelbrecht, I., Van Houdt, H., Van Montagu, M., & Depicker, A. (1994). Posttranscriptional silencing of reporter transgenes in tobacco correlates with DNA methylation. *Proc Natl Acad Sci., 91*(22):10502-6.

Jef, L., Jia-Sheng, W., & Kelly, J. (2015). Serum aflatoxin B1-lysine adduct level in adult women from Eastern Province in Kenya depends on household socio-economic status: A cross sectional study. *Social Science and Medicine Journal,* 146:104-110.

Jin, Y., Szabo, L. & Carson, M. (2010). Century-old mystery of *Puccinia striiformis* life history solved with the identification of *Berberis spp.* as an alternate host. *Phytopathology*, 100, 432–435.

Jolly, P.E., Shuaib, F.M., Jiang, Y., Preko, P., Baidoo, J., Stiles, J.K., Wang, J.S., Phillips, T.D., & Williams, J.H. (2011). Association of high viral load and abnormal liver function with high aflatoxin B-1-albumin adducts levels in HIV-positive Ghanaians: preliminary observations. *Food Additives and Contaminants Part A*, 28:1224-1234.

Keon, J., Antoniw, J., Carzaniga, R., Deller, S., Ward, J.L., Baker, J.M., Beale, M.H., Hammond-Kosack, K. & Rudd, J.J. (2007). Transcriptional adaptation of *Mycosphaerella graminicola* to programmed cell death of its susceptible wheat host. Mol. *Plant–Microbe Interact.* 20, 178–193.

Khan, R., Ghazali, F. M., Mahyudin, N. A., & Samsudin, N. (2021). Aflatoxin Biosynthesis, Genetic Regulation, Toxicity, and Control Strategies: A Review. *Journal of fungi (Basel, Switzerland)*, *7*(8), 606.

Kimberlin, A. N., Han, G., Luttgeharm, K. D., Chen, M., Cahoon, R. E., Stone, J. M., Markham, J. E., Dunn, T. M., & Cahoon, E. B. (2016). ORM Expression Alters Sphingolipid Homeostasis and Differentially Affects Ceramide Synthase Activity. *Plant physiology*, *172*(2), 889–900.

Koch, A., Biedenkopf, D., Furch, A., Weber, L., Rossbach, O., Abdellatef, E., Linicus, L., Johannsmeier, J., Jelonek, L., Goesmann, A., Cardoza, V., McMillan, J., Mentzel, T., & Kogel, K. H. (2016). An RNAi-Based Control of Fusarium graminearum Infections Through Spraying of Long dsRNAs Involves a Plant Passage and Is Controlled by the Fungal Silencing Machinery. *PLoS pathogens*, *12*(10), e1005901.

Koch, A., Kumar, N., Weber, L., Keller, H., Imani, J., & Kogel, K. H. (2013). Host-induced gene silencing of cytochrome P450 lanosterol C14α-demethylase-encoding genes confers strong resistance to Fusarium species. *Proceedings of the National Academy of Sciences of the United States of America*, *110*(48), 19324–19329.

Kowalska, K., Habrowska-Górczyńska, D. E., Urbanek, K. A., Domińska, K., & Piastowska-Ciesielska, A. W. (2018). Estrogen Receptor α Is Crucial in Zearalenone-Induced Invasion and Migration of Prostate Cancer Cells. *Toxins*, 10(3), 98.

Kuc, J. (1972). Phytoalexins. *Annu. Rev. Phytopathol*. 10, 207–232.

Lawrence, G.J., Dodds, P.N. & Ellis, J.G. (2010). Transformation of the flax rust fungus, *Melampsora lini*: selection via silencing of an avirulence gene. *Plant J.,* 61, 364–369.

Leonard, K.J. & Szabo, L.S. (2005). Stem rust of small grains and grasses caused by *Puccinia graminis*. *Mol. Plant Pathol*. 6, 99–111.

Li, L.D., Chang, S.S. & Liu, Y. (2010). RNA interference pathways in filamentous fungi. *Cell Mol Life Sci*, 67:3849–3863.

Lopez-Berges, M.S., Rispail, N., Prados-Rosales, R.C. & Di Pietro, A. (2010). A nitrogen response pathway regulates virulence functions in Fusarium oxysporum via the protein kinase TOR and the bZIP protein MeaB. *Plant Cell*, 22, 2459– 2475.

Machado, A. K., Brown, N. A., Urban, M., Kanyuka, K., & Hammond-Kosack, K. E. (2018). RNAi as an emerging approach to control Fusarium head blight disease and mycotoxin contamination in cereals. *Pest management science*, *74*(4), 790–799.

Magan, N., Aldred, D., Mylona, K. & Lambert, R.J.W. (2010). Limiting mycotoxins in stored wheat. *Food Addit. Contam. A,* 27, 644–650.

Majeed, S., De Boevre, M., De Saeger, S., RaufWaqa, R., Tawab, A., Habib, F., Rahman, M., & Iqbal, M. (2018). Multiple Mycotoxins in Rice; Occurrence and Health Risk Assessment in Children and Adults of Punjab, Pakistan. *Toxins,* 10:77-107.

Majumdar, R., Rajasekaran, K., & Cary, J. W. (2017). RNA Interference (RNAi) as a Potential Tool for Control of Mycotoxin Contamination in Crop Plants: Concepts and Considerations. *Frontiers in plant science*, *8*, 200.

Marshall, R., Kombrink, A., Motteram, J., Loza-Reyes, E., Lucas, J., Hammond-Kosack, K.E., Thomma, B.P.H.J. & Rudd, J.J. (2011). Analysis of two in planta expressed LysM effector homologs from the fungus *Mycosphaerella graminicola* reveals novel functional properties and varying contributions to virulence on wheat. *Plant Physiol.*, 156, 756–769.

Masanga, J.O., Matheka, J.M., Omer, R.A., Ommeh, S.C., Monda, E.O. & Alakonya, A.E. (2015). Downregulation of transcription factor aflR in *Aspergillus flavus* confers reduction to aflatoxin accumulation in transgenic maize with alteration of host plant architecture. *Plant Cell Rep,* 34:1379–1387.

Medina, A., Sejakhosi, M., Nik, I., Putra, S., Alicia, R-S, Alicia, R., & Naresh, M. (2017). Biocontrol of mycotoxins: dynamics and mechanisms of action. *Current Opinion in Food Science,* 17:41-48.

Micali, C.O., Neumann, U., Grunewald, D., Panstruga, R. & O'Connell, R. (2011). Biogenesis of a specialized plant–fungal interface during host cell internalization of *Golovinomyces orontii* haustoria. *Cell Microbiol*, 13:210–226.

Michielse, C.B., van Wijk, R., Reijnen, L., Cornelissen, B.J. & Rep, M. (2009). Insight into the molecular requirements for pathogenicity of *Fusarium oxysporum f. sp. lycopersici* through large-scale insertional mutagenesis. *Gen. Biol.,* 10, R4.

Mitter, N., Worrall, E. A., Robinson, K. E., Li, P., Jain, R. G., Taochy, C., Fletcher, S. J., Carroll, B. J., Lu, G. Q., & Xu, Z. P. (2017). Clay nanosheets for topical delivery of RNAi for sustained protection against plant viruses. *Nature plants*, *3*, 16207.

Mueth, N. A., Ramachandran, S. R., & Hulbert, S. H. (2015). Small RNAs from the wheat stripe rust fungus (Puccinia striiformis f.sp. tritici). *BMC genomics*, *16*(1), 718.

Napoli, C., Lemieux, C. & Jorgensen, R. (1990). Introduction of chimeric chalcone synthase gene into *Petunia* results in reversible cosuppression of homologous genes in trans. Plant Cell 2**:**279-289.

Nowara, D., Gay, A., Lacomme, C., Shaw, J., Ridout, C., Douchkov, D., Hensel, G., Kumlehn, J., & Schweizer, P. (2010). HIGS: host-induced gene silencing in the obligate biotrophic fungal pathogen Blumeria graminis. *The Plant cell*, *22*(9), 3130–3141.

Nucci, M., & Anaissie, E. (2007). Fusarium infections in immunocompromised patients. *Clin. Microbiol. Rev.*, 20, 695–704.

Ogara, I.M., Zarafi, A.B., Alabi, O., Banwo, O., Ezekiel, C.N., Warth, B., Sulyok, M., & Krska, R. (2017). Mycotoxin patterns in ear rot-infected maize: a comprehensive case study in Nigeria. *Food Control,* 73:1159-1168.

Orton, E.S., Deller, S., & Brown, J.K.M. (2011). *Mycosphaerella graminicola*: from genomics to disease control. *Mol. Plant Pathol.,* 12, 413–424.

Panstruga, R. & Dodds, P.N. (2009). Terrific protein traffic: the mystery of effector protein delivery by filamentous plant pathogens. *Science*, 324, 748–750.

Panwar, V., McCallum, B., & Bakkeren, G. (2013). Host-induced gene silencing of wheat leaf rust fungus *Puccinia triticina* pathogenicity genes mediated by the Barley stripe mosaic virus. *Plant Mol Biol*. 81(6):595-608.

Perez-Nadales, E. & Di Pietro, A. (2011). The membrane mucin Msb2 regulates invasive growth and plant infection in *Fusarium oxysporum*. *Plant Cell,* 23, 1171– 1185.

Power, I. L., Faustinelli, P. C., Orner, V. A., Sobolev, V. S., & Arias, R. S. (2020). Analysis of small RNA populations generated in peanut leaves after exogenous application of dsRNA and dsDNA targeting aflatoxin synthesis genes. *Scientific reports*, *10*(1), 13820.

Rajasekaran, K., Sayler, R. J., Majumdar, R., Sickler, C. M., & Cary, J. W. (2019). Inhibition of Aspergillus flavus Growth and Aflatoxin Production in Transgenic Maize Expressing the α-amylase Inhibitor from Lablab purpureus L. *Journal of visualized experiments: JoVE*, (144), 10.3791/59169.

Ridout, C.J., Skamnioti, P., Porritt, O., Sacristan, S., Jones, J.D.G. & Brown, J.K.M. (2006). Multiple avirulence paralogues in cereal powdery mildew fungi may contribute to parasite fitness and defeat of plant resistance. *Plant Cell*, 18, 2402– 2414.

Rocha, O., Ansari, K., & Doohan, F. M. (2005). Effects of trichothecene mycotoxins on eukaryotic cells: a review. Food additives and contaminants, 22(4), 369–378.

Romano, N. & Macino G. (1992). Quelling - Transient inactivation of gene-expression in *Neurospora crassa* by transformation with homologous sequences. *Mol Microbiol*, 6:3343–3353.

Rutter, B.D. & Innes, R.W. (2017). Extracellular vesicles isolated from the leaf apoplast carry stress-response proteins. *Plant Physiol*, 173:728–741.

Sacristán, S., Vigouroux, M., Pedersen, C., Skamnioti, P., Thordal-Christensen, H., Micali, C., Brown, J.K.M. & Ridout, C.J. (2009). Coevolution between a family of parasite virulence effectors and a class of LINE-1 retrotransposons. *PLoS ONE*, 4, e7463.

Sarkar, A., & Roy-Barman, S. (2021). Spray-Induced Silencing of Pathogenicity Gene *MoDES1 via* Exogenous Double-Stranded RNA Can Confer Partial Resistance Against Fungal Blast in Rice. *Frontiers in plant science*, *12*, 733129.

Simons, G., Groenendijk, J., Wijbrandi, J., Reijans, M.G.J., Diergaarde, P., Van Der Lee, T., Bleeker, M., Onstenk, J., De Both, M., Haring, M.A., Mes, J.J., Cornelissen, B.J.C., Zabeau, M. & Vos, P. (1998). Dissection of the Fusarium I2 gene cluster in tomato reveals six homologs and one active gene copy. *Plant Cell,* 10, 1055–1068.

Sobolev, V., Walk, T., Arias, R., Massa, A., & Lamb, M. (2019). Inhibition of Aflatoxin Formation in Aspergillus Species by Peanut (*Arachis hypogaea*) Seed Stilbenoids in the Course of Peanut-Fungus Interaction. *Journal of agricultural and food chemistry*, *67*(22), 6212–6221.

Sobrova, P., Adam, V., Vasatkova, A., Beklova, M., Zeman, L., & Kizek, R. (2010). Deoxynivalenol and its toxicity. *Interdiscip. Toxicol.*, 3, 94–99.

Spanu, P.D., Abbott, J.C., Amselem, J., Burgis, T.A., Soanes, D.M., Stuber, K., ... (2010). Genome expansion and gene loss in powdery mildew fungi reveal tradeoffs in extreme parasitism. *Science,* 330, 1543–1546.

Spolti, P., Del Ponte, E.M., Dong, Y.H., Cummings, J.A. & Bergstrom, G.C. (2014). Triazole sensitivity in a contemporary population of *Fusarium graminearum* from New York wheat and competitiveness of a tebuconazole-resistant isolate. *Plant Dis*, 98:607–613.

Sutton, B.C. (1992). The genus Glomerella and its anamorph Colletotrichum. Colletotrichum: Biology, Pathology, and Control (Bailey, J.A. and Jeger, M.J., eds), 1–26. Wallingford: CAB International.

Takamatsu, S. (2004) Phylogeny and evolution of the powdery mildew fungi (Erysiphales, Ascomycota) inferred from nuclear ribosomal DNA sequences. *Mycoscience,* 45, 147–157.

Takano, Y., Kikuchi, T., Kubo, Y., Hamer, J.E., Mise, K. & Furusawa, I. (2000). The *Colletotrichum lagenarium* MAP kinase gene CMK1 regulates diverse aspects of fungal pathogenesis. *Mol. Plant–Microbe Interact.,* 13, 374–383.

Tetorya, M., & Rajam, M. V. (2021). RNAi-mediated silencing of *PEX6* and *GAS1* genes of *Fusarium oxysporum* f. sp. *Lycopersici* confers resistance against Fusarium wilt in tomato. *3 Biotech*, *11*(10), 443.

Tinoco, M. L., Dias, B. B., Dall'Astta, R. C., Pamphile, J. A., & Aragão, F. J. (2010). In vivo trans-specific gene silencing in fungal cells by in planta expression of a double-stranded RNA. *BMC biology*, *8*, 27.

Trieu, T. A., Calo, S., Nicolás, F. E., Vila, A., Moxon, S., Dalmay, T., Torres-Martínez, S., Garre, V., & Ruiz-Vázquez, R. M. (2015). A non-canonical RNA silencing pathway promotes mRNA degradation in basal Fungi. *PLoS genetics*, *11*(4), e1005168.

Turner, N.W., Subrahmanyam, S., & Piletsky, S.A. (2009). Analytical methods for determination of mycotoxins: a review. *Analytica Chimica Acta*, 632(2):168-80.

Urban, M. & Hammond-Kosack, K.E. (2012). Molecular genetics and genomic approaches to explore Fusarium infection of wheat floral tissue. Fusarium Genomics and Molecular and Cellular Biology Norwich, Norfolk, UK: Horizon Scientific Press

Van Baarlen, P., Woltering, E.J., Staats, M. & van Kan, J.A.L. (2007). Histochemical and genetic analysis of host and non-host interactions of Arabidopsis with three Botrytis species: an important role for cell death control. *Mol. Plant Pathol.*, 8, 41–54.

Van der Krol, A.R., Mur, L.A., Beld, M., Mol, J.N., Stuitje, A.R. (1990). Flavonoid genes in petunia: addition of a limited number of gene copies may lead to a suppression of gene expression. *Plant Cell. Apr; 2(4):291-9.*

Voegele, R.T. & Mendgen, K.W. (2011). Nutrient uptake in rust fungi: how sweet is parasitic life? *Euphytica*, 179, 41–55.

Wagacha, J.M., & Muthomi, J.W. (2008). Mycotoxin problem in Africa: current status, implications to food safety and health and possible management strategies. *International Journal of Food Microbiology,* 124:1-12.

Wang, B., Sun, Y., Song, N., Zhao, M., Liu, R., Feng, H., Wang, X., & Kang, Z. (2017). Puccinia striiformis f. sp. tritici microRNA-like RNA 1 (Pst-milR1), an important pathogenicity factor of Pst, impairs wheat resistance to Pst by suppressing the wheat pathogenesis-related 2 gene. *The New phytologist*, *215*(1), 338–350.

Wang, M., Weiberg, A., Lin, F.M., Thomma, B.P., Huang, H.D., & Jin, H. (2016). Bidirectional cross-kingdom RNAi and fungal uptake of external RNAs confer plant protection. *Nat Plants*, 2:16151.

Wang, M., Weiberg, A., Dellota, E., Jr, Yamane, D., & Jin, H. (2017). Botrytis small RNA Bc-siR37 suppresses plant defense genes by cross-kingdom RNAi. *RNA biology*, *14*(4), 421–428.

Wang, M., Weiberg, A., Lin, F. M., Thomma, B. P., Huang, H. D., & Jin, H. (2016). Bidirectional cross-kingdom RNAi and fungal uptake of external RNAs confer plant protection. *Nature plants*, *2*, 16151.

Weiberg, A., Wang, M., Lin, FM., Zhao, H., Zhang, Z., Kaloshian, I., Huang, H.D. & Jin H. (2013). Fungal small RNAs suppress plant immunity by hijacking host RNA interference pathways. *Science*, 342:118-223.

Werner, B. T., Koch, A., Šečić, E., Engelhardt, J., Jelonek, L., Steinbrenner, J., & Kogel, K. H. (2021). Fusarium graminearum DICER-like-dependent sRNAs are required for the suppression of host immune genes and full virulence. *PloS one*, *16*(8), e0252365.

Winston, W. M., Molodowitch, C., & Hunter, C. P. (2002). Systemic RNAi in *C. elegans* requires the putative transmembrane protein SID-1. *Science (New York, N.Y.),* 295(5564), 2456–2459.

Witwer, K.W. & Hirschi, K.D. (2014). Transfer and functional consequences of dietary microRNAs in vertebrates: concepts in search of corroboration: negative results challenge the hypothesis that dietary xenomiRs cross the gut and regulate genes in ingesting vertebrates, but important questions persist. *Bioessays*, 36:394–406.

Zhang, K., Yuan, X., Zang, J., Wang, M., Zhao, F., Li, P., Cao, H., Han, J., Xing, J., & Dong, J. (2018). The Kynurenine 3-Monooxygenase Encoding Gene, *BcKMO*, Is Involved in the Growth, Development, and Pathogenicity of *Botrytis cinerea*. *Frontiers in microbiology*, *9*, 1039.

Zhong, L., Carere, J., Lu, Z., Lu, F., & Zhou, T. (2018). Patulin in Apples and Apple-Based Food Products: The Burdens and the Mitigation Strategies. *Toxins,* 10(11), 475.

DETERMINATION OF ELECTRON TRAJECTORIES FOR SEM-EDS ANALYSIS OF BI-(2212) BULK SUPERCONDUCTORS: A MONTE CARLO SIMULATION FOR SURFACE IMPURITY DIFFUSION

Şenol KAYA[1]

1 Assist. Prof. Dr., Bolu Abant Izzet Baysal University Vocational School of Health Services, Turkey, 14030. Orcid ID: 0000-0001-8152-9122

1. A Brief Introduction to Superconductivity

The superconducting phenomenon was found out by Onnes in 1911 for mercury metal cooled in liquid Helium temperatures (4.2K) (Onnes, 1911). On his experiment, Onnes realized that the resistance of the mercury drops to zero in the liquid Helium. The phenomenon of the superconductivity was obtained below the certain temperature called as critical temperature, T_c. Superconductors are the special materials, i.e., naturally not all conductors exhibits superconductor behaviors. A typical resistance vs temperature relation of superconductor and normal conductors was illustrated in Figure 1a (Saxena, 2012; Yildirim, 2012). As temperature above T_c, the materials resistance obeys the conventional Ohm law (Dikici, 2013). As temperature approaches to T_c, the resistance of the superconductor materials drops almost zero below the transition zone. The width of this transition zone strictly connected to impurities on the superconductor materials (Semerci, 2015). The width of the transition region is narrow and sharp for the pure and single phase superconductors while the region can be broadened with the effects of impurities (Pakdil, Bekiroglu, Oz, Saritekin, & Yildirim, 2016; Yildirim et al., 2012). In addition, externally applied magnetic field may also changes the width of transition region (Dogruer, Aksoy, Yildirim, Ozturk, & Terzioglu, 2021) due to Meissner Effect explained following section.

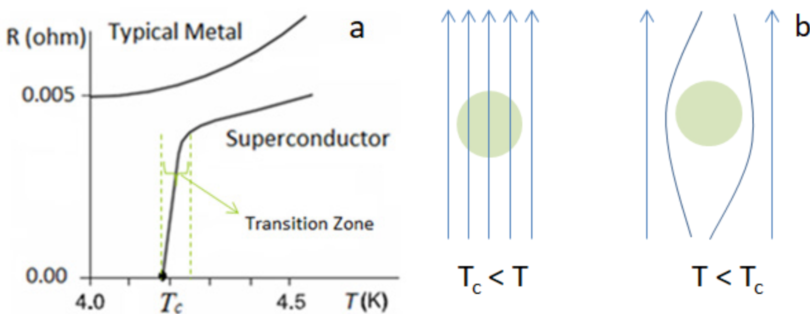

Figures 1: *a) Temperature versus resistance correlation of a normal metal and a superconductor (Yildirim, 2012), b-) Schematics of Meissner Effects (Dikici, 2013), (in figure 1b: green: superconductor, arrows: magnetic flux)*

After discovery of the superconductivity, a second milestone was discovered by W. Meissner and R. Ochsenfield in 1933s (Meissner & Ochsenfeld, 1933). As cooling the superconductor materials below the T_c in the presence of the magnetic field, it was found that the magnetic flux inside the superconductor materials vanished, i.e., flux was expelled from interior of superconductor (Semerci, 2015). This observation is called as Meissner Effect as shown in Figure 1b (Dikici, 2013). Meissner Effect demonstrates that together the superconductor with zero resistivity exhibits also perfect diamagnetism features. Discovery of this unique properties of

the superconductors open a new gate for the applications in magnetics such as magnetic levitation that is the virtual part of recent high-speed railways. This Meissner state can be broken as the magnetic field whether applied externally or generated by superconductor during current conduction enhances above a specific value which is called critical magnetic field, H_c. Beyond this H_c superconductors behave like an ordinary conductor. The value of the H_c can be varied by temperature. The value of the H_c enhances as the ambient temperature decreases lower then T_c. There may be also an additional parameter that causes degradation of the superconductor states. Above a certain current values superconductor state changes to normal state (Semerci, 2015). This certain values are called as critical current and denoted as J_c in the literatures (Cabassi, Delmonte, Abbas, Abdulridha, & Gilioli, 2020).

Considering to magnetic flux exclusion features, superconducting materials can be divided into two groups as Type I superconductors and Type II superconductors. The transition edge between the normal to superconductor states is narrow, i.e., penetrating distance (λ) of the magnetic flux is low (varied with Ae^{-p}, and approximately below the 100 nm) (Dikici, 2013). Hence, a sharp modulation between these two phases is observed. Therefore, the H_c values are relatively small than Type II superconductors. On the other hand, together with sharp edge, there exists a broad transition region where mixtures of both normal and superconducting states present (Dikici, 2013; Semerci, 2015). Owing to these mixture phases, magnetic fields penetrate in form of small cylinder called as vortices. The core radius of each cylindrical vortex is called as coherent length, (β). Further increase the magnetic field enhances the vortex number. This causes the phase transition from superconductor to normal conductor. The λ is smaller than β for the Type I superconductor, while the β is lower than λ for the Type II superconductors (Yildirim, 2012). Schematic illustrations for the Type I and II superconductors are depicted in Figures 2a-b, respectively (Dikici, 2013; Semerci, 2015). Type I superconductors are almost pure metals (Dikici, 2013) and they are not useful for the fabrication of the magnet due to the low H_c values (Semerci, 2015). In general perspective, the Type II superconductors exhibits greater critical temperature and carry grater current than Type I superconductors. In addition to these features of the Type II uperconductors, the high H_c values make them suitable to magnet fabrication.

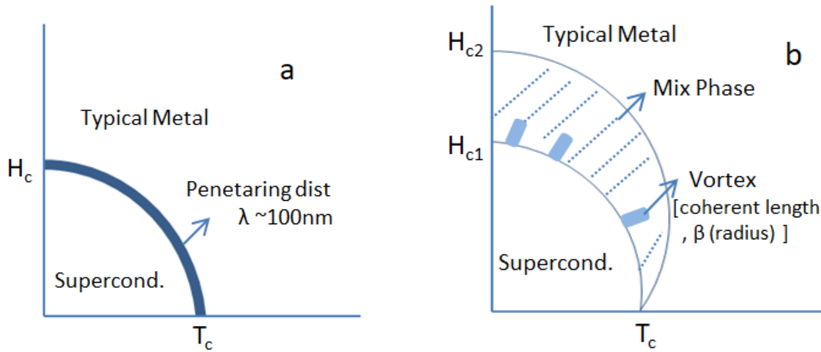

Figures 2: Schematic illustration of a) Type I and b) Type II Superconductors with penetrating distance and coherent length (Semerci, 2015).

The theory of the superconductors is rather complicated. In 1934, researchers developed different models for the mechanisms for the Type I superconductors in order to understand material behaviors under a magnetic field. By the year 1950, Ginzburg-Landau's phenomenological macroscopic theory achieved great success in explaining superconductivity. This theory is used a mathematical and physical formulation of the Landau second-order phase transition theory which assumes superconductivity is a type of macroscopic quantum state (Ketterson, 2016). A milestone for the superconductor theory was achieved in 1957. John Bardeen, Leon N. Cooper and J. Robert Schrieffer explained the superconducting behavior of the materials with the quantum mechanics in microscopic level known as the BCS theory (Bardeen, Cooper, & Schrieffer, 1957; Ray, 2015). Though its estimation power is restricted, compared to present ab initio methods, it is still valid phenomena for the classification and understanding of the superconductors (Flores-Livas et al., 2020). The BCS theory defines how electrons couple in bosonic pairs known as Cooper pairs intermediated by phonon lattice vibrations in the crystal where they circulate (Ray, 2015). In other words, it is expected that two electrons in the bound state with some kind of attractive interaction between them pair up to form a single system. These electrons resulting from the electron-lattice-electron interaction, which are coupled owing to adhesive property of the phonon, are called Cooper pairs (Yildirim, 2012). Together with BCS theory, applications on the Josephson Junction in 1962s based on quantum tunneling of the electron paved the way for the technology of superconducting materials (Dikici, 2013).

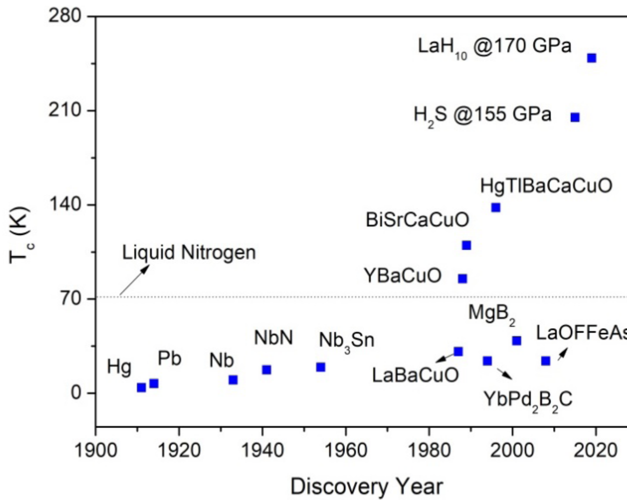

Figure 3: A century of critical temperatures of some discovered superconductor materials (Ray, 2015)

The BCS theory defines the superconducting behaviors of the materials close the zero Kelvin, typically below the 30 K. This is due to the fact that Coulomb repulsion force between electrons is larger than bonding via phonons above the 30 K (Ray, 2015). Therefore, by the invention of the superconductors with T_c above the 30 K, the BCS theory becomes insufficient. Hence, the theory of superconductivity is rather intricate (Flores-Livas et al., 2020). Since discovery of the superconductor, various elements and compounds in the form of bulk, ceramic and wire have been investigated for the technological applications (Bednorz & Muller, 1986; Gajda et al., 2016; Karaboga, Yetis, Akdogan, Gajda, & Belenli, 2018; Liu et al., 2021; Poole, Canfield, & Ramirez, 2000; Wilson, 2012; Zalaoglu, Karaboga, Terzioglu, & Yildirim, 2017). The evolution of the superconducting materials in the last century is depicted in Figure 3 (Ray, 2015; Wilson, 2012). The invention of the superconductors exhibiting the T_c above the 30 K can be accepted another milestone for the superconductor technology. Bednorz and Müller reported a possible new class of the superconductor like La-Ba-CuO_x (Bednorz & Muller, 1986) in 1986 and following studies including the Y-Ba-CuO_x and Bi-Sr-Ca-CuO_x etc. were supported their inventions (Hazen et al., 1988; Kirschner et al., 1987; Ray, 2015; Takahashi et al., 2008). The superconductors exhibiting the T_c above the 30 K was called as high temperature superconductors. These types of superconductors are classified as the Type II Superconductors materials. The discovery of the superconductor materials with the T_c above the 77 K is also important landmark. Above the 77 K, the liquid nitrogen can be

used as cooling agent which significantly decrease the usage cost of the superconductor based devices. Although discovery of the novel materials, such as the iron based structure, MgB_2 or etc. seen in Figure 3, a special attention on have been still devoted on the Cupper oxide (CuO_x) based (T_c above the 77 K and useful at atmospheric pressure) superconductors. The CuO_x based superconductors known as cuprates superconductors. Together with BCS theory, some researchers explain superconductivity of the cuprates in the line of the fluctuation/overlapping mechanism between Cu 3d and O 2p wave functions (Aftabi & Mozaffari, 2021; Pakdil et al., 2016). In addition, the anisotropic crystalline structure of the multilayer CuO also contribution of the high T_c features of the cuprate superconductors (Dikici, 2013). Thanks to these unique characteristics of the cuprates, large numbers of the studies will be performed in the next few decades.

2. Motivation of the Study and Simulation Procedure

Since the nineteenth century, society has developed in parallel with electricity generation and related technologies with electricity. This development gained a great momentum especially in the second half of the 19th century with the invention of the telephone and the light bulb, and in the following years it came to an end with the discovery of electrical machines. Since the invention of the electricity, energy usage has increased significantly as can be seen in Figure 4 (Smil, 2017). The reason for this huge increase in energy use is the production of complex and powerful devices/machines to increase the quality of life of societies with the emerging technology.

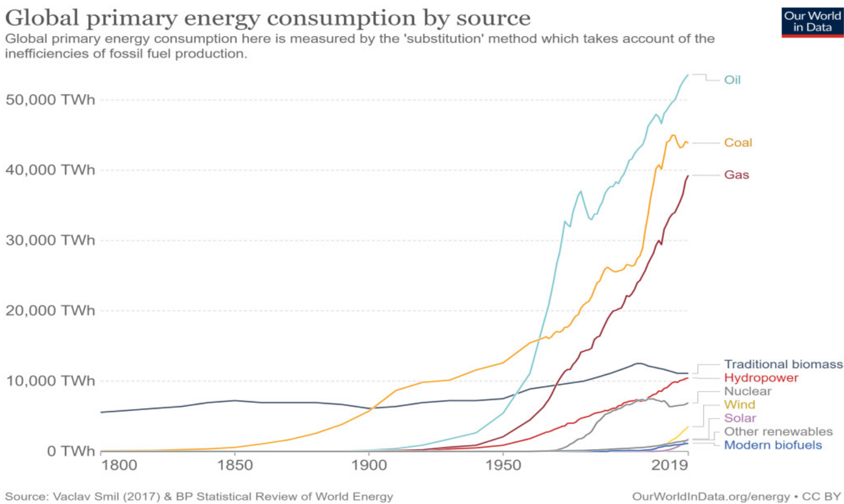

Figure 4: Global energy consumption by source between 1800 and 2019 (Smil, 2017)

Considering that more than eighty percent of the electrical energy used worldwide is obtained from fossil fuels, it is obvious that the increase in the energy used causes carbon dioxide emissions. When CO_2 emissions are examined on a sectoral basis in a global sense, industry-oriented energy use and transportation-based energy consumption constitute the big portion (Ritchie, 2020). Despite increasing energy use and sectoral developments, it is emphasized that CO_2 emissions should be reduced by sixty percent by 2050 compared to today in order to avoid climate changes (Yeatman, 2009). In order to achieve these goals, it is clearly seen that besides the widespread use of renewable energy sources, the effective and optimum use of electrical energy is required. Losses in electrical energy systems originate from generation, transmission and delivery systems. It is globally accepted that 50% of the system costs come from generation, 20% from transmission and 30% is due to delivery of the electricity (Yasar, Aslan, & Bicer, 2010). The energy loses during the transmission and deliveries of electricity originate from the formation of the heat due to the internal parasitic resistance of the wire and transformers used in the grid system. Low resistance, R, increases efficiency by reducing internal losses ($P=RI^2$) that can turn into heat, especially in high power applications (She, Huang, Lucia, & Ozpineci, 2017). In order to increase efficiency of the electrical energy systems and high power application, some elements must be have ideally zero internal resistance which decreases the waste consumption of the energy. In line with these requirements, superconducting technologies stand out with their superior properties. As temperature drops below the specific level depending on the materials, electrons carried current cannot release heat due to internal resistance of the materials approaches to almost zero ohm. Thus, the usage of the superconducting based systems affords a strong motivation for the efficiency of energy consumption.

Among the various superconductor materials, Type II high temperature cuprate superconductors are more attractive for the technological applications due to their unique properties as mentioned above section. Superconducting behaviors of copper-oxide with Bi-based, Tl-based and Hg-based systems has been still studied in the literatures (Abd-Shukor, 2018; Al-Sharabi & Abd-Shukor, 2013; Brylewski et al., 2016; Dogruer et al., 2021; Lee et al., 2009; Zalaoglu et al., 2021). The Bi-based materials are among the most useful in ordinary industrial applications and it is a first high-T_c superconductor without a rare element that decrease the fabrication cost. The most common application fields of Bi- based superconductors are magnetic coil, wire cable, particle accelerators, energy storage devices, motors and generators, transformers and current limiting (Chen et al., 2002; Kharissova et al., 2014; Oh, Kim, Jeong, Hyun, & Kim, 2007; Sato, 2015). Hence, the possible usage of the Bi based superconductor technology in

the energy applications may significantly decrease the waste heat loses. Bismuth materials have three distinct superconducting phases, depending on the chemical component which is connected with the number of Cu–O_2 layers in the unit cell. The critical temperatures of these phases are approximately 20 K for Bi–2201 phase, 85 K for Bi–2212 phase and 110 K for Bi–2223 high phase. The crystallographic c axis length bounds of these three phases are 24.6 Å, 30.7 Å and 37.1 Å for Bi-2201, Bi-2212 and Bi-2223, respectively. Both a-axis length bounds for all phases is approximately 5.4 Å (Doğruer, 2021). Among the others, the Bi-2212 called the low phase has superior properties compared to the other phases in terms of morphology and structural, thermodynamic stability, electrical and superconductivity properties (Cabassi et al., 2020; Kumar, Sharma, Ahluwalia, & Awana, 2013). The large void and multilayered anisotropic crystal structure, weak bonds between superconducting grains and structural defects inherent in materials are among the factors that prevent the use of these materials in novel technology and sustainable energy fields. In order to solve these issues and improve superconductive features Bi-based materials may be doped impurities such as hole type cation substitution (e.g., Pb^+ for Bi^+) or materials may have extra interstitial oxygen deficiencies. It should be note that T_c varies with the doping amount, material type and the annealing procedure (Kharissova et al., 2014). Doping can be performed via two different methods. One may add impurity materials with a specific ratio to powder form of the BiSrCaCuO (BSCCO) system. After that following the experimental recipe, the impurity-doped BSCCO superconductor device can be fabricated (Doğruer, 2021; Ulgen, Erdem, Zalaoglu, Turgay, & Yildirim, 2020). Doping impurities via surface diffusion is another method for generating some additional interstitial non-stoichiometric oxygen atoms/deficiencies and/or cation substitution. This second type doping can be performed via deposition of impurity materials onto surface of the bulk BSCCO samples. Following the deposition of the impurities, the impurity materials drive-inside the BSCCO thanks to the high temperature annealing process (Aydin et al., 2013; Ozturk et al., 2012; Yildirim, 2017). The parameters during the surface diffusion doping process are particularly important due to the impurity materials only effectively diffuse in the few ten micrometers depth of the bulk BSCCO surface (Ozturk et al., 2012; Zalaoglu & Yildirim, 2017). Hence, surface characterization methods becomes particularly significant for the understanding the physical background of the possible variation on the superconducting characteristics of the materials.

Various surface characterization methods including the XRD for crystallography, Vickers for microhardness specification etc., can be performed. Among them, evolution on the surface morphology of the samples is particularly important which can be carried out via Scanning

Electron Microscopy (SEM) measurements. Indentation size effect behavior, types of the grains and their distribution, local structural distortions and porosity between the superconducting grains can be specified via SEM images (Aydin et al., 2013; Ozturk et al., 2012). The parameters including the angle of the electron beam and energy of the incident electrons directly affect resolution of SEM image. In addition, depending on the beam energy of the incident electron, the penetrating distance of electron can be varied. It means that by adjusting the energy of the electron, images can be taken from different depths. Thus, surface morphology of the BSCOO system can be efficiently controlled. The controlling the parameters provide a reliable information particularly for the surface impurity diffusion studies of the BSCCO systems. Hence in this study, the electron trajectories at different angles, penetrating depth of the incident electron at various beam energies and polar angular distributions of emerging secondary irradiation for the Bi-2212 superconductor surface have been investigated in detail via pyPENELOPE (Penetration and Energy Loss of Positrons and Electrons in matter) Monte Carlo package. The pyPENELOPE is free and open-source Monte Carlo code. The number of electron shower is 10^5 for the electron trajectory simulation and primary electrons come from z-axis to sample surface. The simulation of the electron trajectories were performed for 10 keV, 20 keV and 30 keV incident electrons. The simulation was performed for zero, 30 degree and 60 degree tilt angles in each energy, separately. Absorption and backscattering distribution of particles, and characteristic X-ray distribution under 30 keV electron beam for the SEM/EDS analysis was also specified via Monte Carlo Simulation package.

3. Simulation Results

A SEM measurement is a useful tool to investigate surface morphology of the samples. The image from SEM measurements is obtained via scanning the surface with focused primary electron beam. During the SEM measurements two different types of electrons are typically detected which are called as secondary electrons (SE) and backscattered electrons (BE). Primary electrons lose its energy predominantly through collisions with electrons of Bi-2212 samples. In other words, as the electron radiation propagates through the sample structure, multiple scattering interactions, which are basically Coulomb scattering and radiative loss (Bremsstrahlung), deflect electrons (Lundh et al., 2012). Due to these interactions, primary electrons lose their energies and generate secondary irradiations which are photons and electron. The SE is particularly important for the SEM image formation.

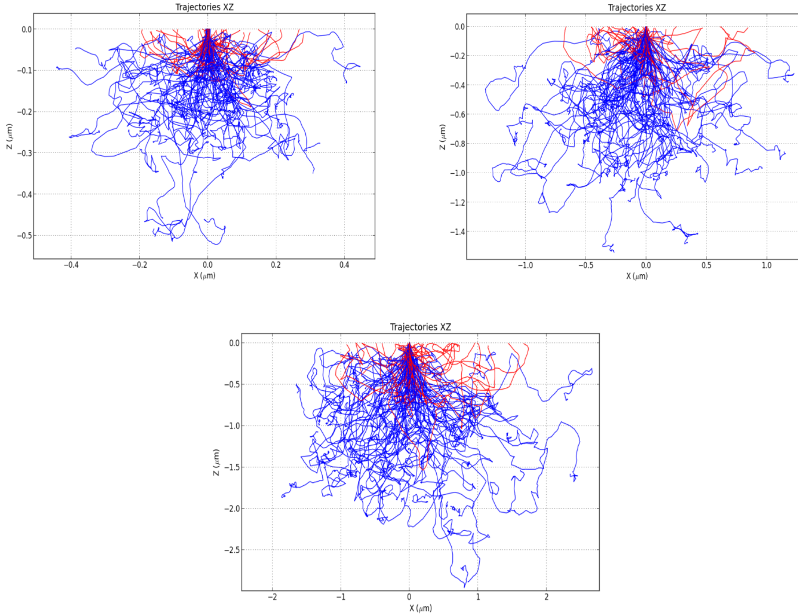

Figures 5: Monte Carlo simulations of electron trajectories for a-) 10 keV BE-zero TA, b-) 20 keV-zero TA, c-) 30 keV-zero TA (where BE: Beam Energy, TA: Tilt Angle and absorbed primary electrons are depicted in blue, with back-scattered electrons in red)

On the other hand, some of the primary electron can be also backscattered. Hence, possible path of the primary electrons provides significant information for the SEM image. By tracking the primary electrons, the depth of the SE and BE signals can be found. This is particularly important for the morphological determination of the surface impurity diffusion of the Bi-2212 samples. Electron shower simulation can be specified the electrons trajectories when they lose energy during their propagation inside the Bi-2212 bulk. The simulated trajectories are illustrated in Figure 5a-c for 10 keV, 20 keV and 30 keV energetic incident electron beam, respectively. The primary electrons were directly sent to BSCCO surface, i.e., tilt angle is zero. The trajectories of the primary particles are denoted as blue color, while the backscattered electrons are denoted as red color in Figure 5a-c. The primary electrons penetrates up to 500 nm depth of the Bi-2212 and mean depth values are approximately 200 nm for 10 keV electron beam. It is known that the secondary electrons are generated by primary electrons. Therefore, secondary electron SEM (SE-SEM) images of Bi-2212 contain intense resolutions for a depth of about 200 nm. The means penetrations depth values are approximately 600 nm and 1100 nm for the 20 keV and 30 keV electron beam, respectively. These results demonstrate that influence of the impurity diffusion on the surface

morphology of the Bi-2212 can be effectively scanned up to 1100 nm depth from the surface of the BSCCO layer by using the SE-SEM images. Similarly, mean penetration depths of the backscattered electrons are 70 nm, 250 nm and 550 nm for the 10 keV, 20 keV and 30 keV electron beam energies, respectively.

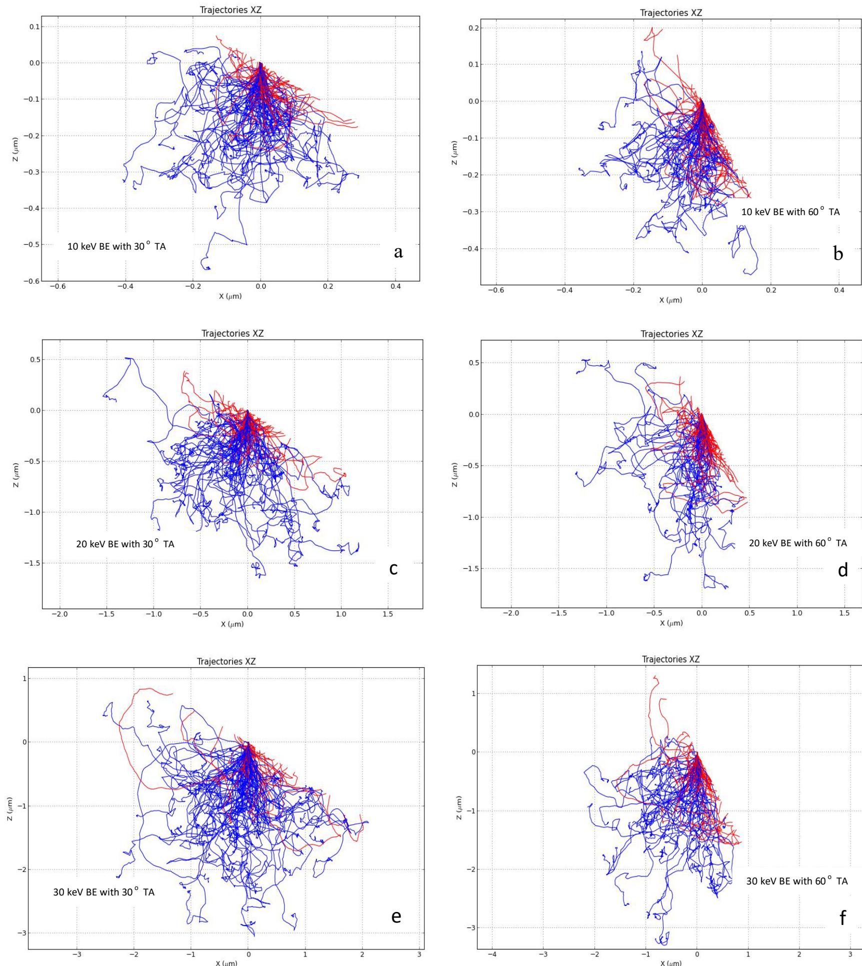

Figures 6: Monte Carlo simulations of electron trajectories for a) 10 keV BE-30° TA, b) 10 keV BE-60° TA, c) 20 keV BE-30° TA, d) 20 keV BE-60° TA, e) 30 keV BE-30° TA, f) 30 keV BE-60° TA

Influences of the angle between the incident electron beam and Bi-2212 sample on electron trajectories have been also investigated. The Figures 6a-f have depicted the electron trajectories for 30° and 60° tilt angles between the 10 keV, 20 keV and 30 keV electron beam energies. Due to the momentum transfer depends on the beam angle the trajectories of the electron naturally oriented different orbits. As we analyses the Figures 6, it can be seen that the penetration depth length of the electrons in z-axis are

almost similar with the values obtained in Figures 5. However, it seems that the intensity of the backscattered electron that leave the Bi-2212 surface is higher than the values for the incident electrons comes perpendicular to Bi-2212 surface. Hence resolution of the BE-SEM image may be better for the higher tilt angles. The absorption, backscattered and transmission fraction of the primary and secondary electrons have been also investigated via pyPENELOPE simulation. This simulation was performed for only 30 keV electron beams. The obtained fraction parameters are listed in Table 1.

Table 1: Some simulation results for the primary and secondary irradiations

	Primary Irradiation		Secondary electron	
	Fraction	Uncertainty x 10^{-4}	Fraction	Uncertainty x 10^{-4}
Absorbed	0.61	4.60	-	-
Backscattered	0.39	5.80	0.015	1.12
Transmitted	0	0	0	0

Bi-2212 sample with 1 mm thickness was designed during the simulation. Due to the high interaction probability of the electron with matter no ant particles were transmitted from Bi-2212 structure. This means that all the electrons either absorbed by samples or backscattered from Bi-2212 structure. The absorption fraction of the primary electrons is 61% indicating the majority of the incident electron absorbed by Bi-2212 structure. Some of these absorbed particles generate secondary electrons and that leaves the Bi-2212 structure. These SE is used for the SEM image of the Bi-2212. Moreover the 39% percent of the primary electrons is backscattered. These BE were formed the BE-SEM image of the Bi-2212 structure. It should be also noted that BE-SEM image may also have contribution of the backscattered SE. As seen in Table 1, the backscattered fraction of the generated SE is only 1.5 % which does not significantly effects the BE-SEM image.

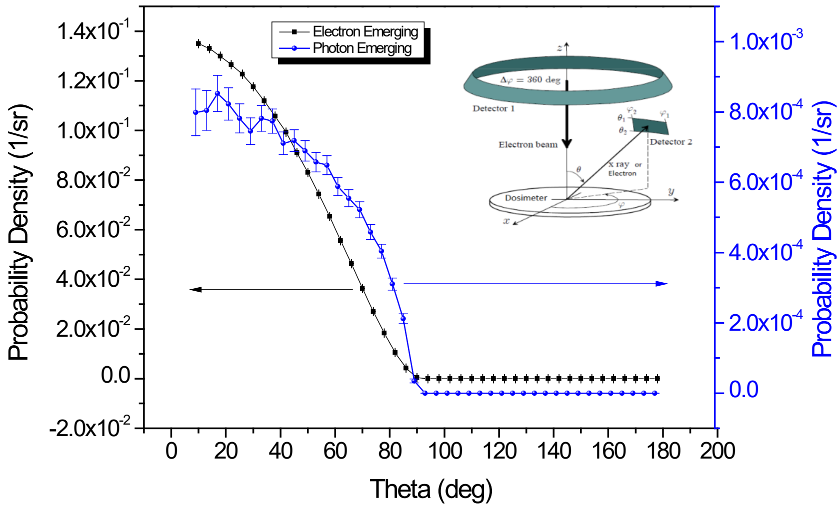

Figure 7: Polar angular distributions of emerging photons and electrons emitted from Bi-2212 bulk surface, and schematic distribution of simulation structure (Llovet & Salvat, 2017)

The scattered angle dependency of the generated electrons and photons which are called as secondary irradiation are depicted in the Figure 7. The electron beam energy was 30keV and incident electrons were perpendicularly oriented to Bi-2212 surface. The schematic simulation structure including the polar angle (Theta) distribution has been illustrated on the right corner (Llovet & Salvat, 2017). In order to obtain intense SEM image the BE and SE detectors should be located between zero and 40° theta angles. Higher angles from 40° emerging electron intensity decreases more that 40% percentage compared to zero degree.

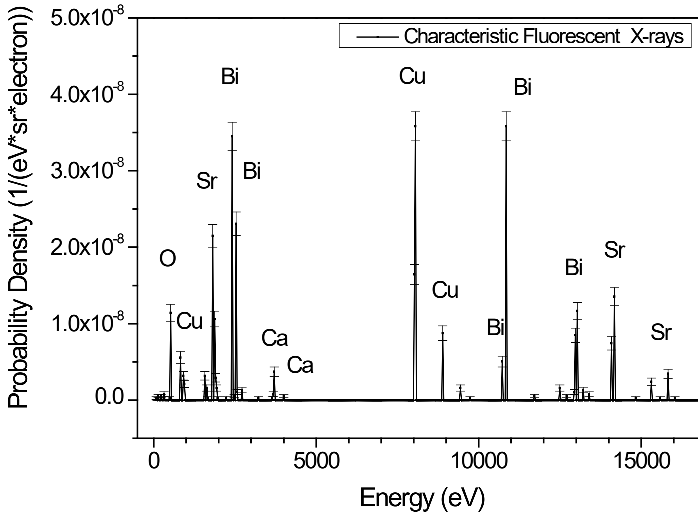

Figure 8: Characteristics Fluorescent X-ray spectra for Bi-(2212) for elemental analysis in EDS

Secondary photon, which may be used for the EDS elemental analysis during the SEM measurements, angular distribution does not significantly varied up to the 60 ^{o} theta angles. In order to obtain reliable elemental SEM/EDS analysis, the detectors should be located at angles from zero to 60 ^{o} theta angles. Moreover, the characteristics X-rays for the simulated Bi-2212 phase were also specified via pyPENELOPE Monte Carlo simulations. The characteristics fluorescent X-ray spectra are depicted in Figure 8. The peaks in the Figure 8 belongs the characteristics energy of the elements in the BSCCO structure. The peaks were indexed with elements and elemental analysis is in harmony with the literature given in Ref. (Cabassi et al., 2020; Mohammed, Awad, Abou-Aly, Ibrahim, & Hassan, 2012).

4. Conclusion

Electron trajectories and elemental analysis were specified for the SEM/EDS analysis of the Bi-2212 phase bulk superconductor materials via pyPENELOPE Monte Carlo Simulation package. This simulation study is particularly important for the impurity surface diffusion morphological evolution of the Bi-2212 bulk superconductors. The results demonstrates that the signals for the SE-SEM images of the Bi-2212 effectively comes from the mean penetrations depth of about 200 nm, 600 nm and 1100 nm for the 10 keV, 20 keV and 30 keV electron beam, respectively. Similarly, mean penetration depths of the backscattered electrons are 70 nm, 250 nm and 550 nm for the 10 keV, 20 keV and 30 keV electron beam

energies, respectively. Tilt angle between the sample and ground which affects the incident electron direction to sample influences the intensity of the backscattered electrons. It is observed that backscattered electron intensity slightly increase with increasing the tilt angles. The absorption fraction of the primary electrons is 61%, while the backscattered fraction of the primary particles 39%. No any significant contribution of the backscattered SE on the BE-SEM images was assessed. In order to obtain reliable elemental SEM/EDS analysis, the detectors should be located at angles from zero to 60° theta angles for emerging photons, and it should be zero to 40° theta angles for emerging electron. It can be concluded that the surface morphology of the Bi-2212 superconductors bulk can be specified up to 1100 nm depth after the impurity diffusion studies.

Acknowledgments

This simulation performed Bolu Abant Izzet Baysal Univeristy-Mehmet Tanrıkulu Vocational School for providing an office type computer. The author would like to thank to pyPENELOPE development group (http://pypenelope.sourceforge.net) for open source and free usage of the simulation package. The author would like to thank Assoc. prof. Dr. Fırat KARABOĞA and Prof. Dr. Cabir TERZİOĞLU for proof reading of the first section of the study.

References

Abd-Shukor, R. (2018). Ultrasonic and elastic properties of Tl- and Hg-Based cuprate superconductors: a review. *Phase Transitions, 91*(1), 48-57.

Aftabi, A., & Mozaffari, M. (2021). Fluctuation induced conductivity and pseudogap state studies of $Bi_{1.6}Pb_{0.4}Sr_2Ca_2Cu_3O_{10}$ delta superconductor added with ZnO nanoparticles. *Scientific Reports, 11*(1), 4341.

Al-Sharabi, A., & Abd-Shukor, R. (2013). Effect of Hf Substitutions on the Formation and Superconductivity of Tl-1212 Type Phase $TlSr_2(Ca_{1-x}Hf_x)Cu_2O_7$-delta. *2013 Ukm Fst Postgraduate Colloquium, 1571*, 102-107.

Aydin, H., Babanli, A., Altintas, S. P., Asikuzun, E., Soylu, N., Ozturk, O., . . . Yildirim, G. (2013). Breaking point of the harmony between Gd diffused Bi-2223 slabs with diffusion annealing temperature. *Journal of Materials Science-Materials in Electronics, 24*(11), 4566-4573.

Bardeen, J., Cooper, L.N., & Schrieffer, J.R. (1957). Microscopic Theory of Superconductivity. *Physical Review, 108*, 162.

Bednorz, J. G., & Muller, K. A. (1986). Possible High-Tc Superconductivity in the Ba-La-Cu-O System. *Zeitschrift Fur Physik B-Condensed Matter, 64*(2), 189-193.

Brylewski, T., Przybylski, K., Morawski, A., Gajda, D., Cetner, T., & Chmist, J. (2016). Soft-chemistry synthesis of Ba2Ca2Cu3Ox precursor and characterization of high-T-c $Hg_{0.8}Pb_{0.2}Ba_2Ca_2Cu_3O_8$ delta superconductor. *Journal of Advanced Ceramics, 5*(3), 185-196.

Cabassi, R., Delmonte, D., Abbas, M. M., Abdulridha, A. R., & Gilioli, E. (2020). The Role of Chemical Substitutions on Bi-2212 Superconductors. *Crystals, 10*(6). doi:ARTN 462

Chen, M., Paul, W., Lakner, M., Donzel, L., Hoidis, M., Unternaehrer, P., . . . Mendik, M. (2002). 6.4 MVA resitive fault current limiter based on Bi-2212 superconductor. *Physica C-Superconductivity and Its Applications, 372*, 1657-1663.

Dikici, M. (2013). *Katıhal Fiziği*: Seckin Yayınları.

Dogruer, M., Aksoy, C., Yildirim, G., Ozturk, O., & Terzioglu, C. (2021). Influence of Sr/Nd partial replacement on fundamental properties of Bi-2223 superconducting system. *Journal of Materials Science-Materials in Electronics, 32*(6), 7073-7089.

Doğruer, M. (2021). *Full Characterization of Sr Site Nd Substituted Bulk Bi-2223 Superconducting Samples with Standard Experimental Methods and Theoretical Approaches.* (Ph.D. Thesis), Bolu Abant İzzet Baysal University

Flores-Livas, J. A., Boeri, L., Sanna, A., Profeta, G., Arita, R., & Eremets, M. (2020). A perspective on conventional high-temperature superconductors at high pressure: Methods and materials. *Physics Reports-Review Section of Physics Letters, 856*, 1-78.

Gajda, D., Morawski, A., Zaleski, A. J., Akdogan, M., Yetis, H., Karaboga, F., . . . Belenli, I. (2016). The influence of HIP process on critical parameters of MgB_2/Fe wires with big boron grains and without barriers. *Journal of Alloys and Compounds, 687*, 616-622.

Hazen, R. M., Prewitt, C. T., Angel, R. J., Ross, N. L., Finger, L. W., Hadidiacos, C. G., . . . Chu, C. W. (1988). Superconductivity in the High-Tc Bi-Ca-Sr-Cu-O System - Phase Identification. *Physical Review Letters, 60*(12), 1174-1177.

Karaboga, F., Yetis, H., Akdogan, M., Gajda, D., & Belenli, I. (2018). Design, Fabrication, and Testing of MgB_2/Fe Racetrack Coils. *Ieee Transactions on Applied Superconductivity, 28*(6), 6200805.

Ketterson, J.B. . (2016). *The Physics of Solids*: Oxford Scholarship.

Kharissova, O. V., Kopnin, E. M., Maltsev, V. V., Leonyuk, N. I., Leon-Rossano, L. M., Pinus, I. Y., & Kharisov, B. I. (2014). Recent Advances on Bismuth-based 2223 and 2212 Superconductors: Synthesis, Chemical Properties, and Principal Applications. *Critical Reviews in Solid State and Materials Sciences, 39*(4), 253-276.

Kirschner, I., Bankuti, J., Gal, M., Torkos, K., Solymos, K. G., & Horvath, G. (1987). High-Tc Superconductivity in La-Ba-Cu-O and Y-Ba-Cu-O Compounds. *Europhysics Letters, 3*(12), 1309-1314.

Kumar, Jagdish, Sharma, Devina, Ahluwalia, P. K., & Awana, V. P. S. (2013). Enhanced superconducting performance of melt quenched $Bi_2Sr_2CaCu_2O_8$ (Bi-2212) superconductor. *Materials Chemistry and Physics, 139*(2), 681-688.

Lee, W. S., Tanaka, K., Vishik, I. M., Lu, D. H., Moore, R. G., Eisaki, H., . . . Shen, Z. X. (2009). Dependence of Band-Renormalization Effects on the Number of Copper Oxide Layers in Tl-Based Copper Oxide Superconductors Revealed by Angle-Resolved Photoemission Spectroscopy. *Physical Review Letters, 103*(6), 067003.

Liu, Z., Zheng, J., Chen, J. Z., Hu, Z. X., Deng, Z. G., Shi, Y. H., & Cardwell, D. A. (2021). The magnetic and levitation characteristics of single-grain YBaCuO and GdBaCuO-Ag bulk superconductors in high magnetic fields. *Journal of Applied Physics, 130*(18), 183904.

Llovet, X., & Salvat, F. (2017). PENEPMA: A Monte Carlo Program for the Simulation of X-Ray Emission in Electron Probe Microanalysis. *Microscopy and Microanalysis, 23*(3), 634-646.

Lundh, O., Rechatin, C., Faure, J., Ben-Ismail, A., Lim, J., De Wagter, C., . . . Malka, V. (2012). Comparison of measured with calculated dose distribution from a 120-MeV electron beam from a laser-plasma accelerator. *Medical Physics, 39*(6), 3501-3508.

Meissner, W., & Ochsenfeld, R. (1933). Ein neuer effect bei eintritt der supraleitfahigkeit. *Naturwissenschaften 21*, 787.

Mohammed, N.H., Awad, R., Abou-Aly, A.I., Ibrahim, I.H., & Hassan, M.S. (2012). Optimizing the Preparation Conditions of Bi-2223 Superconducting Phase Using PbO and PbO_2. *Materials Sciences and Applications, 3*, 224.

Oh, S. Y., Kim, H. R., Jeong, Y. H., Hyun, O. B., & Kim, C. J. (2007). Joining of Bi-2212 high-T-c superconductors and metals using indium solders. *Physica C-Superconductivity and Its Applications, 463*, 464-467.

Onnes, H.K. . (1911). The Resistance of Pure Mercury at Helium Temperatures. *Comm. Phys. Lab. Univ. Leiden, 12*, 120.

Ozturk, O., Asikuzun, E., Kaya, S., Coskunyurek, M., Yildirim, G., Yilmazlar, M., & Terzioglu, C. (2012). Physical Properties and Diffusion-Coefficient Calculation of Iron Diffused Bi-2223 System. *Journal of Superconductivity and Novel Magnetism, 25*(7), 2481-2487.

Pakdil, M., Bekiroglu, E., Oz, M., Saritekin, N. K., & Yildirim, G. (2016). Role of preparation conditions of Bi-2223 ceramic materials and optimization of Bi-2223 phase in bulk materials with experimental and statistical approaches. *Journal of Alloys and Compounds, 673*, 205-214.

Poole, C., Canfield, P., & Ramirez. (2000). *Handbook of Superconductivity*: Academic Press.

Ray, P.J. (2015). *Structural investigation of* $La_{2-x}Sr_xCuO_{4+y}$. (M.Sc. Thesis), University of Copanhagen.

Ritchie, H. (2020). Sector by sector: where do global greenhouse gas emissions come from. *Available in: https://ourworldindata.org/ghg-emissions-by-sector*.

Sato, K. (2015). 3 - Bismuth-based oxide (BSCCO) high-temperature superconducting wires for power grid applications: Properties and fabrication. In Christopher Rey (Ed.), *Superconductors in the Power Grid* (pp. 75-95): Woodhead Publishing.

Saxena, A.K. (2012). *High-Temperature Superconductors*: Springer- Verlag.

Semerci, T. (2015). *Terahertz Wave Sensitive Superconducting Bolometric Detector.* (M.Sc. Thesis), İzmir Institute of Technology.

She, X., Huang, A. Q., Lucia, O., & Ozpineci, B. (2017). Review of Silicon Carbide Power Devices and Their Applications. *Ieee Transactions on Industrial Electronics, 64*(10), 8193-8205.

Smil, Vaclav. (2017). Energy Transitions: Global and National Perspectives. *BP Statistical Review of World Energy*. doi:https://ourworldindata.org/grapher/global-energy-consumption-source? country=~OWID_WRL

Takahashi, H., Igawa, K., Arii, K., Kamihara, Y., Hirano, M., & Hosono, H. (2008). Superconductivity at 43 K in an iron-based layered compound LaO1-xFxFeAs. *Nature, 453*(7193), 376-378.

Ulgen, A. T., Erdem, U., Zalaoglu, Y., Turgay, T., & Yildirim, G. (2020). Effect of vanadium addition on fundamental electrical quantities of Bi-2223 crystal structure and semi-empirical model on structural disorders-defects. *Journal of Materials Science-Materials in Electronics, 31*(16), 13765-13777.

Wilson, M. N. (2012). A Century of Superconducting Technology. *Advances in Cryogenic Engineering, Vol 58, 1435*, 11-35.

Yasar, C., Aslan, Y., & Bicer, T. (2010). Investigation of Power Losses in a Power Distribution Transformer Zone. *DPÜ Fen Bilimleri Enstitüsü Dergisi, 20*, 9 22.

Yeatman, W. (2009). Global Warming 101: Costs. Retrieved from http://www.globalwarming.org /2009/02/04/global-warming-101-costs/

Yildirim, G. (2012). *Electrical and Magnetic Properties of Bi(Pb)SrCaCuO Superconductor Thin Film Produced by Sputtering Method.* (Ph.D. Thesis), Bolu Abant Izzet Baysal University.

Yildirim, G. (2017). Determination of optimum diffusion annealing temperature for Au surface-layered Bi-2212 ceramics and dependence of transition temperatures on disorders. *Journal of Alloys and Compounds, 699*, 247-255.

Yildirim, G., Bal, S., Yucel, E., Dogruer, M., Akdogan, M., Varilci, A., & Terzioglu, C. (2012). Effect of Mn Addition on Structural and Superconducting Properties of (Bi, Pb)-2223 Superconducting Ceramics. *Journal of Superconductivity and Novel Magnetism, 25*(2), 381-390.

Zalaoglu, Y., Erdem, U., Bolat, F. C., Akkurt, B., Turgay, T., & Yildirim, G. (2021). Improvement in fundamental electronic properties of Bi-2212 electroceramics with trivalent Bi/Tm substitution: a combined experimental and empirical model approach. *Journal of Materials Science-Materials in Electronics, 32*(14), 19846-19858.

Zalaoglu, Y., Karaboga, F., Terzioglu, C., & Yildirim, G. (2017). Improvement of mechanical performances and characteristics of bulk Bi-2212 materials exposed to Au diffusion and stabilization of durable tetragonal phase by Au. *Ceramics International, 43*(9), 6836-6844.

Zalaoglu, Y., & Yildirim, G. (2017). An effective research for diffusion annealing temperature and activation energy in Au surface-layered Bi-2212 ceramic composites. *Journal of Materials Science-Materials in Electronics, 28*(23), 17693-17701.

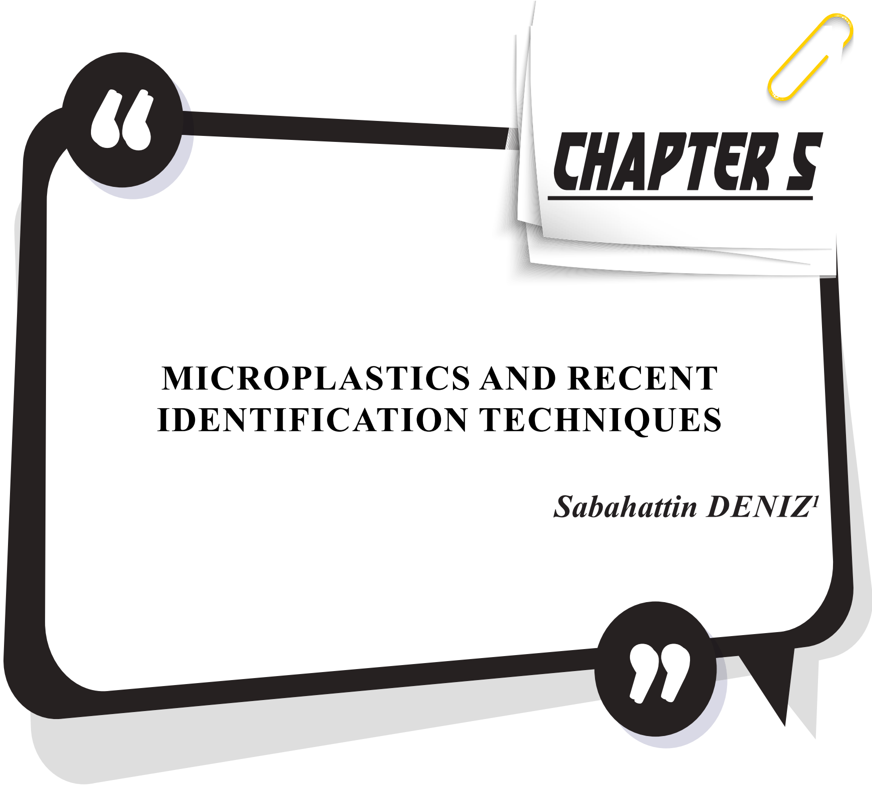

MICROPLASTICS AND RECENT IDENTIFICATION TECHNIQUES

Sabahattin DENIZ[1]

1 Dr. Öğr. Üyesi Sabahattin Deniz, Marmara Üniversitesi, Teknoloji Fakültesi, Tekstil Mühendisliği Bölümü, sdeniz@marma.edu.tr

Introduction

Plastics are a part of our daily life. There are everywhere. After 1950's the usage of plastics started and increased their popularity every year. Plastic products are preferred to be used instead of glass, metal and wooden products. They have some advantages such as; cheapness, lightness, flexibility and provide benefits to individuals. That's why plastics have become an inseparable part of our lives. Now, products made of plastic are used in all areas of our lives, including industry and health. Plastic products are now produced worldwide at about 200 million tons per year (Gündoğdu et al, 2017a).

Despite its many advantages, plastics continue to exist in nature for a long time when they become waste, making them a significant threat to the environment. Plastic waste, which cannot be easily destroyed in nature due to its strong structure, can be transported to distant points due to streams, albeit for a long time after reaching the sea. It is stated that there are 180 times more plastic types than sea creatures on the surface of the Great Pacific Ocean, which constitutes the world's largest plastic garbage area (Aytamam, 2018).

What is the microplastic?

In 2004 Thomas et al. have published an article published in Science, and they brought up the issue of microplastic with the question "Lost at sea: where is all the plastic?" (Thompson et al, 2004).

Microplastic means a material consisting of solid polymer containing particles, to which additives or other substances may have been added, and where ≥ 1% w/w of particles have -all dimensions 1nm ≤ x ≤ 5mm, - or, for fibers, a length of 3nm ≤ x ≤ 15mm and length to diameter ratio of >3 (Gündoğdu, 2017b).

Microplastics can be classified into two groups;

Primary microplastics: It is released directly into the environment in the form of small particles. They are produced for a purpose as a micro particles and mostly used in cosmetics and personal care products.

Secondary microplastics: These microplastics are formed when larger plastic materials break down into smaller pieces over time by various factors such as UV, waves, wind and living things.

Microplastic Sources

The main sources of Microplastics was given by International Union for Conservation of Nature (IUCN). IUCN has divided source of microplastics into 7 main categories and given in Figure 1 (Boucher & Friot, 2017).

Synthetic textiles:

Synthetic textiles, making up 35% of the total volume, are the biggest source of microplastics released to aquatic environment. To wash textiles especially made of synthetic fibers, releases microplastics from fabrics thru abrasion of fibers. This is caused chemical and mechanical stresses to which fabrics are exposed during the washing process in a washing machine. Some studies have shown that a single clothes releases about two thousand microplastics per wash cycle. (Browne et al. 2011) It is estimated that there are nearly nine hundred million washing machines in the world. So, it is clearly can said that synthetic textiles are the main source of microplastics (Cesa et al., 2017).

Tires:

The main structure of an ordinary tire is plastic polymer, synthetic and natural rubber, while the rest consists of metals and other compounds. Wear on tires is caused by friction and heat generated by the contact of the tire with the road. Breeze and rain also cause tire dust, namely microplastics, to spread to the environment. Tires is the second source of microplastics in aquatic environment.

City dust:

City dust includes damages from abrasion of objects such as synthetic shoe soles, plastic cookware, plastic plates, cups, forks, spoons, and materials such as synthetic turf, house dust, ports and marine coatings and it also contains various abrasives and particulates from the weathering of plastic materials.

Road marking:

Road signs are applied when roads are built and maintained. These markings mostly include polymer based products. They are converted into microplastics by exposure to wear from vehicles and weather conditions.

Marine coatings:

To protect ships from the corrosive effects of saltwater, protective marine coatings are applied to all parts of them and various plastic containing materials are used for marine coatings. The most common are epoxy and polyurethane coatings and varnishes. Wear and pour out of surface during the application, maintenance, and disposal of these coatings cause the release of microplastics.

Cosmetics:

A type of microplastic, known as microbeads, is found in many personal care and cosmetic products. Microbeads used in cosmetics; such as facial cleansing and peeling gels, shampoos and soaps, toothpaste, eyeliner, mascara, lip gloss, deodorant and sunscreens can be sources of microplastics.

Plastic pellets:

Plastic raw materials to be used in the production of plastic products are generally produced as small pellets or powders. The pellets are then transported to machines that produce final material. During production, processing, transportation, and recycling, accidentally dumping of these pellets to the environment resulting in the release of microplastics into the environment.

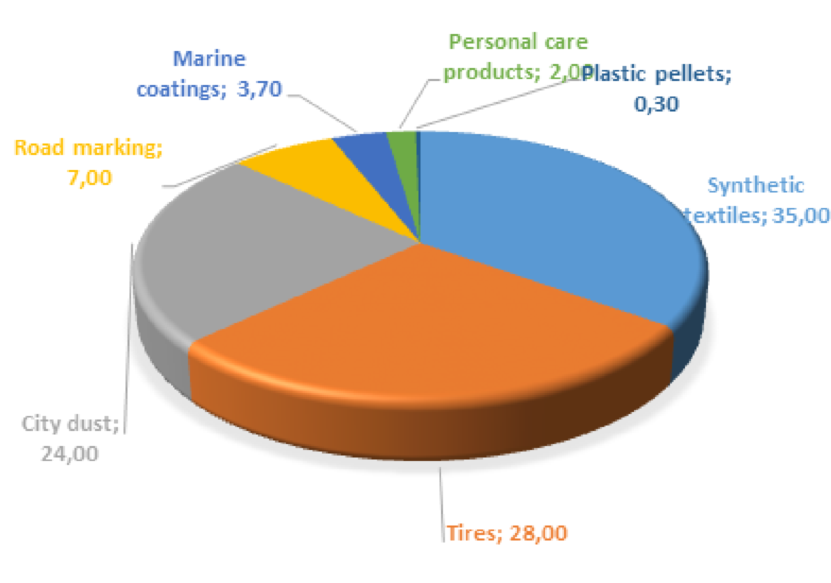

Figure 1. *Source of microplastics in oceans by source (in %)*

Classification of plastic particles

Microplastics can be classified three main groups such as size, shape and color, chemical structure.

Size:

Microplastics can be classified differently by different researchers in terms of their sizes. But general approach was given in Table 1 (Aytamam 2018).

Table1. *Classification of plastic particles*

Category	Size
Macroplastics	≥25mm
Mezoplastics	25mm ≤ 5mm
Microplastics	5mm – 1mm
Mini microplastics	1mm – 1µm
Nanoplastics	< 1µm

Shape and color:

Microplastic particles, which are formed as a result of the fragmentation of macro-sized particles, do not have a specific shape and color. However, it can be spherical, film, oval, fiber and irregular in general. Although parts of plastic-containing fabrics are in the form of fibers, microplastics produced for personal care products are generally spherical. The presence of microplastics in every color can be mentioned. However, color is an important factor by some marine organisms, and sea creatures may swallow them, likened to their prey. Therefore, the amount of some colored microplastics may be less than they should be. (Song et al., 2015).

Chemical structure:

Plastics are used for various purposes due to their low cost, moisture retention and light weight. Since plastics with very different chemical structures are used to produce materials with different properties, the microplastics formed from these will also have different chemical structures. Blumenröder et al. found chemical structure of microplastics in intertidal sediments such as; polytetrafluorodiethylene, polyethylene, polyamide; polyester and polyacrylonitrate (Blumenröder et al., 2017) Gies et al. identified chemical structure of microplastics in wastewater effluent and found polystyrene, polyester, modified cellulose, nylon, polypropylene, and cotton (Gies et al., 2018). It is possible to see a lot type of chemical structure of microplastics in literature. It can be said that the chemical structure of microplastics varies according to the polluting plastics in their environment.

Exposure to microplastics

We are exposed to microplastics in many areas. Microplastics accumulate especially in aquatic environment and enter the bodies of living organisms. For this reason, microplastics are found in many living species. Apart from that, it is also present in a wide variety of foods that we consume in our daily lives. The size of microplastics, micro- or even nano-scale makes us think that they can also exist in the human body, and in a recent study, the presence of microplastics in the placenta was detected, proving that microplastics can circulate in the human body as well. Although the human toxicity of the presence of microplastics has not yet been proven, the potential harm is thought to be high. (Yang et al., 2015; Rochman et al., 2015; Leibzeit et al., 2013; Mason et al., 2018; Schwabl et al., 2019; Ragusa et al., 2021)

Exposure to microplastics by food chain is illustrated in Figure 2.

Figure 2. *Exposure to microplastics. (Adapted from Horiba Scientific 2021)*

Toxicity of microplastics

Three possible toxic effects of plastic particles are estimated. The first is the plastic particles themselves, the second is the release of persistent organic pollutant absorbed into the plastics, and the third is the leaching of plastic additives. Unfortunately, limited data on the presence of microplastics in food has a negative impact on our estimate of the adverse effects of these pollutants or additives. The possible toxicity of nanoplastics to humans has not been adequately studied. (Bouwmeester et al., 2015). Despite all this limited information, it should be considered that microplastics are likely to have harmful effects on health.

Analysis of microplastics

Microplastic analysis can generally be performed in five steps: sampling, sample preparation-purification, filtering, measurement-data collection, and analysis-reporting.

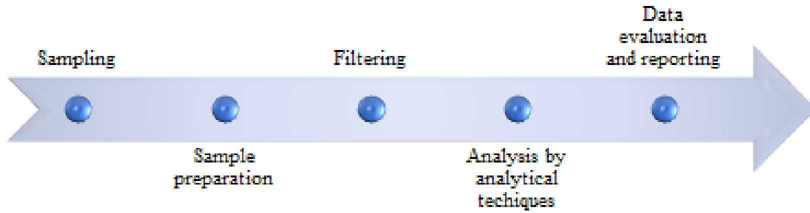

Figure 3. *Analysis workflow for microplastics analysis*

Sampling

The appropriate sampling step depends on the nature of the environment in which the microplastics are found. This largely depends on the matrix to be analyzed, where the microplastics are present. Some of the matrixes that contain microplastics are:

- Water
  - Wastewater
  - Tap water
  - Bottled water
- Sediments
- Biota
- Foods
  - Honey and sugar
  - Salts

Appropriate sampling methods can be found in various studies. (Hidalgo-Ruz, et al.,2012; Lusher et al., 2017; Liebezeit et al., 2013; Yang et al., 2015; Kim et al., 2018; Kosuth M. et al., 2018; Mason at al., 2018)

Sample preparation

Before a sample can be analyzed correctly, the analyte must be free of contaminants that would negative effect the analysis. Even when analyzing bottled water, these contaminants are always encountered and their amount varies depending on the matrix being analyzed. Even if we apply very sensitive analysis techniques, it can be said that sample preparation is the most important step for microplastic analysis. Because when the sample preparation is done correctly, the contaminants that may affect the chemical identification are removed and the correct result is achieved.

A blank or reference sample should be prepared using filtered deionized water to avoid contamination from the laboratory environment and materials used. It is essential for understanding plastic contamination and it is strongly suggested that preparation of samples under a laminar flow hood. It is passed through sieve pans larger than 20 **µm** to separate the coarse particles in the sample (Wong C, S. and Coffin S., 2021).

After physical separation, the removal of chemical contaminants should also be considered. For this, digestion procedures should be carried out and most of the digestion procedures face up to use of concentrated alkali or acid solutions which can be destroy organic macro molecules such as proteins, carbohydrates and fats. These organic molecules interfere chemical identification using the common analytical methods for microplastics. Enzymatic methods also can be applied (Cole et al, 2014; Courtene-Jones W. et al, 2017).

Filtration

There are a lot of filter/membrane can be chosen for identification of microplastics. But three significant properties should be considered: size of filter in diameter, material of filter (PTFE-polytetrafluoroethylene, alumina, PC-polycarbonate etc.) and pore size. For sure, appropriate filter must be selected according to the size of microplastics and on the techniques used. Borosilicate glass fibers, Alumina, Silicon and Polycarbonate filters are the most commonly used. Schematic diagram for filtration was shown by Wong C, S. and Coffin S. and given in Figure 4.

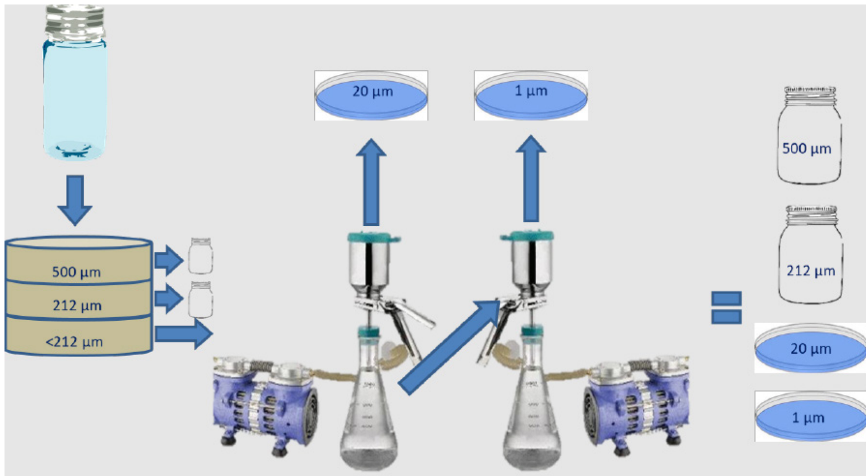

Figure 4. *Schematic diagram for filtration (Wong C, S. and Coffin S., 2021)*

Analysis

After sample preparation, samples are examined with various microscopes. Microplastic can be characterized by color, and morphology using visual examination. After that chemical structure of microplastics can be identified different analytical techniques. These techniques are;

- Infrared coupled with Microscopy
- Raman coupled with Microscopy

- Scanning Electron Microscopy - Energy Dispersive X-ray Spectroscopy (SEM-EDX)
- Fluorescence microscopy using Nile Red fluorescent dye.
- Pyrolysis Gas Chromatography Mass Spectrometry (Pyr-GCMS)

Infrared spectroscopy is non-destructive method and can provide qualitative and quantitative analysis almost whole organic molecules. Infrared spectrum encompasses radiation wavelengths from 0.78 to 1000 μm or 12,800 to 10 cm^{-1}. Using the infrared spectra, the functional groups in the plastics can be determined (Skoog, D. and Lary, J., 1992). IR spectroscopy uses the principle that IR radiation of different wavelengths is absorbed by molecules in a sample by their functional groups in the molecule. The absorbed frequency of IR radiation is the same as the intramolecular vibrational frequency of the analyte molecule. By passing a beam of IR radiation through the sample and detecting the light passing through the sample, we can obtain IR spectra for different molecules. This shows us the absorbed wavelengths and is called the IR spectrum. A typical IR spectrum is an absorption spectrum.

Raman and Infrared spectrum can ensure a more elaborate picture. Raman spectroscopy is more flexible about dimensions and microplastics below 10 μm, can be detected. Microplastics below 10 μm in the placenta have been detected by this method (Ragusa et al., 2021).

IR or Raman spectrometers with software (libraries) are much more efficient. These libraries allow high accuracy detection of large numbers of organic compounds in seconds. Instrument manufacturers can also offer these libraries. It can be said that these libraries are just as important as the device. An example of Infrared spectrum taken from Interactive IRUG Spectrum, was given in Figure 5.

The second most common technique, Raman microscopy is a non-destructive technique like Infrared spectroscopy. It also includes standard optical microscopy and provides morphological information, particle count, and chemical identification of microplastics (comparison of obtained Raman spectra with those in libraries using a software). Like infrared spectroscopy, Raman spectroscopy relies on the interaction of electromagnetic waves with chemical bonds within a molecule. However, the frequency of electromagnetic radiation used in this technique is higher than infrared. The main difference between IR and Raman spectra is that IR spectra can be obtained from light absorption whereas Raman spectra can be obtained from light scattering. The types of scattering processes that can occur when a molecule interact with light are shown in Figure 6.

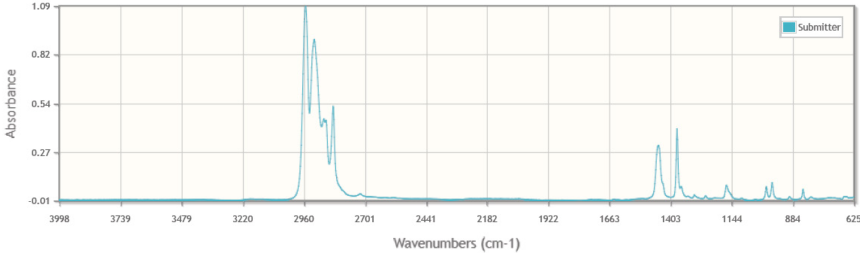

Figure 5. *IR spectra of polypropylene*

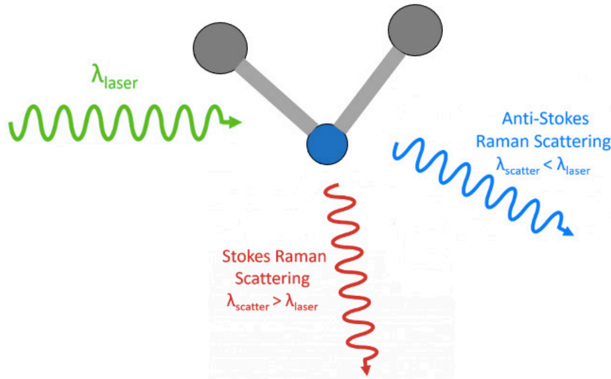

Figure 6. *Types of Raman scatterings*

Nile Red is a fluorescent dye is commonly used for the quantitation of lipids, but it also has affinity to most plastic molecules, allowing their identification by fluorescence spectroscopy. Nile Red binds to lipids and environmental samples, that's why care should be taken during the sample preparation step.

SEM-EDX allows morphological characterization of microplastics and provides the elemental composition of the sample. Some plastics including inorganics such as; PVC (due to presence chlorine) or Al, Ca, Mg, Si containing microplastics can be detected. But it does not provide chemical information for all microplastics.

The chemical composition of microplastics also can be determined by pyrolysis combined with GC-MS. This is a destructive method, so the sample cannot be re-analyzed. In this method, microplastics are pyrolyzed and pyrolysis products are analyzed at high accuracy. There are also library softwares which prepared by instrument manufacturers. The main advantage of this method is very low amount of sample is needed to be analyzed. However, its biggest disadvantages are that it does not provide information about the morphology of microplastics, and samples cannot be re-analyzed.

Table 2. *Classification of analysis methods for microplastics*

Samples, analysis	Methods
Polymers Additives Dyes/Pigments Natural particles Chemical identification Morphological information Quantitative analysis of microplastics	Raman Spectroscopy IR Spectroscopy
Nanoplastics Dissolved organic matter Toxicology studies for microplastics	Fluorescence Spectroscopy
Metals accumulated on microplastics Elemental analysis	SEM-EDX, XRF
Quantitative analysis of microplastics Chemical identification	Pyr-GCMS
Morphological information Quantitative analysis (number of particles)	Nile Red coupled with Fluorescence microscopy

Data evaluation and reporting

In this part of microplastic analysis, especially software technology is used.

After the IR or Raman spectrums are taken, the evaluation of these spectra is usually done by computer software. Device manufacturers take the IR and Raman spectra of plastic molecules that may need to be analyzed one by one in their own centers, with the device they produce, and create a library of these spectra. They also make this library available with the device.

The analyzer takes the IR or Raman spectra of microplastics identified with the microscope and examines these spectra for comparison with the spectra stored in the library. The device software determines the chemical structure of the microplastic by specifying the matching ratio, according to the spectrum in the library that best matches the spectrum of the microplastic in the sample.

In conclusion, the identification of microplastics is a very important issue and requires careful to work at all stages of microplastic analysis. A mistake made at one stage of the analysis will also affect the other steps of the analysis and the result will be wrong.

References

Gündoğdu, S., Çevik, C., & Karaca, S. (2017a). Fouling assemblage of benthic plastic debris collected from Mersin Bay, NE Levantine coast of Turkey. *Marine pollution bulletin, 124 1*, 147-154.

Aytamam, O. (2018). Okyanuslar ve denizlerimizde 5 trilyonu aşan plastik parçasının yüzdüğünü biliyor muydunuz? *The Deloltte Times*, *Kasım*, 51-53.

Thompson, R.C., Olsen, Y.S., Mitchell, R., Davis, A., Rowland, S.J., John, A.W., McGonigle, D.F., & Russell, A.E. (2004). Lost at Sea: Where Is All the Plastic? *Science, 304*, 838 - 838.

Gündoğdu, S., & *Çevik*, C. (2017b). Micro- and mesoplastics in Northeast Levantine coast of Turkey: The preliminary results from surface samples. *Marine pollution bulletin, 118 1-2*, 341-347.

Boucher, J., & Friot, D. (2017). Primary microplastics in the oceans: A global evaluation of sources.

Browne, M.A., Crump, P., Niven, S.J., Louise, E., Tonkin, A., Galloway, T.S., & Thompson, R.C. (2011). Accumulations of microplastic on shorelines worldwide: sources and sinks.

Salvador Cesa, F., Turra, A., & Baruque-Ramos, J. (2017). Synthetic fibers as microplastics in the marine environment: A review from textile perspective with a focus on domestic washings. *The Science of the total environment, 598*, 1116-1129.

Song, Y.K., Hong, S.H., Jang, M., Han, G.M., Rani, M., Lee, J., & Shim, W.J. (2015). A comparison of microscopic and spectroscopic identification methods for analysis of microplastics in environmental samples. *Marine pollution bulletin, 93 1-2*, 202-9.

Blumenröder, J., Séchet, P., Kakkonen, J.E., & Hartl, M.G. (2017). Microplastic contamination of intertidal sediments of Scapa Flow, Orkney: A first assessment. *Marine pollution bulletin, 124 1*, 112-120.

Gies, E.A., Lenoble, J.L., Noël, M., Etemadifar, A., Bishay, F., Hall, E.R., & Ross, P.S. (2018). Retention of microplastics in a major secondary wastewater treatment plant in Vancouver, Canada. *Marine pollution bulletin, 133*, 553-561.

Yang, D., Shi, H., Li, L., Li, J., Jabeen, K., & Kolandhasamy, P. (2015). Microplastic Pollution in Table Salts from China. Environmental science & technology, 49 22, 13622-7.

Rochman, C., Tahir, A., Williams, S. *et al.* (2015). Anthropogenic debris in seafood: Plastic debris and fibers from textiles in fish and bivalves sold for human consumption. *Sci Rep* **5,** 14340.

Liebezeit, G., & Liebezeit, E. (2013). Non-pollen particulates in honey and sugar. Food Additives & Contaminants: Part A, 30, 2136 - 2140.

Mason, S.A., Welch, V.G., & Neratko, J. (2018). Synthetic Polymer Contamination in Bottled Water. Frontiers in Chemistry, 6, 1-11.

Schwabl, P., Kppel, S., Knigshofer, P., Bucsics, T., Trauner, M., Reiberger, T., & Liebmann, B. (2019). Detection of Various Microplastics in Human Stool. Annals of Internal Medicine, 171, 453-457.

Ragusa, A., Svelato, A., Santacroce, C., Catalano, P., Notarstefano, V., Carnevali, O., Papa, F., Rongioletti, M.C., Baiocco, F., Draghi, S., D'Amore, E., Rinaldo, D., Matta, M., & Giorgini, E. (2021). Plasticenta: First evidence of microplastics in human placenta. Environment international, 146, 106274.

Horiba Scientific, The microplastics solutions for a better life, www.horiba.com/microplastics (2021).

Bouwmeester, H., Hollman, P.C., & Peters, R. (2015). Potential Health Impact of Environmentally Released Micro- and Nanoplastics in the Human Food Production Chain: Experiences from Nanotoxicology. Environmental science & technology, 49 15, 8932-47.

Hidalgo-Ruz, V., Gutow, L., Thompson, R.C., & Thiel, M. (2012). Microplastics in the marine environment: a review of the methods used for identification and quantification. *Environmental science & technology, 46 6*, 3060-75 .

Lusher, A.L., Welden, N.A., Sobral, P., & Cole, M. (2017). Sampling, isolating and identifying microplastics ingested by fish and invertebrates. Analytical Methods, 9, 1346-1360.

Kim, J., Lee, H., Kim, S., & Kim, H. (2018). Global Pattern of Microplastics (MPs) in Commercial Food-Grade Salts: Sea Salt as an Indicator of Seawater MP Pollution. Environmental science & technology, 52 21, 12819-12828.

Košuth, M., Mason, S.A., & Wattenberg, E.V. (2018). Anthropogenic contamination of tap water, beer, and sea salt. PLoS ONE, 13.

Wong C.,S., Coffin S., Standard Operating Procedures for Extraction and Measurement by Infrared Spectroscopy of Microplastic Particles in Drinking Water, *Southern California Coastal Water Research Project Authority*, 2021.

Cole, M., Webb, H., Lindeque, P., Fileman, E.S., Halsband, C., & Galloway, T.S. (2014). Isolation of microplastics in biota-rich seawater samples and marine organisms. Scientific Reports, 4.

Courtene-Jones, W., Quinn, B., Murphy, F., Gary, S.F., & Narayanaswamy, B.E. (2017). Optimisation of enzymatic digestion and validation of specimen preservation methods for the analysis of ingested microplastics. Analytical Methods, 9, 1437-1445.

Skoog, D. and Lary, J., *Princples of Instrumental Analysis,* Fourth Edition, Saunders College Publishing, USA, 1992.